UNIVERSITY OF CALIFORNIA, SAN DIEGO

The kinase-independent roles of the *C. elegans* Eph receptor in axon guidance involve PI 3-kinase and the Abl tyrosine kinase

A dissertation submitted in partial satisfaction of the requirements for the degree Doctor of Philosophy

in

Biology

by

Emily Nicole Grossman

Committee in charge:

Professor Andrew D. Chisholm, Chair
Professor Kuo-Fen Lee
Professor Elena B. Pasquale
Professor Emily R. Troemel
Professor Binhai Zheng
Professor Yimin Zou

2013

The Dissertation of Emily Nicole Grossman is approved, and it is acceptable in quality and form for publication on microfilm and electronically:

_____

_____

_____

_____

_____

_____
Chair

University of California, San Diego

2013

DEDICATION

I dedicate this work to the teachers who cultured my love of science, to the friends who supported me unconditionally, to my parents and brother who are proud of me for exactly who I am, but most of all, to Marcy, without whom I probably wouldn't have made it this far.

TABLE OF CONTENTS

LIST OF FIGURES

LIST OF TABLES

ACKNOWLEDGEMENTS

I would like to thank my advisor, Dr. Andrew D. Chisholm, for his guidance and support throughout my graduate career. I would also like to acknowledge the members of both the Chisholm and Jin labs (past and present) for their friendship and support.

I want to thank all the friends I have made here in graduate school, especially Rachel and Michaelanne; I honestly couldn't have made it through without you. Thank you for being there for me, through all the highs and lows. Most of all, I want to thank my beautiful wife Marcy for supporting me in all things that I do.

Chapter 2, in part, has been submitted for publication of the material as it may appear in Genetics, 2013, Grossman, Emily N.; Giurumescu, Claudiu A.; Chisholm, Andrew D. The dissertation author was the primary investigator and author of this paper.

VITA

2006 Bachelor of Science, Biology, University of California, Irvine

2013 Doctor of Philosophy, Biology, University of California, San Diego

Publications:

Milnes MR, Garcia A, **Grossman E**, Grün F, Shiotsugu J, Tabb MM, Kawashima Y, Katsu Y, Watanabe H, Iguchi T, Blumberg B. (2008) Activation of steroid and xenobiotic receptor (SXR, NR1I2) and its orthologs in laboratory, toxicologic, and genome model species. Environ Health Perspect. 116(7): 880-5.

Awards:

2011	3rd place poster, International *C. elegans* Meeting
2006	Inducted into the Phi Beta Kappa Society
2006	Graduated Magna Cum Laude, University of California, Irvine
2006	Excellence in Research, University of California, Irvine
2002-2006	Chancellor's Scholar, University of California, Irvine
2002-2006	Campuswide Honors Program, University of California, Irvine

ABSTRACT OF THE DISSERTATION

The kinase-independent roles of the *C. elegans* Eph receptor in axon guidance involve PI 3-kinase and the Abl tyrosine kinase

by

Emily Nicole Grossman

Doctor of Philosophy in Biology

University of California, San Diego, 2013

Professor Andrew D. Chisholm, Chair

It is only within the last twenty years that scientists have begun to understand the processes of axon guidance. Although a considerable body of work has been published regarding the mechanisms of axon guidance, much is still not known. In this work we seek to elucidate the *in vivo* mechanism of ephrin signaling, using the amphid sensory neurons of *Caenorhabditis elegans* as a model. In contrast to mammalian models, *C. elegans* only encodes a single Eph receptor, VAB-1. We find that guidance of the amphid neurons requires both kinase-dependent and kinase-independent Eph signaling mediated

by EFN-1, a GPI-linked ligand. Expression of VAB-1 was observed in select amphid neurons, and EFN-1 expression was visible in surrounding cells. This expression pattern is consistent with a model of kinase-independent forward Eph signaling by VAB-1. We find that the phosphatidylinositol 3-kinase pathway and the ABL-1 nonreceptor tyrosine kinase have roles in this Eph kinase-independent pathway. Surprisingly, we identified an asymmetry in guidance defects where left-hand neurons are affected significantly more often than right-hand neurons by loss of Eph signaling. Additionally, we find that overexpression of ABL-1 in a single neuron pair can rescue the entire sensory bundle, suggesting a non-cell autonomous relationship between the amphids during outgrowth. Lastly, we report our observation that a hyperactive calcium channel mutant, in combination with ephrin signaling mutants, cause disruption of dendrite attachment. These results shed light on the *in vivo* mechanisms of Eph signaling, and uncover previously unknown roles for ABL-1 in *C. elegans*.

I. Introduction

Ephrin Signaling

Ephrins and their cell surface receptors, the Eph receptor tyrosine kinases (EphR), play critical roles in many axon guidance processes, including midline guidance and growth cone collapse (COWAN *et al.* 2000; DRESCHER *et al.* 1995). Eph receptors make up the largest subfamily of receptor tyrosine kinases (RTKs). In vertebrates, each receptor has an ephrin binding domain, a cysteine-rich region, and two fibronectin III repeats as part of its extracellular domain. The receptor also has a transmembrane component linking it to the intracellular domain, which contains a juxtamembrane segment, the catalytically active kinase domain, and a sterile α-motif domain (SAM) (VAN DER GEER *et al.* 1994). In contrast to long-range guidance cues, which are secreted, ephrin ligands are cell membrane bound. This means that Eph signaling consists of contact mediated interactions, and active signaling requires membrane bound or artificially clustered ephrin ligands (DAVIS *et al.* 1994). Ephrin ligands can be classified into two types, either transmembrane (ephrin-B) or GPI linked (ephrin-A). Receptors are also classified into type-A or type-B depending on which type of ligand they usually bind. Although this is the case, there can be "cross-talk" between receptors and ligands of different types (HIMANEN *et al.* 2004). Eph signaling is complex and multi-functional, capable of mediating both repulsion and attraction depending on ephrin concentration even in the same neurons (HANSEN *et al.* 2004). Many of the signaling pathways downstream of Eph receptors and ephrins regulate cell movement or cell adhesion

(KULLANDER and KLEIN 2002; PASQUALE 2005).

Because Eph receptors and ephrins are cell surface molecules, they can operate in a variety of signaling modes (EGEA and KLEIN 2007; KULLANDER and KLEIN 2002; PASQUALE 2008). Eph receptors can generate kinase-dependent "forward" signals, in which ligand binding triggers receptor dimerization, activating the intrinsic kinase activity of the receptor and initiating response in the receptor-expressing cell. Kinase-dependent forward Eph signaling contributes to many processes including retinotopic mapping (HINDGES *et al.* 2002), axonal midline avoidance after crossing (YOKOYAMA *et al.* 2001), neural crest cell migration (SMITH *et al.* 1997), and migration of neural progenitors (CATCHPOLE and HENKEMEYER 2011). This regulation of diverse developmental processes occurs in part via kinase-dependent interactions with downstream effectors including Src-family kinases (KNOLL and DRESCHER 2004; ZISCH *et al.* 1998), Rho GTPases (NOREN and PASQUALE 2004; WAHL *et al.* 2000), and RhoGEFs (SAHIN *et al.* 2005; SHAMAH *et al.* 2001).

In addition to kinase-dependent signaling, some Eph receptors initiate kinase-independent forward signals. In HEK293 cells EphA8 signals promote integrin activity via the phosphatidylinositol 3-kinase (PI3K) pathway; the juxtamembrane domain of EphA8 directly interacts with the PI3K catalytic subunit p110γ, independent of EphA8 kinase activity (GU and PARK 2001; GU and PARK 2003). EphA8 can also interact with the Anks (Ankyrin and Sterile Alpha Motif) proteins AIDA and Odin in a kinase-independent manner (SHIN *et al.* 2007). However, the significance of kinase-independent forward signaling *in vivo* has not been extensively analyzed. Reverse signaling via ephrin ligands can also contribute to kinase-independent functions. Although both ephrin-B and

ephrin-A ligands are capable of reverse signaling (BRUCKNER *et al.* 1999; DAVY *et al.* 1999), ephrin-A ligands do not contain a transmembrane domain and therefore require a co-receptor, such as p75 (LIM *et al.* 2008), TrkB (MARLER *et al.* 2008), or Ret (BONANOMI *et al.* 2012). Finally, bidirectional signaling can occur where both the receptor and its membrane-bound ephrin ligand are involved in transmission of the signal into their respective cells (EGEA and KLEIN 2007). Bidirectional signaling was first shown for the EphB2(Nuk) receptor, which guides anterior commissure axons in the mouse brain (HENKEMEYER *et al.* 1996; HOLLAND *et al.* 1996).

Ephrin Signaling in *C. elegans*

In contrast to the many Eph receptors and ligands in vertebrates, *C. elegans* encodes a single Eph receptor, VAB-1 (GEORGE *et al.* 1998) and four ephrins, EFN-1-4 (CHIN-SANG *et al.* 1999; WANG *et al.* 1999). The *C. elegans* ligands resemble vertebrate ephrin-As in topology, in that they are attached to the cell membrane by a glycosylphosphatidylinositol (GPI) linker. Ephrins EFN-1 to 3 have partly redundant roles in VAB-1 signaling, depending on the developmental context (CHIN-SANG *et al.* 1999; WANG *et al.* 1999) whereas the divergent ephrin EFN-4 functions independently of VAB-1 (CHIN-SANG *et al.* 2002; IKEGAMI *et al.* 2004).

C. elegans Eph signaling acts in many cell types and processes. For example, VAB-1 and its ephrin ligands control neuroblast migrations during embryonic morphogenesis (CHIN-SANG *et al.* 1999; GEORGE *et al.* 1998; WANG *et al.* 1999). VAB-1 function in embryonic neuroblast migration requires both kinase-dependent and kinase-independent signaling, and involves partly redundant signaling by all three ephrin

ligands. VAB-1 signaling also regulates oocyte maturation and gonadal sheath cell contractions in response to a distinct set of ligands, the major sperm proteins (MSPs) (CHENG *et al.* 2008; MILLER *et al.* 2003). Although the VAB-1 kinase domain is required for inhibition of oocyte maturation in the absence of sperm, it is dispensable for regulation of the basal gonadal sheath cell contraction rate (MILLER *et al.* 2003). *C. elegans* Eph signaling has been implicated in outgrowth or guidance of several axon types, including PLM outgrowth (MOHAMED and CHIN-SANG 2006) and pathfinding of PVQ and HSN axons (BOULIN *et al.* 2006). In most of these situations, the defects of VAB-1/Eph receptor null mutants are more severe than those of kinase-dead alleles (BOULIN *et al.* 2006; GEORGE *et al.* 1998; MOHAMED and CHIN-SANG 2006), implying that a portion of VAB-1 signaling is kinase-independent. However the *in vivo* mechanism of VAB-1 kinase-independent signaling has remained elusive.

Sensory Neurons as a Model of Ephrin Signaling

To elucidate *in vivo* mechanisms of kinase-independent ephrin signaling we used the amphid commisure of *C. elegans* as a model. The amphid consists of twelve pairs of bilaterally symmetric neurons in the head of the worm that are responsible for detecting chemicals, odors, and temperature. Most are continuous with the outside environment through the amphid pore, but AWA, AWB, and AWC invaginate the amphid sheath cell (PERKINS *et al.* 1986; WARD *et al.* 1975). Each amphid neuron has a dendrite, which is exposed to environmental cues, as well as an axon, which extends into the nerve ring. By using the amphids as a model for axon outgrowth, this allows us to examine both dendritic and axonal morphology in the same neuron in response to genetic modification.

The initial step of amphid neuron development begins with dendritic anchoring during embryogenesis. This process begins when the amphid cell body anchors its dendritic tip to the anterior part of the embryo. DYF-7 and DEX-1, which share homology with zona pellucida (ZP), ZP-binding proteins, and tectorin proteins, are required for proper anchoring of the dendritic tip (HEIMAN and SHAHAM 2009). It is thought that these proteins form a matrix-like structure to hold the dendrite in place, although more work is required to ascertain all the players involved (HEIMAN and SHAHAM 2009). After the dendritic tip is secured, dendrites extend as a coordinated bundle by a process known as "retrograde extension" where the dendritic tip of the amphid neuron remains stationary while the cell body moves posteriorly and lays down dendrite as it goes (HEIMAN and SHAHAM 2009). The sheath and socket glial cells, which surround the amphid sensory organ (WARD *et al.* 1975), also serve as important support structures to the amphids. They are essential for sensory function, and may also contribute to dendrite anchoring (BACAJ *et al.* 2008; PROCKO and SHAHAM 2010). As development progresses, the dendrites must scale almost two times their original length in order to keep pace with overall larval growth (HEIMAN and SHAHAM 2009).

ABL-1, a Non-Receptor Tyrosine Kinase

One of the first protein tyrosine kinases discovered (SEFTON *et al.* 1981; WITTE *et al.* 1981), Abl is a non-receptor tyrosine kinase with multiple functional regions, including a Src homology 3 (SH3), Src homology 2 (SH2), and a tyrosine kinase domain (VAN ETTEN 1999). Abl has been studied intently for its contributing role to chronic myelogenous leukemia; recombination of the Abl gene with the BCR gene produces the

BCR-Abl fusion protein, which leads to deregulation of kinase activity and disease (LUGO *et al.* 1990; SHTIVELMAN *et al.* 1985). Abl was found to be constitutively active in aggressive and invasive breast cancer cell lines, and seems to promote cell invasion (SRINIVASAN and PLATTNER 2006). Over the years, Eph signaling has also been intensely investigated to determine its contribution to cancer progression (GENANDER 2012). To investigate if Eph and Abl physically interact in cancer cell culture, yeast-two-hybrid experiments were conducted. In these, the SH2 domain of Abl was determined to bind to the cytoplasmic domains of the EphA4 and EphB2 receptors. Furthermore, a motif in the C-terminal tail of Abl was also found to mediate binding to EphB2, but does so independently of Eph kinase activity (YU *et al.* 2001).

In addition to regulating cell migration during cancer proliferation, Abl also interacts with both the Roundabout (Robo) receptor and the Netrin receptor to regulate neuron guidance in *D. melanogaster* (BASHAW *et al.* 2000; FORSTHOEFEL *et al.* 2005). Although Abl has not been shown to act downstream of Eph receptors in invertebrates, it has been demonstrated to be required downstream of the EphA receptor for growth cone collapse in vertebrate neuron cell culture (HARBOTT and NOBES 2005). In *C. elegans*, ABL-1 encodes a non-receptor tyrosine kinase containing both SH2 and SH3 domains. Although shown to inhibit both germline apoptosis in response to ionizing radiation (DENG *et al.* 2004) as well as engulfment of apoptotic cells (HURWITZ *et al.* 2009), its role in neuron guidance in *C. elegans* is still unclear.

Phosphatidylinositol 3-Kinase Signaling

The phosphatidylinositol 3-kinase (PI3K) pathway has been previously implicated downstream of Eph receptors in regulation of integrin activity (GU and PARK 2001), migration of endothelial cells contributing to angiogenesis (BRANTLEY-SIEDERS *et al.* 2004; MAEKAWA *et al.* 2003), and cell positioning of intestinal cells (GENANDER *et al.* 2009). In addition to regulation of cell migration, components of PI3K signaling also have been shown to play a role downstream of guidance receptors. In *Xenopus*, PI3K signaling is required downstream of TrkA receptors for attractive turning towards NGF (MING *et al.* 1999). Additionally, PI3K signaling mediates outgrowth of the AVM neuron in *C. elegans* in response to slit and netrin (CHANG *et al.* 2006). Currently, the role of PI3K signaling downstream of Eph receptors during axon guidance is not well understood.

Left/Right Asymmetry in the Nervous System

Many bilaterally symmetric organisms have structural and functional left/right asymmetries as a normal part of development. For example, in humans the heart, spleen, and liver are asymmetric with respect to the ventral midline. Asymmetries are not restricted to gross morphology though, and occur even in the design of neural circuits. These neural asymmetries result as a consequence of genetics and environmental factors, and can be roughly grouped into two classes (CONCHA *et al.* 2012). In the first class, an asymmetry can occur in a system that has similar cell types that are present in different ratios on the left and right. For example, in the zebrafish dorsal diencephalon, neurogenesis is under genetic control of Notch, which suppresses neurogenesis on the

right side and leads to a smaller lateral subnucleus (CONCHA *et al.* 2009). The second class of asymmetries can result from a unilateral circuit component such as receptor-expression that is restricted to one side or the other. This case is observed in *C. elegans* in the ASE and AWC chemosensory neurons (HOBERT *et al.* 2002; TROEMEL *et al.* 1999; YU *et al.* 1997), where right or left specific expression of receptors gives these neurons different functional sensitivities to chemicals.

Role of Calcium in Regulation of Axon Guidance

Calcium signaling is crucial to life, starting with fertilization, and required for a multitude of processes in every organism. Regulation of calcium signaling is partially mediated by voltage gated calcium channels (VGCCs), which typically consist of the poreforming $\alpha 1$ subunit and the accessory subunits β, $\alpha 2/\ \delta$, and γ (SINGER *et al.* 1991). The $\alpha 1$ subunit contains a pore-forming structure in the center, which selectively allows Ca^{2+} ion flux across the membrane. There are three main types of vertebrate VGCCs, and their classification is dependent on their $\alpha 1$ subunits as well as what type of molecule can block the channel's function. There are L-type, non-L-type, and T-type channels. non-L type can further be classified into N-, P/Q-, and R-type depending on what specific peptide toxins can block the channel. While both the L-type and non-L type are high voltage activated, T-type are low voltage activated (for review see (CATTERALL 2000)).

Developing neurons are highly reliant on calcium signaling to regulate cell differentiation, rate of outgrowth, and function (ROSENBERG and SPITZER 2011; TROEMEL *et al.* 1999). During development, transient calcium spikes were found to reduce the rate of axon outgrowth both *in vitro* (GOMEZ *et al.* 1995; TANG *et al.* 2003) and *in vivo*

(GOMEZ and SPITZER 1999). Growth cones producing a high frequency of calcium transients were found to migrate slowly or retract, whereas growth cones generating a low frequency of calicum transients migrate rapidly.

In addition to regulating rate of outgrowth, calcium-dependent pathways also regulate axon pathfinding in response to molecular guidance cues. For example, in cultured *Xenopus* spinal neurons, axons turning toward a netrin-1 source depend on calcium signaling (HONG *et al.* 2000; MING *et al.* 1997). Although L-type channels primarily regulate calcium signaling downstream of guidance cues, they are not the only channel type because when L-type channel blockers were applied to spinal neuron cultures, calcium signaling in response to netrin cues were reduced, but not eliminated (HONG *et al.* 2000). This implies that other non-L-type or non-VGCCs may be regulating calcium influx in response to cues. Although netrin has been found to trigger calcium-dependent signaling, there is no evidence that Eph/ephrin signaling also has a Calcium-dependent component. However, a recent report using *Drosophila* suggests that Eph receptors form a complex with ephexin, Cdc42, and CaV2.1 (P/Q-type VGCC) to maintain synaptic homeostasis (FRANK *et al.* 2009).

II. Ephrin signaling in *C. elegans* amphid guidance

Abstract

Eph receptors and their ephrin ligands are key conserved regulators of axon guidance, and can function in a variety of signaling modes. Here we analyze the genetic and cellular requirements for Eph signaling in a *C. elegans* axon guidance choice point, the ventral guidance of axons in the amphid commissure. The *C. elegans* Eph receptor VAB-1 has both kinase-dependent and kinase-independent roles in amphid guidance. Of the four *C. elegans* ephrins, we find that only EFN-1 has a major role in amphid axon guidance, and signals in both a receptor kinase-dependent and kinase-independent manner. Analysis of VAB-1 and EFN-1 expression and tissue specific requirements is consistent with a model in which VAB-1 acts in amphid neurons, interacting with EFN-1 expressed on surrounding cells. Unexpectedly, left-hand neurons are more strongly affected than right-hand neurons by loss of Eph signaling, indicating a previously undetected left-right asymmetry in the requirement for Eph signaling. By screening candidate genes involved in Eph signaling we find that the Eph kinase-independent pathway involves phosphatidylinositol 3-kinase pathway and the ABL-1 nonreceptor tyrosine kinase. Overexpression of ABL-1 is sufficient to rescue *vab-1* guidance defects cell-autonomously, and can restore normal guidance to other amphid axons non-autonomously. Our results reveal new aspects of Eph signaling in a single axon guidance decision *in vivo*.

Introduction

To understand the basis of VAB-1 kinase-independent signaling at the level of individual cells we have focused on a simple axon guidance decision, the ventral guidance of amphid sensory axons. Ventral guidance of amphid sensory axons involves VAB-1 and at least two other partly redundant guidance systems: netrin (UNC-6/UNC-40) signaling, and the SAX-3/Robo receptor (ZALLEN *et al.* 1999). Loss of function in any one of these pathways leads to incompletely penetrant guidance defects in which the amphid commissure extends laterally instead of ventrally. Double mutants between the pathways display strong synergistic enhancement of guidance defects. As VAB-1 is required for many aspects of embryonic morphogenesis it has been unresolved whether VAB-1 acts directly in amphid axon guidance.

We show here that VAB-1 likely functions in amphid neurons to mediate their ventral axonal guidance, interacting with EFN-1 in non-amphid neurons. The requirement for Eph signaling displays an unexpected left-right asymmetry. VAB-1's role in amphid axon guidance involves at least two pathways, both of which are partly kinase-independent. PI3K signaling promotes amphid axon guidance, in part downstream of VAB-1. Additionally, ABL-1, a non-receptor tyrosine kinase, signals in the amphid neurons as part of a VAB-1 kinase-independent pathway. These results elucidate mechanisms of VAB-1 kinase-independent forward signaling in amphid axon guidance.

Results

Amphid ventral guidance involves both kinase-dependent and kinase-independent functions of VAB-1/Eph receptor

Amphids are sensory organs containing 12 bilaterally symmetric pairs of neurons whose cell bodies are located in the lateral ganglia of the head. Amphid neuron cell bodies are born in the anterior head in mid-embryogenesis, move anteriorly to anchor their dendrite tip, then migrate posteriorly, laying down their sensory processes by 'retrograde extension' (HEIMAN and SHAHAM 2009; SULSTON *et al.* 1983). Once the amphid cell body reaches its final place in the lateral ganglia, the amphid axons grow out ventrally then turn and extend anteriorly and dorsally into the nerve ring. Amphid axons are fasciculated in their ventral trajectories, forming two bundles known as the amphid commissures. Previous work revealed that amphid commissure guidance was strongly dependent on VAB-1/EphR signaling: *vab-1(dx31)* null mutants display 30-40% guidance defects in which amphid axons leave the cell body laterally and enter the nerve ring without following the normal ventral trajectory (ZALLEN *et al.* 1999). Defects were significantly less penetrant in the kinase-dead allele *vab-1(e2)* suggesting amphid axon guidance is a suitable model of VAB-1/EphR kinase-independent signaling.

To confirm the requirement for VAB-1 we examined amphid axon guidance in the entire *vab-1* allelic series using the AWB marker P*str-1*-GFP (*kyIs104)* (**Fig 2.1A**). Axon guidance defect penetrance correlated strongly with penetrance of lethality or body morphology defects (GEORGE ET AL., 1998). Putative *vab-1* null alleles (*e2027, dx31, ju8,*

ok1699, dx14, ju307) cause between 31%-38% axon guidance defects, whereas likely kinase-dead *vab-1* alleles (*e118, e2, zd118)* display 10% defects. These results confirm that both kinase-dependent and kinase-independent VAB-1 functions are involved in amphid axon guidance. Hereafter we refer to the reference null *vab-1(e2027)* as *vab-1(0),* and to the reference kinase dead allele *vab-1(e118)* as *vab-1(kd)*. We next addressed whether VAB-1 signals affected other amphid neurons. Using cell specific markers we find that at least four neurons display similar axon guidance defects in *vab-1* mutants, and are differentially affected in the *vab-1* null and kinase-dead mutants (**Fig 2.1B**). Using dye filling to visualize multiple amphid neurons we find that animals with defective AWB guidance were also defective in the guidance of the entire commissure (**Fig 2.1C**). This is in agreement with previous observations (ZALLEN *et al.* 1999) that *vab-1* mutations affect all amphid axons equally. Below, we focus on a representative neuron, AWB.

Amphid axon guidance is dependent on EFN-1, which signals through both VAB-1 kinase-dependent and -independent pathways

Previous studies had not determined the specific ephrin ligands involved in amphid axon guidance. Of the four *C. elegans* ephrins, only *efn-1(0)* mutants displayed amphid axon guidance defects like those of *vab-1,* at lower penetrance (25%; **Fig 2.1C, 2.1D**). These observations suggested that EFN-1 might be partly redundant with EFN-2 and EFN-3 in regulating ventral guidance. However, *efn-2* or *efn-3* null mutants or *efn-2 efn-3* double mutants displayed completely normal AWB guidance (**Fig 2.1D**). *efn-1 efn-2* and *efn-1 efn-3* double mutants resembled *efn-1* single mutants, as did the *efn-1, efn-2,*

efn-3 triple mutant (**Fig 2.1D**). Thus, EFN-1 is the major ephrin ligand involved in amphid axon guidance. As shown below, EFN-2 may play a minor role in guidance.

To address how EFN-1 may regulate VAB-1 signaling we examined amphid guidance in *efn-1 vab-1* double mutants. The phenotype of *vab-1* null mutants was not enhanced by *efn-1(0)*, consistent with EFN-1 and VAB-1 acting in a linear pathway. We next addressed whether EFN-1 acted in the VAB-1 kinase-dependent or kinase-independent pathway by examining double mutants between each ephrin ligand and the kinase dead receptor. We interpret enhancement of the kinase-dead phenotype as evidence for signaling in a kinase-independent pathway. *efn-1(0) vab-1(kd)* double mutants showed enhancement relative to *vab-1(kd)* but not to *efn-1(0)* alone, consistent with EFN-1 signaling at least in part through a kinase independent pathway (**Fig 2.1E**). Conversely, *efn-2 vab-1(kd)* and *efn-3 vab-1(kd)* mutants displayed significant suppression of axon guidance defects relative to *vab-1(kd)*, suggesting EFN-2 and EFN-3 have a cryptic function antagonizing the kinase independent pathway. *efn-2* or *efn-3* neither enhanced nor suppressed *vab-1(0)* guidance defects, implying that the antagonistic effects of EFN-2/3 require the Eph receptor (**Fig 2.1E**).

To test whether loss of EFN-2 improved VAB-1 signaling by enhancing EFN-1 activity we examined whether *efn-1* partial loss of function mutants could be suppressed by *efn-2(lf)*, and found no significant suppression in these double mutants (**Fig 2.1F**). Loss of EFN-2 may be unable to compensate for the reduced EFN-1 function in these mutants. To address the specificity of *efn-2* suppression, we analyzed double loss-of-function mutants between *efn-2* and the netrin receptor *unc-40* or *sax-3*/Robo. *efn-2* weakly suppressed guidance defects in both cases (**Fig 2.1F**), although these effects were

not statistically significant. These data imply that loss of *efn-2* function might increase EFN-1/VAB-1 signaling via VAB-1, resulting in slight improvement of guidance in the absence of UNC-40 or SAX-3.

VAB-1 is expressed and required in amphid neurons for axon guidance

We considered two general models for how VAB-1 and EFN-1 might promote amphid guidance (**Fig 2.2A**) First, VAB-1 in amphid neurons might interact with EFN-1 on surrounding guidepost cells, mediating a receptor forward signal into axons. EFN-1 might present an attractive cue on ventral guidepost cells or EFN-1 might repel amphid axons from the more lateral pathway. In the second model EFN-1 in amphid neurons might interact with VAB-1 in surrounding cells, mediating an ephrin reverse signal into axons. More complex models in which VAB-1 and EFN-1 are coexpressed in amphids and surrounding cells are possible.

VAB-1 is widely expressed in anterior neurons during embryonic and larval development (BRISBIN *et al.* 2009; GEORGE *et al.* 1998). Although the embryonic VAB-1 expression is complex, at least some VAB-1-expressing cells appear to correspond to amphid neurons (**Fig 2.2B**). During larval stages P*vab-1*-GFP expression becomes more restricted, but is observable in at least one amphid neuron, ASIL, as well as other locations (**Fig 2.2C**). We therefore focused on testing the cellular requirement of VAB-1 using a variety of tissue- or cell-specific promoters (Appendix A). We verified that the *vab-1(0)* axon guidance phenotypes were fully rescuable by genomic *vab-1* DNA or by the VAB-1::GFP transgene (GEORGE *et al.* 1998). Expression of VAB-1 under the control of pan-neuronal promoters such as *unc-33* or *rgef-1* partly rescued *vab-1(0)* phenotypes from 38% to 27% (not significant), suggesting VAB-1 is required at least in part in

neurons. When we expressed VAB-1 using an amphid specific promoter (P*dyf-7*), *vab-1(0)* mutant phenotypes were significantly rescued (18%; **Fig 2.2D**). In contrast, expression of VAB-1 from non-neuronal promoters, including *lin-26* (glial and epidermal cells), *hlh-17* (cephalic sheath cells), or *myo-2* (pharyngeal muscle), did not rescue amphid axon defects. Taken together, our expression and tissue-specific rescue experiments are most consistent with VAB-1 acting directly in amphid neurons to promote axon guidance.

EFN-1 is expressed and required in neurons and can inhibit VAB-1 when expressed in amphid neurons

EFN-1::GFP is expressed widely in anterior neurons during mid-embryogenesis (CHIN-SANG *et al.* 1999), but like VAB-1 becomes more restricted during larval stages. In larvae, EFN-1::GFP was not observed in amphid neurons but was seen in a set of ventral neurons including AIM, AIY, and AVK (**Fig 2.3A**). Tissue-specific expression of EFN-1 under the control of the pan-neuronal *unc-33* promoter significantly suppressed *efn-1(0)* guidance defects, suggesting EFN-1 is at least partly required in neurons. However, amphid specific expression of EFN-1 strongly enhanced guidance defects in an *efn-1(0)* mutant (**Fig 2.3B**). We reasoned that if EFN-1 is normally excluded from VAB-1-expressing amphid neurons, its ectopic expression in amphid neurons could inhibit VAB-1 signaling by a *cis*-interaction similar to that reported in retinal axons (CARVALHO *et al.* 2006). Consistent with this hypothesis, P*dyf-7*-EFN-1 did not enhance guidance defects of a *vab-1(0)* mutant. Thus, guidance defects due to misexpression of EFN-1 require VAB-1/EphR. Expression of EFN-1 under the control of non-neuronal or AWB-specific promoters (*lin-26, hlh-17, myo-2,* or *str-1*) neither rescued nor enhanced *efn-1*

phenotypes. Overall these data are consistent with EFN-1 functioning in non-amphid neurons, presumably guidepost cells for amphid axons.

Eph signaling in amphid axon guidance displays left-right asymmetry

In the course of analyzing axon guidance phenotypes, we noticed that almost all *vab-1* and ephrin mutant strains displayed a strong left-right bias, in that guidance defects were 2-4 times more frequent in the left hand neuron of a bilateral pair (**Fig 2.4A**, **2.4B**). Such asymmetric guidance defects were seen in multiple neuron types and with dye filling. In contrast, *unc-40* (Netrin receptor) or *sax-3* (Robo) mutants displayed symmetrical defects (**Fig 2.4B**). These observations suggest that despite the overt symmetry of axon guidance in the wild type, left-hand neurons are much more dependent on Eph signaling than are right-hand neurons.

Amphid neurons display left-right asymmetries in gene expression and function, determined by cell autonomous gene regulatory cascades (HOBERT *et al.* 2002; JOHNSTON and HOBERT 2003). To distinguish whether an amphid neuron's identity or its environment determines the asymmetric response to loss of ephrin signaling we used *lsy-6* mutants, in which a left-hand neuron (ASEL) is genetically transformed into its right-hand counterpart ASER (JOHNSTON and HOBERT 2003). If left-hand bias in guidance defects reflects an intrinsic aspect of the ASEL fate, ASER should not show higher guidance defects when on the left side. On the other hand, if the left hand environment determines reliance on Eph signaling then the transformed ASER (left) should show enhanced defects compared to the nontransformed ASER (right). In *vab-1(0) lsy*-6 double mutants we observed a strong left-hand bias in defects ($P < 0.01$), equivalent to that in

vab-1(0) alone (**Fig 2.4C**), suggesting it is not the lateralized identity of the cell, but a difference in the environment that leads to the asymmetry of Eph guidance defects.

To better quantify the asymmetry in each mutant we created an "asymmetry index" consisting of the percentage of left hand lateral defects divided by percentage of total lateral defects (1 = all defects on left hand side, 0 = all on right, 0.5 = symmetrical). By examing these ratios, we realized that double mutants with *efn-2* show a more left-skewed ratio of defects when compared with the single mutant alone. For example, loss of function in *efn-1* causes defects with a strong left-hand bias that is exacerbated in *efn-1 efn-2* mutants. Defects on the left side increase from 36% to 50%, and those on the right side decrease from 16% to 8% (**Fig 2.4D**). In contrast, loss of *efn-2* improves left-hand guidance in *vab-1(kd)* mutants, suggesting that the effect of EFN-2 on left hand guidance can be positive or negative depending on the presence of EFN-1. *efn-2* does not modify the left-right asymmetry of *vab-1(0)* consistent with the idea that the inhibitory effect of EFN-2 requires VAB-1. Asymmetric expression of EFN-2 and likely other guidance cues could contribute to the unequal roles of Eph signaling in left and right amphid axon guidance.

Screening candidates for components of Eph signaling in axon guidance

To identify additional components of the Eph pathway involved in axon guidance we screened candidates chosen based on their known involvement in Eph signaling in other cells or organisms (Table 1). We scored guidance in all single mutants and for selected mutants in the *vab-1(kd)* and *vab-1(0)* backgrounds, reasoning that mutations affecting a VAB-1 kinase-independent pathway should enhance *vab-1(kd)* but not *vab-1(0)*. Based on the tissue and cell-specific rescue results we report here, it is likely that

components in this pathway would function downstream of VAB-1 in a "forward signaling" mechanism. As predicted, loss of function in candidate coreceptors for ephrin reverse signaling such as the TrkB homolog *trk-1* (MANNING 2005) did not affect guidance. Other potential VAB-1 ligands such as the atypical ephrin EFN-4 (CHIN-SANG *et al.* 2002; IKEGAMI *et al.* 2004), VPR-1 (TSUDA *et al.* 2008), or the Wrapper/Klingon receptor WRK-1 (BOULIN *et al.* 2006) did not affect amphid axon guidance and were not tested further (Table 1). Some sterile or maternal-effect mutants, such as *src-1* were only tested as single mutants and did not affect guidance. Loss of function in *mig-10/*Lamellipodin or *ngn-1/*Neurogenin caused highly penetrant axon guidance defects as single mutants and may affect parallel pathways or multiple signaling pathways. Most single mutants did not display axon guidance defects, and did not modify the *vab-1(kd)* phenotype, including several genes implicated in Eph signaling in other contexts, such as *nck-1*/Nck (HU *et al.* 2009) or *ephx-1/*Ephexin (SAHIN *et al.* 2005). Below we focus on two pathways that displayed specific roles in amphid guidance*:* the PI3-kinase/Insulin signaling pathway and the non-receptor tyrosine kinase *abl-1*/Abl.

PI 3-kinase signaling promotes amphid axon guidance

The phosphatidylinositol 3-kinase pathway plays widespread roles in Eph signaling. In *C. elegans,* VAB-1's roles in axon outgrowth and lifespan appear to be mediated via PI3K signals (BRISBIN *et al.* 2009). We therefore tested *age-1* and *aap-1*, which encode the *C. elegans* orthologs of the PI3K p110 catalytic and p50/p55 adaptor/regulatory subunit. *age-1* or *aap-1* single mutants displayed normal amphid guidance and both significantly enhanced the *vab-1(kd)* phenotype (**Fig 2.5A**). Loss of *aap-1* or *age-1* also enhanced *efn-1(0)* guidance defects, and *age-1* enhanced *vab-1* null

mutant defects. PI3K signaling has recently been shown to cell-autonomously promote axon outgrowth of the AIY neuron (CHRISTENSEN *et al.* 2011); we found that AWB also displayed outgrowth defects in PI3K mutants, but that these were independent of axon guidance or VAB-1 (not shown). These results suggest PI3-kinase signaling promotes amphid guidance and that loss of VAB-1 function sensitizes amphid axons to loss of PI3K activity. As *vab-1(0)* is enhanced by PI3K mutations, PI3K may act downstream to VAB-1, in parallel, or both.

daf-18 encodes the *C. elegans* PTEN phosphatase and acts antagonistically to PI3K (OGG and RUVKUN 1998). VAB-1 has been shown to interact with and negatively regulate PTEN expression and function in amphid neurons in a kinase-dependent manner (BRISBIN *et al.* 2009). We found that *daf-18 vab-1(kd)* mutants showed significant suppression of amphid guidance defects, consistent with PI3K signaling promoting guidance (**Fig 2.5B**). In *C. elegans* PI(3,4,5)P_3 (PIP_3)is thought to signal via a variety of kinases, including AKT-1/AKT-2 (PARADIS and RUVKUN 1998) and PDK-1 (PARADIS *et al.* 1999). The serum-and glucocorticoid-inducible kinase SGK-1 strictly depends on PDK-1 for its activation, but transduces PIP_3 signals by forming a complex with AKT-1/2 to control life span through regulation of DAF-16 (HERTWECK *et al.* 2004). We therefore tested *pdk-1*/PDK*, sgk-1*/SGK, and the Akt/PKB homologs *akt-1* and *akt-2.* Unexpectedly, loss of function in each of these kinases except *akt-2* suppressed *vab-1(kd)* defects (**Fig 2.5B**). Loss of function in a target of the PI3-kinase/insulin pathway, DAF-16/FOXO (LIN *et al.* 1997; OGG *et al.* 1997), also suppressed *vab-1(kd)* guidance defects.

Overall, these results are consistent with the model that VAB-1 kinase-independent signaling involves the PI3K pathway. However, the roles of PI3K dependent

kinases differ from their canonical roles as defined by their functions in aging or dauer formation (HERTWECK *et al.* 2004; PARADIS *et al.* 1999; PARADIS and RUVKUN 1998). Reduced PI3K activity enhanced guidance defects, yet loss of function in the kinases that transduce PIP_3 activity suppressed guidance defects. These results suggest a more complex and possibly non-canonical relationship between VAB-1 and the PI3K pathway in axon guidance.

The ABL-1 tyrosine kinase acts in Eph signaling in amphid axon guidance

abl-1 mutants display a low penetrance (1%) lateral axon phenotype and significantly enhanced *vab-1(kd),* but not *vab-1(0)* guidance defects (**Fig 2.6A**), suggesting *abl-1* acts in Eph signaling but independent of the Eph kinase. *abl-1 unc-40* double mutants did not display genetic interactions, consistent with ABL-1 acting specifically in Eph signaling (**Fig 2.6A**). *efn-1 abl-1* double mutants displayed significant enhancement, suggesting that although ABL-1 acts within the Eph pathway it is not solely downstream of EFN-1 (**Fig 2.6A**). *age-1 abl-1* double mutants displayed normal guidance. However, the *abl-1 age-1 vab-1(kd)* triple mutant displayed 45% guidance defects, equivalent to or slightly stronger than *vab-1(0)* (**Fig 2.6B**). This synergistic effect in the *vab-1(kd)* background suggest *abl-1* and *age-1* act in distinct pathways in amphid guidance that are redundant with each other and with VAB-1 kinase-dependent signals.

To determine where ABL-1 functions in amphid axon guidance we conducted tissue- and cell- specific rescue experiments. We expressed the ABL-1 cDNA under the control of amphid-specific (*dyf-7*) or AWB-specific (*str-1*) promoters and tested for rescue of the *vab-1(kd) abl-1* enhanced phenotype. Amphid-specific expression of ABL-1 rescued the *vab-1(kd) abl-1* double mutant to the level of the *vab-1(kd)* phenotype alone,

indicating ABL-1 acts in amphid neurons. Strikingly, expression of ABL-1 under the AWB-specific *str-1* promoter was able to suppress *vab-1(kd) abl-1* guidance defects to levels even lower than those of *vab-1(kd)* (**Fig 2.6C**). This suppression of *vab-1* by AWB-specific ABL-1 overexpression is also consistent with ABL-1 acting in AWB downstream of VAB-1. Moreover, when we examined other amphid neurons in the P*str-1*-ABL-1 rescued line, we found that rescue of AWB guidance was almost completely correlated with rescue of other axons in the commissure (**Fig 2.6D**). Thus, AWB-specific expression of ABL-1 not only rescues AWB guidance but appears to non-autonomously rescue guidance of other amphid axons.

Discussion

We were interested in the roles of Eph signaling in amphid axon guidance as a simple model for kinase-independent functions of Eph receptors. Our genetic and cellular analysis suggests the role of VAB-1 signaling in amphid axons is in several respects unlike its function in other cellular contexts in *C. elegans*. Thus, despite expressing a single Eph receptor and a small number of ephrin ligands, *C. elegans* Eph signaling is highly context-specific (MILLER and CHIN-SANG 2012).

EFN-1 is the major ephrin acting in amphid guidance

In contrast to the previously characterized functional redundancy between EFN-1, EFN-2, and EFN-3 in embryonic morphogenesis and ventral neuroblast migration (WANG *et al.* 1999), only EFN-1 is required to properly guide the amphid neurons, and is sufficient to signal in the absence of EFN-2 and EFN-3. Unexpectedly, the *efn-1,-2,-3*

triple mutant fails to phenocopy the *vab-1* receptor null in amphid guidance suggesting that EFN-1,-2, and -3 do not collectively account for all VAB-1 activity. At least three explanations can be considered for this discrepancy. First, EFN ligands might antagonize one another. Removal of *efn-2* appears to slightly enhance *efn-1*, but this effect is negated by loss of *efn-3*. It is possible that EFN-3 acts in an inhibitory way to disrupt the functionality of EFN-1 or EFN-2 during ephrin signaling. We also find that loss of EFN-2 or EFN-3 mildly suppressed *vab-1(kd),* suggesting EFN-2 and EFN-3 inhibit kinase-independent signaling. Loss of EFN-2 or EFN-3 does not affect the *vab-1* null phenotype, suggesting such suppression effect requires the VAB-1 receptor.

A second possibility is that amphid axon guidance involves an additional VAB-1 ligand. However, the best candidate non-ephrin ligand VPR-1 does not appear to be required in amphid guidance. Lastly, VAB-1 could have ligand-independent activity in axon guidance. In cancer cell lines EphRs have been shown to regulate cell migration independently of ephrin stimulation (MIAO *et al.* 2009; NOREN *et al.* 2009). In axon guidance, in which localized ligands should provide directional information, ligand-independent activity of VAB-1 might be permissive for other instructive signals such as netrins to promote ventral guidance.

Cellular requirements for Eph signaling in amphid axon guidance

Our tissue-specific rescue experiments suggest VAB-1 functions at least in part in the nervous system, and most likely in the amphid neurons themselves. This conclusion is consistent with our expression data and previous evidence for VAB-1 functioning in amphid neurons (BRISBIN *et al.* 2009; GEORGE *et al.* 1998). Conversely, EFN-1 does not appear to be expressed or required in amphid neurons; moreover, expression of EFN-1 in

amphid neurons enhances the *efn-1(0)* mutant phenotype. We hypothesize that this enhancement reflects a *cis*-inhibitory interaction between EFN-1 and VAB-1, because amphid specific expression of EFN-1 does not enhance *vab-1(0)*. Although we have not pinpointed the cells in which EFN-1 is expressed at the time of amphid guidance, it is noteworthy that EFN-1::GFP was detected in a set of ventral neurons some of which are postsynaptic to amphid sensory neurons and whose cell bodies are close to the amphid commissure.

A caveat to this analysis is that none of the VAB-1 or EFN-1 tissue-specific transgenes fully rescue the corresponding mutant defects. As amphid or AWB-specific expression of ABL-1 fully rescued *abl-1* defects, these promoters are likely expressed early enough to function during axon guidance. We therefore suspect that the incomplete transgenic rescues are because VAB-1 and EFN-1 are required either in multiple tissues or in a complex subset of neurons, and that pan-neural or pan-amphid expression does not sufficiently recapitulate these patterns to fully rescue the mutant defect.

VAB-1 and phosphatidylinositol 3-kinase signaling in axon guidance

PI3K signaling is a key regulator of axon guidance in many organisms. Eph receptors can physically interact with the p85 subunit of phosphatidylinositol 3-kinase (PI3K)(PANDEY *et al.* 1994), as well as transmit kinase-independent forward signals through a PI3K pathway (GU and PARK 2001). In *C. elegans,* ventral guidance of AVM depends on AGE-1/PI3K to properly respond to netrin and slit cues (CHANG *et al.* 2006). In addition, VAB-1 directly interacts with and inhibits PTEN in PLM axon termination (BRISBIN *et al.* 2009). Here we have shown genetic evidence that PI3-kinase signaling contributes to amphid axon guidance and may function in a VAB-1 kinase-independent

manner. *vab-1(kd)* phenotypes are enhanced by loss of function in PI3K and suppressed by loss of function in DAF-18/PTEN. *age-1* mutations enhance both *vab-1(kd)* and the *vab-1* null mutant, indicating PI3K signals do not solely act in the VAB-1 pathway.

Our results are overall consistent with the model that VAB-1 promotes PI3K signaling, either by inhibiting DAF-18 or promoting PI3K activity. Loss of function in the PI3K target DAF-16/FOXO also suppresses *vab-1* guidance defects. Unexpectedly, loss of function in PIP_3-regulated kinases such as AKT-1, SGK-1, or PDK-1 also suppressed *vab-1(kd)* defects. The downstream mechanisms of PI3K signal transduction in axon guidance may differ from those involved in dauer formation or aging.

The role of ABL-1 in VAB-1 signaling

We have shown that the Src family tyrosine kinase ABL-1 promotes amphid axon guidance, likely downstream of VAB-1 signaling. So far, *C. elegans abl-1* has only been indirectly implicated in axon guidance (FOX *et al.* 2005); our results provide the first functional evidence for this. In mammalian neurons Abl has been shown to mediate EphA dependent axon repulsion (HARBOTT and NOBES 2005). The simplest of interpretation of our findings in *C. elegans* is that ABL-1 promotes attractive responses to guidance cues. ABL-1 appears to be required in a kinase-independent and EFN-1-independent branch of VAB-1 signaling. ABL-1 might be activated by a non-ephrin ligand, or by a ligand-independent activity of VAB-1 as discussed above. In mammalian cells Abl can interact with Eph receptors in multiple ways. In breast cancers EphB4 can directly interact with Abl, dependent on ligand and kinase activity (NOREN *et al.* 2006). Eph receptors can also interact with Abl independent of Eph kinase activity (YU *et al.* 2001). Although the ABL-1 SH2 domain did not interact with VAB-1 in two-hybrid

assays (MOHAMED *et al.* 2012), ABL-1 might interact with VAB-1 indirectly, or via one of the other modes described by Yu et al. Further work will be required to determine the mechanism by which ABL-1 might mediate VAB-1 signals.

Our finding that PI3K and ABL-1 act as parallel outputs in VAB-1-mediated axon guidance (**Fig 2.7A**) is interesting in light of evidence that EphB2 signaling in intestinal stem cells also involves PI3K and Abl signals (GENANDER *et al.* 2009). EphB2 regulates cell positioning in a kinase-independent pathway via PI3K, and regulates cell proliferation via a kinase-dependent Abl pathway. Although our results are more compatible with ABL-1 functioning in a kinase-independent forward signaling pathway, these comparisons suggest Eph signaling operates via a small number of signaling cascades whose outputs are ultimately cell type specific.

Eph signaling has unexpected left-right asymmetry in axon guidance

It is now well established that amphid neurons display extensive left-right asymmetry in function and in structure. Such asymmetry can be stochastic, as in AWC receptor expression (TROEMEL *et al.* 1999), or biased, as in ASE receptor expression, sensory function, and axon diameter (BARGMANN and HORVITZ 1991; CHANG *et al.* 2003; GOLDSMITH *et al.* 2010; PIERCE-SHIMOMURA *et al.* 2001). Left-right asymmetry in axon outgrowth has been reported in AIY amphid interneurons (BERTRAND *et al.* 2011). Our findings are the first evidence that amphid neurons also display biased asymmetry in their axon guidance.

vab-1 and *efn* mutants display a consistent and significant left-hand bias in defects. This bias has been seen in multiple neuron types and may extend to all amphid sensory neurons. The inability of the left-to-right fate transformation in *lsy-6* mutants to

alter this bias is suggestive that the bias reflects one or more asymmetric signaling cues. Although these studies do not directly address the signaling environment at the time of axon guidance, they are consistent with ephrins playing asymmetric roles. As *vab-1* null mutants also display asymmetry, one inference would be that other non-ephrin cues must also be asymmetric and that this is revealed in the absence of VAB-1. However no obvious asymmetry has been found in the expression or function of the two other main pathways in amphid axon guidance, netrin and SAX-3/Robo.

Our results imply a differential reliance on kinase-dependent or kinase-independent signaling on the left and right sides (**Fig 2.7B**). As over 90% of aberrantly guided axons in *vab-1(kd)* mutants are on the left, the kinase-dependent pathway seems to be most important in left side outgrowth. Loss of *efn-2* improves left hand guidance of *vab-1(kd)*, indicating EFN-2 is inhibitory in this context. However, in animals lacking EFN-1, loss of EFN-2 exacerbates left-hand guidance defects and improves right-hand defects. In the absence of EFN-1, EFN-2 may play a positive role in left-hand guidance.

Axons in the amphid commissure may be guided by pioneer neurons

A prime question in analyzing guidance of an axon bundle such as the amphid commissure is the extent to which axons are guided independently or by fasciculation with pioneer axons (LEE *et al.* 1997). The all-or-nothing nature of amphid commissure guidance defects has been previously noted (BULOW *et al.* 2002), and suggests amphid axons might follow single pioneer axons. Our analysis extends this picture in that ABL-1 overexpression in a single neuron, AWB, is not only able to rescue guidance of that neuron cell autonomously, but also non-autonomously rescues guidance of other amphid neurons. It is possible that AWB is normally a pioneer axon whose guidance determines

the direction of the commissure. Alternatively, ABL-1 overexpression may sensitize or otherwise give a growth advantage to AWB such that it is able to assume a pioneer function that it does not normally have. An important future goal will be to examine the dynamics of amphid axon outgrowth in these genetic backgrounds.

Materials and Methods

Strains and culture conditions

Worms were cultured on *E. coli* OP50 seeded NGM agar plates. Animals were grown and analyzed at room temperature (21-23°) with the exception of *pdk-1(sa709)* strains, which were analyzed at 22.5°, and *age-1(hx546)* and *aap-1(m889)*, which were analyzed at 25°. The following mutants were used: **LGI:** *unc-40(e1430); aap-1(m889); shc-1(ok198); src-1(cj293), src-2(ok819), vpr-1(tm1411), daf-16(mu86), goa-1(sa734)* **LGII:** *vab-1(ju8, e2027, ju307, ok1699, dx14, dx31, ju220, ju275, e858, e699, ju306, tn2, e118, zd118, e2, ju63, ju426, e116, ju22, e1063, qa2211), ephx-1(ok494), tag-341(ok1498), age-1(hx546), shc-2(tm328), cog-1(sy275)* **LGIII:** *ina-1(gm144), mig-10(ct41)*. **LGIV:** *efn-1(e96, ju90), efn-2(ev658), arf-6(tm1447), daf-18(ok480), rga-5(ok2241), jac-1(ok3000), ngn-1(ok2200)* **LGV:** *akt-1(ok525); lsy-6(ot71); fmi-1(tm306)* **LGX:** *efn-3(ev696), abl-1(ok171), sax-3(ky123), git-1(tm1962), gap-2(tm748), nck-1(ok694), wrk-1(ok695), trk-1(tm3985, tm4054), akt-2(ok393, tm812), unc-6(ev400), sgk-1(ok538, ft15), pdk-1(mg142, sa709)*. Published transgenes used: P*str-1*-GFP(*kyIs104)* (TROEMEL *et al.* 1997); P*str-3*-GFP(*kyIs128*) (ZALLEN *et al.* 1999), P*gcy-5*-GFP(*ntIs1*)(ALTUN-GULTEKIN *et al.* 2001), Pgcy-*7*-GFP(*otIs3*) (CHANG *et al.* 2003),

P*gcy-8*-GFP*(oyIs17)* (SATTERLEE *et al.* 2001), P*vab-1*-Venus*(evIs190*) (IKEGAMI *et al.* 2012).

Scoring of amphid axon guidance and dendrite extension

To visualize amphid neuron morphology we used dye filling (HEDGECOCK *et al.* 1985). To visualize individual neurons we used transgenic markers labeling single amphid neuron types. We immobilized L4 stage hermaphrodites using 1% phenoxy-1-propanol in M9 and scored the morphology of 100-200 neurons per genotype under compound microscopy. In the wild type essentially 100% of amphid axons extend ventrally in the commissure and then turn anteriorly into the nerve ring. We classified amphid axon guidance as Normal, Lateral, or Other. The "other" category was rare (<5%) and only used if no axon was visible. As far as possible we scored the initial guidance of the axon even if it changed direction subsequently; such changes in direction were rare. For screening, mutations were crossed into the *vab-1(e118)* kinase-dead background. To assess significance of differences in proportions we used the Fisher exact test or the chi-squared test.

Transgenic rescue of *vab-1* and *efn-1* phenotypes

To assess rescue of the *vab-1* phenotypes, transgenic lines containing *vab-1* genomic cosmid DNA (M03A1; pRF4 coinjection marker) (GEORGE *et al.* 1998), fosmid DNA (WRM0617bA10 in *juEx2870)* or the rescuing VAB-1::GFP minigene (pCZ55) (GEORGE *et al.* 1998) were generated. These lines were crossed into the *vab-1(e2027); kyIs104* background and scored for rescue of guidance defects. Similarly, a transgene containing wild type *efn-1* genomic DNA (pCZ126), as well as a rescuing GFP::EFN-1

fusion (pCZ131 in *juIs52)*(CHIN-SANG *et al.* 1999) were crossed into the *efn-1(e96); kyIs104* mutant background.

Tissue specific rescue experiments

We amplified full length coding sequences and 3'UTRs from cDNA clones yk497d6 (VAB-1A), yk338g11 (EFN-1), yk708d1 (EFN-2), yk1482h02 (ABL-1A), and yk1500a12 (AAP-1) and cloned them into pCR8 to create Gateway entry clones pCZGY1146, pCZGY1145, pCZGY1148, pCZGY1835, and pCZGY1834. All entry clones were sequenced. We used the following tissue specific promoters: *unc-33* and *rgef-1* (ALTUN-GULTEKIN *et al.* 2001), *unc-119* (MADURO and PILGRIM 1995), *myo-2* (FROKJAER-JENSEN *et al.* 2006), *dyf-7* (HEIMAN and SHAHAM 2009), *lin-26* (LABOUESSE *et al.* 1994), *str-1* (TROEMEL *et al.* 1997), and *hlh-17* (YOSHIMURA *et al.* 2008). After recombination with entry vectors containing the desired cDNA, final constructs were injected into wild type (N2) worms at 1 ng/µl together with 15 ng/µl *sur-5*-mCherry as a co-injection marker; see Appendix A for list of clones and transgenes. Each transgene was crossed into the relevant mutant background; at least two transgenes per construct were scored, and representative lines are reported.

Expression Analysis

To determine cellular expression patterns of VAB-1 and EFN-1, we examined animals expressing the rescuing transgenes *juIs24* (VAB-1::GFP), *juIs52* (EFN-1::GFP), and the *vab-1* transcriptional reporters *juEx101* and *evIs190*. To examine fixed animals we performed fixation and staining as described (Finney and Ruvkun, 1990). Fixed animals were incubated with rabbit anti-GFP polyclonal (A11122, Invitrogen, 1:1000

dilution) and mouse anti-AJM-1 monoclonal (MH27, 1:500) overnight at 4° and staining visualized with appropriate 2° antibodies.

Acknowledgements

We thank Max Heiman, Joe Culotti, and Ian Chin-Sang for reagents. We thank Nese Cinar, Jennifer Gotenstein, and Andy Nguyen for help with strain constructions. Deletion mutations were generated by the *C. elegans* Gene Knockout Consortium and the Japan National Bioresource Project. Some mutations were provided by the *Caenorhabditis* Genetics Center, which is funded by the NIH Office of Research Infrastructure Programs (P40 OD010440). E.N.G. was supported by the 27 UCSD/Salk Training Grant in Developmental Biology of Neural Diseases (T32 HD007495). Supported by an award from the US Public Health Service (NIH R01 GM054657) to A.D.C.

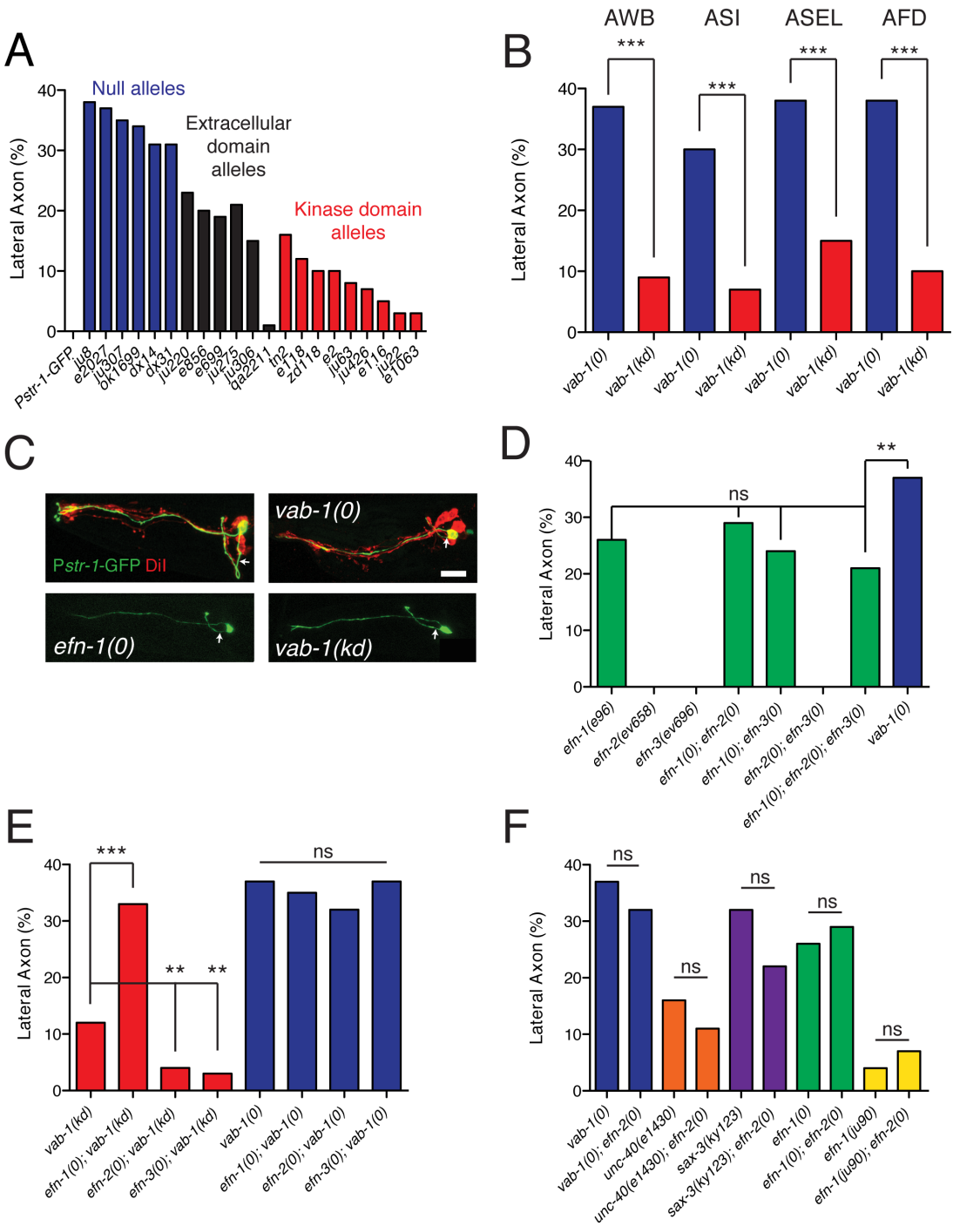

Figure 2.1 Ventral guidance of amphid commissure axons is dependent on EFN-1-VAB-1 signaling. (A) Quantitation of AWB guidance defects in Eph receptor mutants (C) Amphid axon guidance in *vab-1* and *efn-1* mutants; AWB (P*str-1*-GFP, green) and DiI staining (red). Confocal projections; anterior, left; Dorsal, up. Scale, 10µm. Arrows indicate axon extending from cell body. (D) Quantitation of AWB guidance defects in *efn* mutants and double mutants. (E) Quantitation of guidance defects in double mutants between each ligand and the *vab-1(e118)* kinase dead receptor strain, or doubles between each ligand and the receptor null *vab-1(e2027)*. Statistics, Fisher exact test: *, $P < 0.05$; **, $P < 0.01$; ***, $P < 0.001$.

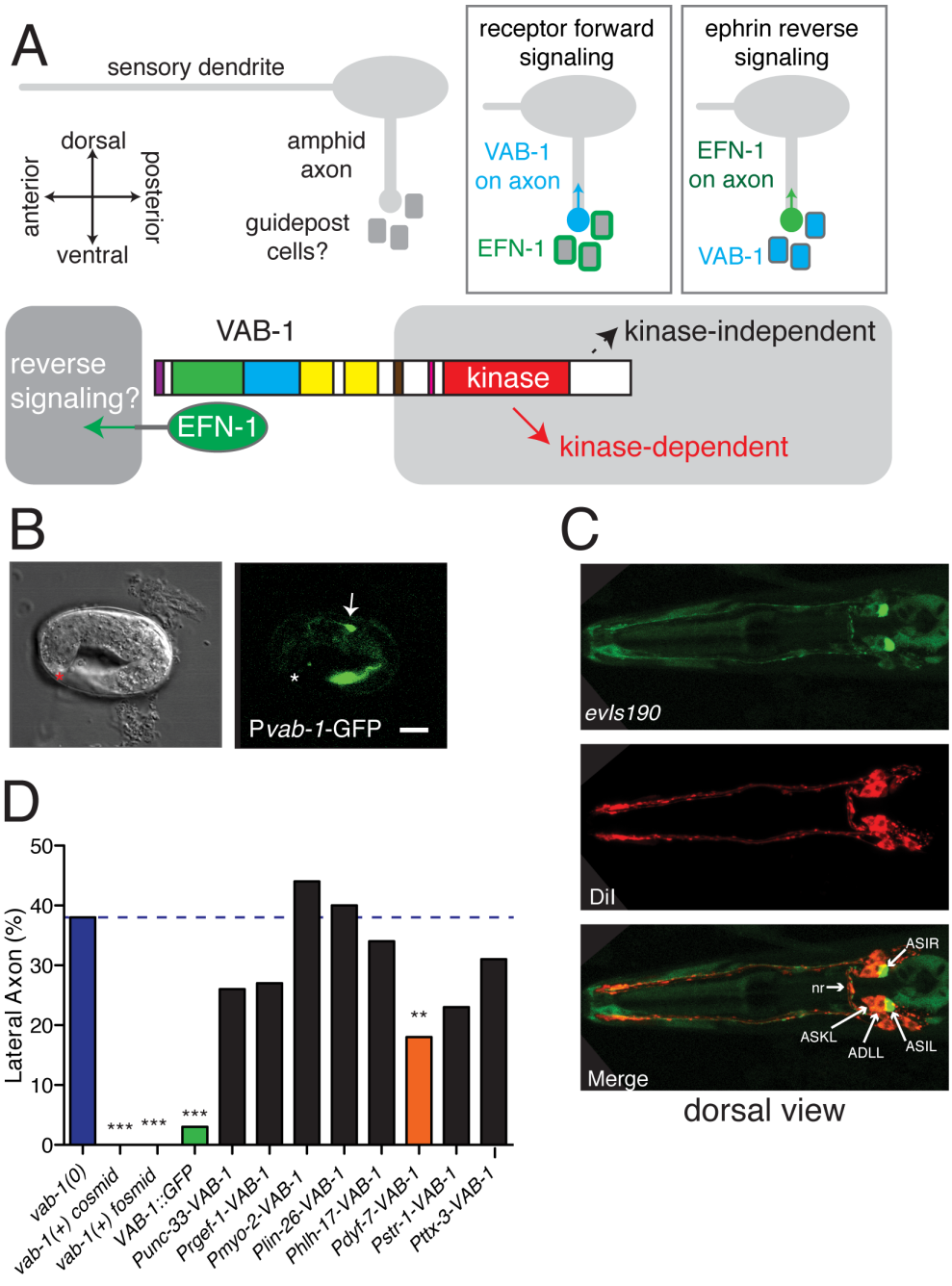

Figure 2.2 Expression and tissue-specific rescue of VAB-1 (A) Model for location of VAB-1 and ephrins in amphid axon guidance. (B) P*vab-1*-Venus (*evIs190*) expression in putative amphid neurons in embryos. Anterior tip of the head indicated by asterisk. Scale, 10µm. (C) *evIs190* expression in ASI amphid neurons, dorsal view. (D) Tissue and cell specific rescue of *vab-1* guidance defects. All transgenic rescue assays were conducted in *vab-1(e2027); kyIs104* mutant background. Asterisks indicate significant differences from *vab-1* single mutant by Fisher exact test: *, $P < 0.05$; **, $P < 0.01$; ***, $P < 0.001$.

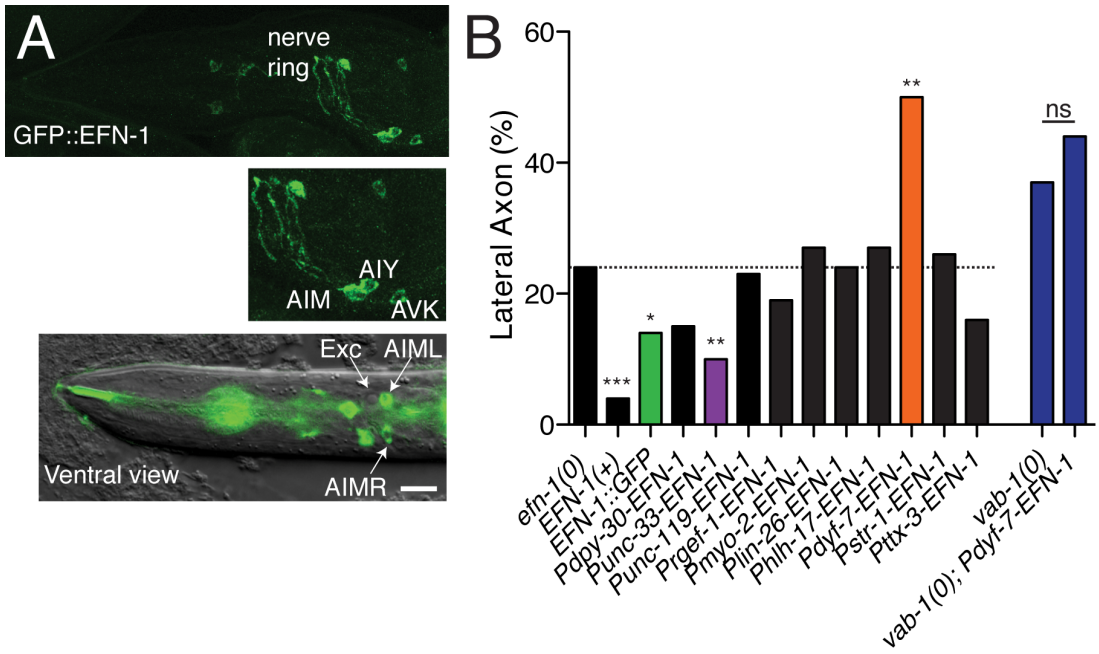

Figure 2.3 EFN-1 expression and tissue specific rescue (A) EFN-1::GFP (*juIs52*) expression in larvae and adults. EFN-1::GFP is expressed in a small number of anterior neurons, identified as AIM, AIY, and AVK. Scale, 10µm. (B) Tissue and cell specific rescue of *efn-1* axon guidance defects, scored in the *efn-1(e96); kyIs104* background. Asterisks indicate significant difference from *efn-1* single mutant defects, by Fisher exact test.*, $P < 0.05$; **, $P < 0.01$; ***, $P < 0.001$.

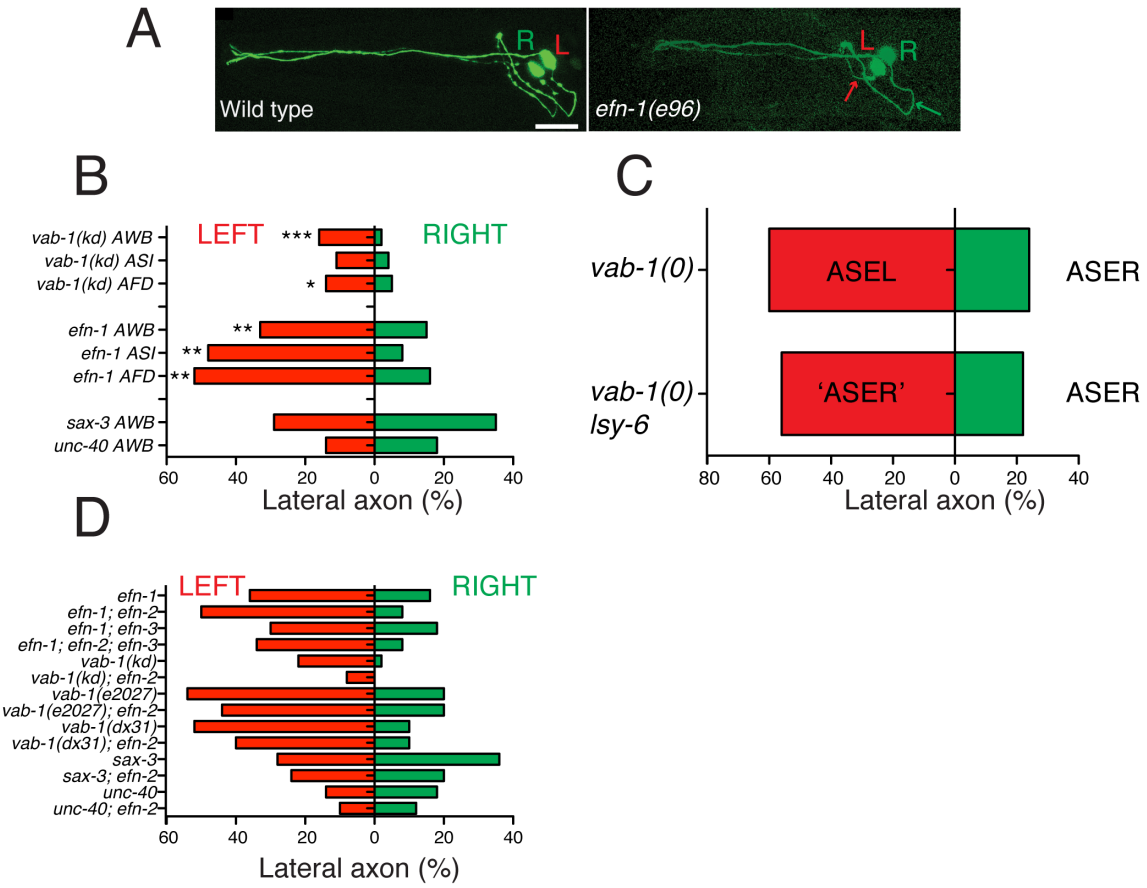

Figure 2.4 Ephrin signaling has asymmetric requirements in amphid commissure guidance (A) Amphid outgrowth defects display left-hand bias; representative example from *efn-1(e96)*. Scale, 10 µm. (B) Quantitation of axon guidance defects in left versus right hand AWB, ASI or AFD axons in *efn-1* or *vab-1(e118)* mutants. *unc-40* and *sax-3* display symmetric guidance defects in AWB. Red bars are left side axons and green bars right. (C) Transformation of ASEL into an ASER-like fate by *lsy-6* does not alter the left-hand bias in guidance defects in *vab-1(e2027)* background. (D) Loss of *efn-2* function increases asymmetry of *efn-1* mutants but decreases penetrance and asymmetry in *vab-1(kd)*.

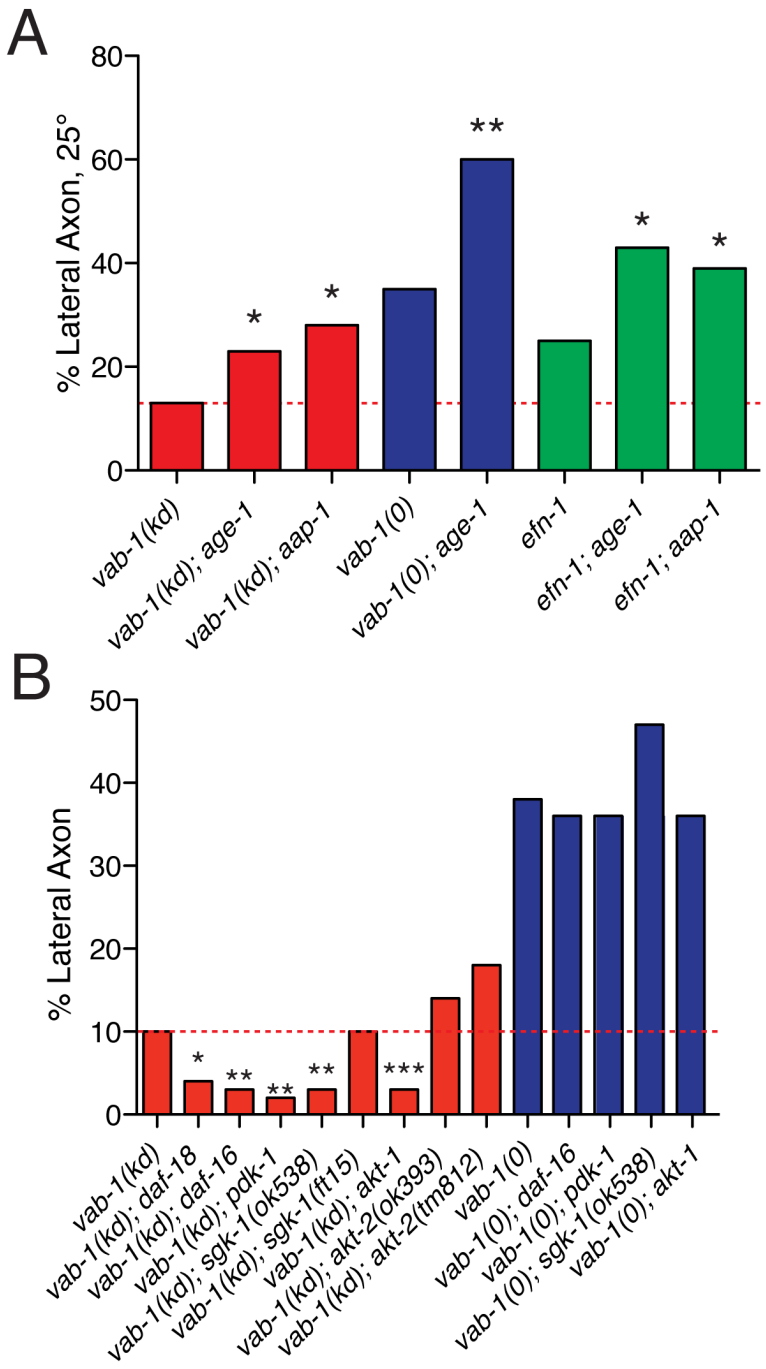

Figure 2.5 Phosphatidylinositol 3-kinase signaling promotes amphid axon guidance. (A) Enhancement of *vab-1(kd)* amphid axon guidance defects by reduction of function in PI3-kinase activity. *age-1* and *aap-1* were tested at 25°. Significance is relative to the single *vab-1(kd)* mutant (red dashed line). (B) Loss of function in *daf-18*/PTEN, *daf-16*/FOXO and in downstream PI3K signaling kinases suppresses *vab-1(kd)* guidance defects. Statistics, Fisher exact test: *, $P < 0.05$; **, $P < 0.01$; ***, $P < 0.001$.

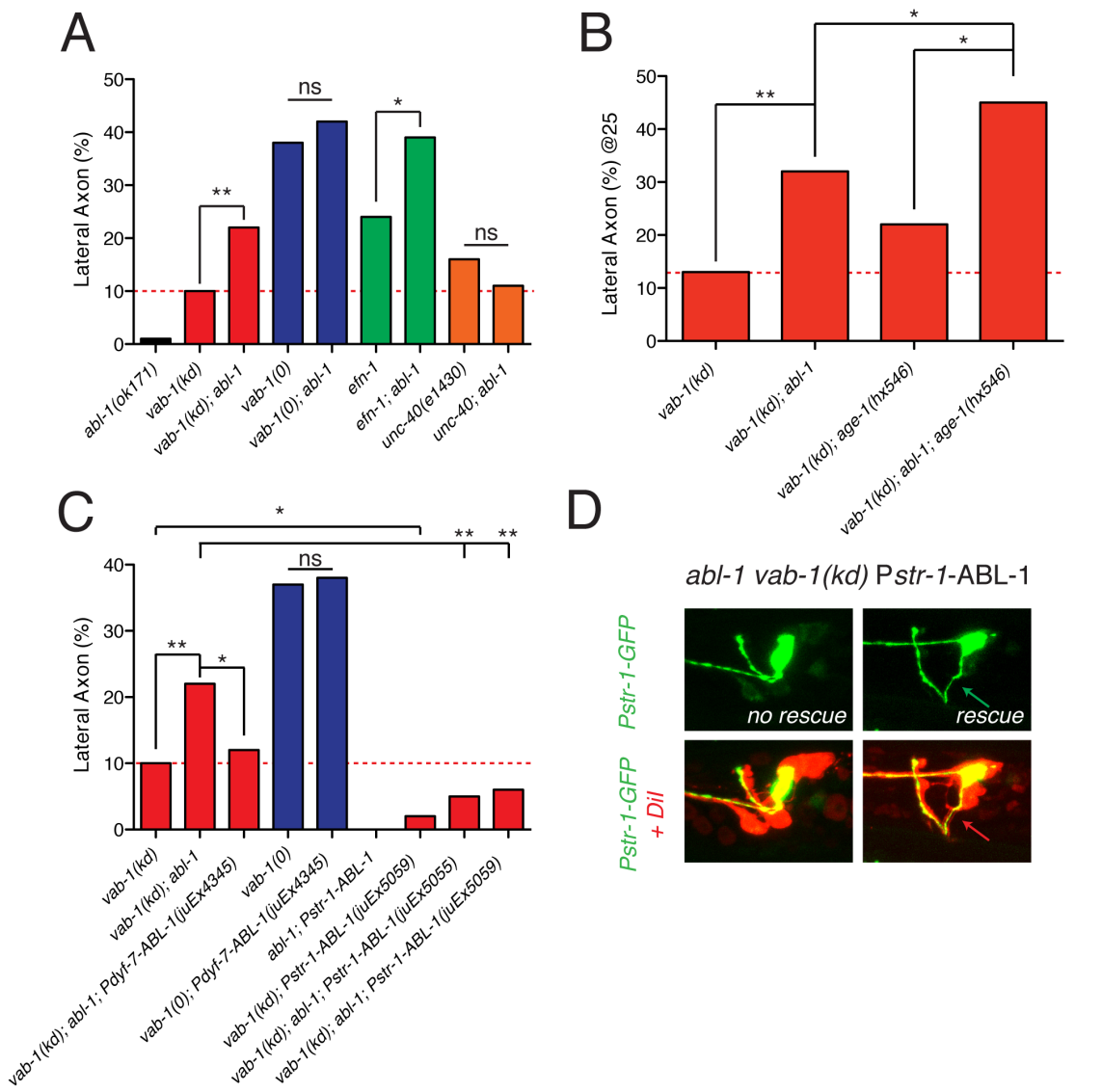

Figure 2.6 ABL-1 signals in VAB-1-dependent amphid axon guidance (A) Quantification of amphid axon guidance defects in *abl-1* mutants. (B) Synergism of guidance defects in the *vab-1(kd) abl-1 age-1* triple mutant indicates ABL-1 and PI3K act in parallel and are redundant with VAB-1 kinase signaling. (C) *dyf-7* driven (pan-amphid) expression of ABL-1 rescues *abl-1* enhancement of *vab-1(kd)* guidance defects but not *vab-1(0)* defects. *str-1*-driven AWB-specific expression of ABL-1 suppresses the *vab-1(kd) abl-1(ok171)* double mutant and the *vab-1(kd)* single mutant. (D) Rescue of guidance of multiple amphid axons by expression of ABL-1 in AWB. Images of *vab-1(kd); abl-1;* P*str-1*-ABL-1*(juEx5059) kyIs104* transgenic animals with other amphid axons visualized by DiI staining. Guidance of AWB correlates with guidance of other amphid axons in non-rescued and rescued animals (N > 50 axons). Statistics, Fisher exact test: *, $P < 0.05$; **, $P < 0.01$; ***, $P < 0.001$.

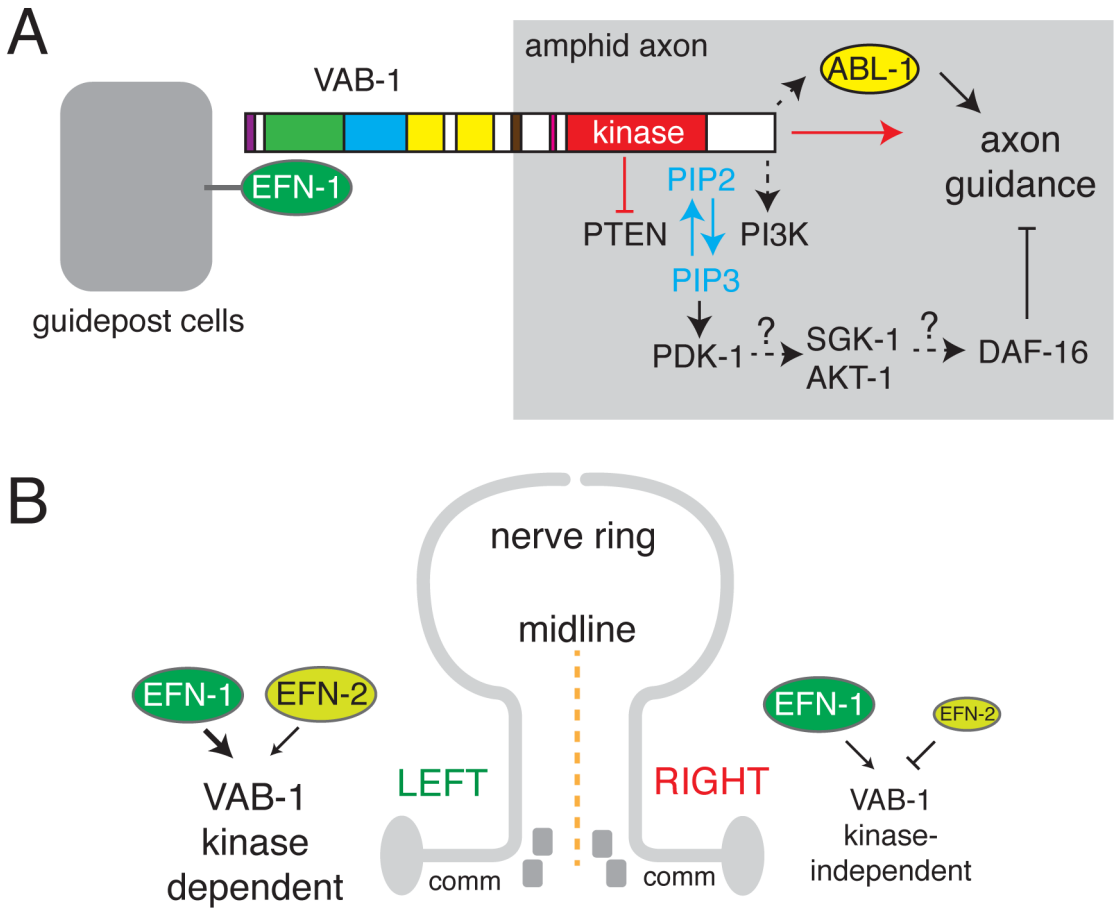

Figure 2.7 Models of Eph signaling in amphid axon guidance (A) Possible relationships between EFN-1, VAB-1 and the PI3K and ABL-1 pathways in axon guidance. (B) Model for the left-right asymmetry. Amphid guidance on the left side of the animal is primarily mediated by a VAB-1 kinase-dependent signaling pathway. In the presence of EFN-1, EFN-2 is inhibitory. In the absence of EFN-1, EFN-2 can promote signaling. The right side relies mostly on a kinase-independent signaling mechanism that is inhibited by EFN-2.

Table 2.1 Candidate Genes in Kinase-Independent Eph Pathway

	Single Mutant Lateral Axon (%)	**Double *vab-1(kd)* Mutant Lateral Axon (%)**	**Compound vs *vab-1(kd)* (p-value)**	**Mammalian Homologs**
vab-1(e118)	-	12%	-	
Class I: Suppressors of *vab-1(kd)*				
pdk-1(sa709)	0%	2%	**0.005, N=100	PDK
akt-1(ok525)	0%	3%	***0.0009, N=200	Akt/PKB
sgk-1(ok538)	0%	3%	**0.002, N=160	SGK/serum-and glucocorticoid-inducible kinase
daf-16(mu86)	0%	3%	**0.003, N=200	FOXO
efn-3(ev696)	0%	3%	**0.008, N=134	ephrin-A ligands
efn-2(ev658)	0%	4%	**0.006, N=268	ephrin-A ligands
egl-19(ad695gf)	0%	4%	*0.024, N=164	VGCC a subunit
daf-18(ok480)	0%	4%	*0.036, N=100	PTEN
Class II: Specific Enhancers of *vab-1(kd)*				
efn-1(e96)	26%	33%	***0.0001, N=122	ephrin-A ligands
abl-1(ok171) @ 25C	0%	32%	**0.002, N=100	Abl/Abelson kinase
abl-1(ok171)	1%	22%	**0.008, N=100	Abl/Abelson kinase
aap-1(m889) @25C	0%	28%	*0.041, N=50	PI3K *p50/p55*
age-1(hx546) @25C	0%	23%	*0.038, N=130	PI3K *p110*

Table 2.1 continued

	Single Mutant Lateral Axon Phenotype (%)	Double *vab-1(kd)* Mutant Lateral Axon Phenotype (%)	Compound vs *vab-1(kd)* (p-value)	Mammalian Homologs
Class III: Non-specific enhancers of *vab-1(kd)*				
ngn-1(ok2200)	32%	50%	***0.0001, N=100	Neurogenin
mig-10(ct41)	2%	22%	*0.05, N=200	Lamellipodin
Class IV: No significant change				
ina-1(gm144)	3%	11%	0.825, N=100	alpha integrin subunit
git-1(tm1962)	0%	8%	0.355, N=100	GIT1
arf-6(tm1447)	0%	11%	0.825, N=100	ARF6
nck-1(ok694)	0%	14%	0.834, N=100	NCK adapter protein
shc-1(ok198)	0%	8%	0.347, N=100	Shc proteins
shc-2(tm328)	1%	-	-	Shc proteins
ephx-1(ok494)	0%	15%	0.683, N=100	Ephexin
rga-5(ok2241)	0%	12%	1.0, N=100	Rho GTPase Activating protein
gap-2(tm748)	0%	-	-	nGAP/synGAP
vpr-1(tm1411)	0%	-	-	VAPB
wrk-1(ok695)	0%	9%	0.490, N=100	Wrapper/Rega-1/Klingon
trk-1(tm3895)	0%	14%	0.822, N=72	TRK neurotrophin receptor
trk-1(tm4054)	0%	6%	0.139; N=100	TRK neurotrophin receptor

Table 2.1 continued

	Single Mutant Lateral Axon Phenotype (%)	**Double *vab-1(kd)* Mutant Lateral Axon Phenotype (%)**	**Compound vs *vab-1(kd)* (p-value)**	**Mammalian Homologs**
src-1(cj293)	0%	-	-	Src family kinase member
src-2(ok819)	0%	12%	1.0, N=50	Src family kinase member
egl-19(n2368cs)	4%	6%	0.138, N=100	VGCC a subunit
jac-1(ok3000)	0%	5%	0.125, N=100	*p120* catenin
tag-341(ok1498)	1%	5%	0.056, N=200	F-BAR and RhoGAP domains
akt-2(ok393)	0%	14%	0.836, N=100	Akt/PKB
akt-2(tm812)	0%	18%	0.326, N=100	Akt/PKB
lsy-6(ot71)	0%	19%	0.248, N=100	N/A
*cog-1(sy275)**	5%	-	-	Nkx6 homeodomain protein
wsp-1(gm324)	0%	10%	0.652, N=100	N-WASP
goa-1(sa734)	1%	sterile	-	heterotrimeric G protein alpha subunit Go (Go/Gi class)
fmi-1(tm306)	7%	-	-	Celsr/Flamingo
efn-4(bx80)	3%	-	-	ephrin-A ligands
kdin-1(ok750)	0%	-	-	ARMS

References

ALTUN-GULTEKIN, Z., Y. ANDACHI, E. L. TSALIK, D. PILGRIM, Y. KOHARA and O. HOBERT, 2001 A regulatory cascade of three homeobox genes, *ceh-10*, *ttx-3* and *ceh-23*, controls cell fate specification of a defined interneuron class in *C. elegans*. Development **128:** 1951-1969.

BACAJ, T., M. TEVLIN, Y. LU and S. SHAHAM, 2008 Glia are essential for sensory organ function in *C. elegans*. Science **322:** 744-747.

BARGMANN, C. I., and H. R. HORVITZ, 1991 Chemosensory neurons with overlapping functions direct chemotaxis to multiple chemicals in *C. elegans*. Neuron **7:** 729-742.

BASHAW, G. J., T. KIDD, D. MURRAY, T. PAWSON and C. S. GOODMAN, 2000 Repulsive axon guidance: Abelson and Enabled play opposing roles downstream of the roundabout receptor. Cell **101:** 703-715.

BERTRAND, V., P. BISSO, R. J. POOLE and O. HOBERT, 2011 Notch-dependent induction of left/right asymmetry in *C. elegans* interneurons and motoneurons. Curr Biol **21:** 1225-1231.

BONANOMI, D., O. CHIVATAKARN, G. BAI, H. ABDESSELEM, K. LETTIERI, T. MARQUARDT, B. A. PIERCHALA and S. L. PFAFF, 2012 Ret is a multifunctional coreceptor that integrates diffusible- and contact-axon guidance signals. Cell **148:** 568-582.

BOULIN, T., R. POCOCK and O. HOBERT, 2006 A novel Eph receptor-interacting IgSF protein provides *C. elegans* motoneurons with midline guidepost function. Curr Biol **16:** 1871-1883.

BRANTLEY-SIEDERS, D. M., J. CAUGHRON, D. HICKS, A. POZZI, J. C. RUIZ and J. CHEN, 2004 EphA2 receptor tyrosine kinase regulates endothelial cell migration and vascular assembly through phosphoinositide 3-kinase-mediated Rac1 GTPase activation. J Cell Sci **117:** 2037-2049.

BRISBIN, S., J. LIU, J. BOUDREAU, J. PENG, M. EVANGELISTA and I. CHIN-SANG, 2009 A role for *C. elegans* Eph RTK signaling in PTEN regulation. Dev Cell **17:** 459-469.

BRUCKNER, K., J. PABLO LABRADOR, P. SCHEIFFELE, A. HERB, P. H. SEEBURG and R. KLEIN, 1999 EphrinB ligands recruit GRIP family PDZ adaptor proteins into raft membrane microdomains. Neuron **22:** 511-524.

BULOW, H. E., K. L. BERRY, L. H. TOPPER, E. PELES and O. HOBERT, 2002 Heparan sulfate proteoglycan-dependent induction of axon branching and axon misrouting by the Kallmann syndrome gene *kal-1*. Proc Natl Acad Sci U S A **99:** 6346-6351.

CARVALHO, R. F., M. BEUTLER, K. J. MARLER, B. KNOLL, E. BECKER-BARROSO, R. HEINTZMANN, T. NG and U. DRESCHER, 2006 Silencing of EphA3 through a cis interaction with ephrinA5. Nature neuroscience **9:** 322-330.

CATCHPOLE, T., and M. HENKEMEYER, 2011 EphB2 tyrosine kinase-dependent forward signaling in migration of neuronal progenitors that populate and form a distinct region of the dentate niche. J Neurosci **31:** 11472-11483.

CATTERALL, W. A., 2000 Structure and regulation of voltage-gated Ca2+ channels. Annu Rev Cell Dev Biol **16:** 521-555.

CHANG, C., C. E. ADLER, M. KRAUSE, S. G. CLARK, F. B. GERTLER, M. TESSIER-LAVIGNE and C. I. BARGMANN, 2006 MIG-10/lamellipodin and AGE-1/PI3K promote axon guidance and outgrowth in response to slit and netrin. Curr Biol **16:** 854-862.

CHANG, S., R. J. JOHNSTON, JR. and O. HOBERT, 2003 A transcriptional regulatory cascade that controls left/right asymmetry in chemosensory neurons of *C. elegans*. Genes Dev **17:** 2123-2137.

CHENG, H., J. A. GOVINDAN and D. GREENSTEIN, 2008 Regulated trafficking of the MSP/Eph receptor during oocyte meiotic maturation in *C. elegans*. Curr Biol **18:** 705-714.

CHIN-SANG, I. D., S. E. GEORGE, M. DING, S. L. MOSELEY, A. S. LYNCH and A. D. CHISHOLM, 1999 The ephrin VAB-2/EFN-1 functions in neuronal signaling to regulate epidermal morphogenesis in *C. elegans*. Cell **99:** 781-790.

CHIN-SANG, I. D., S. L. MOSELEY, M. DING, R. J. HARRINGTON, S. E. GEORGE and A. D. CHISHOLM, 2002 The divergent *C. elegans* ephrin EFN-4 functions inembryonic morphogenesis in a pathway independent of the VAB-1 Eph receptor. Development **129:** 5499-5510.

CHRISTENSEN, R., L. DE LA TORRE-UBIETA, A. BONNI and D. A. COLON-RAMOS, 2011 A conserved PTEN/FOXO pathway regulates neuronal morphology during *C. elegans* development. Development **138:** 5257-5267.

CONCHA, M. L., I. H. BIANCO and S. W. WILSON, 2012 Encoding asymmetry within neural circuits. Nat Rev Neurosci **13:** 832-843.

CONCHA, M. L., I. A. SIGNORE and A. COLOMBO, 2009 Mechanisms of directional asymmetry in the zebrafish epithalamus. Semin Cell Dev Biol **20:** 498-509.

COWAN, C. A., N. YOKOYAMA, L. M. BIANCHI, M. HENKEMEYER and B. FRITZSCH, 2000 EphB2 guides axons at the midline and is necessary for normal vestibular function. Neuron **26:** 417-430.

DAVIS, S., N. W. GALE, T. H. ALDRICH, P. C. MAISONPIERRE, V. LHOTAK, T. PAWSON, M. GOLDFARB and G. D. YANCOPOULOS, 1994 Ligands for EPH-related receptor tyrosine kinases that require membrane attachment or clustering for activity. Science **266:** 816-819.

DAVY, A., N. W. GALE, E. W. MURRAY, R. A. KLINGHOFFER, P. SORIANO, C. FEUERSTEIN and S. M. ROBBINS, 1999 Compartmentalized signaling by GPI-anchored ephrin-A5 requires the Fyn tyrosine kinase to regulate cellular adhesion. Genes Dev **13:** 3125-3135.

DENG, X., E. R. HOFMANN, A. VILLANUEVA, O. HOBERT, P. CAPODIECI, D. R. VEACH, X. YIN, L. CAMPODONICO, A. GLEKAS, C. CORDON-CARDO, B. CLARKSON, W. G. BORNMANN, Z. FUKS, M. O. HENGARTNER and R. KOLESNICK, 2004 *Caenorhabditis elegans* ABL-1 antagonizes p53-mediated germline apoptosis after ionizing irradiation. Nat Genet **36:** 906-912.

DRESCHER, U., C. KREMOSER, C. HANDWERKER, J. LOSCHINGER, M. NODA and F. BONHOEFFER, 1995 In vitro guidance of retinal ganglion cell axons by RAGS, a 25 kDa tectal protein related to ligands for Eph receptor tyrosine kinases. Cell **82:** 359-370.

EGEA, J., and R. KLEIN, 2007 Bidirectional Eph-ephrin signaling during axon guidance. Trends Cell Biol **17:** 230-238.

FORSTHOEFEL, D. J., E. C. LIEBL, P. A. KOLODZIEJ and M. A. SEEGER, 2005 The Abelson tyrosine kinase, the Trio GEF and Enabled interact with the Netrin receptor Frazzled in *Drosophila*. Development **132:** 1983-1994.

FOX, R. M., S. E. VON STETINA, S. J. BARLOW, C. SHAFFER, K. L. OLSZEWSKI, J. H. MOORE, D. DUPUY, M. VIDAL and D. M. MILLER, 3RD, 2005 A gene expression fingerprint of *C. elegans* embryonic motor neurons. BMC genomics **6:** 42.

FRANK, C. A., J. PIELAGE and G. W. DAVIS, 2009 A presynaptic homeostatic signaling system composed of the Eph receptor, ephexin, Cdc42, and CaV2.1 calcium channels. Neuron **61:** 556-569.

FROKJAER-JENSEN, C., K. S. KINDT, R. A. KERR, H. SUZUKI, K. MELNIK-MARTINEZ, B. GERSTBREIH, M. DRISCOL and W. R. SCHAFER, 2006 Effects of voltage-gated calcium channel subunit genes on calcium influx in cultured *C. elegans* mechanosensory neurons. J Neurobiol **66:** 1125-1139.

GENANDER, M., 2012 Eph and ephrins in epithelial stem cell niches and cancer. Cell Adh Migr **6:** 126-130.

GENANDER, M., M. M. HALFORD, N. J. XU, M. ERIKSSON, Z. YU, Z. QIU, A. MARTLING, G. GREICIUS, S. THAKAR, T. CATCHPOLE, M. J. CHUMLEY, S. ZDUNEK, C. WANG, T. HOLM, S. P. GOFF, S. PETTERSSON, R. G. PESTELL, M. HENKEMEYER and J. FRISEN, 2009 Dissociation of EphB2 signaling pathways mediating progenitor cell proliferation and tumor suppression. Cell **139:** 679-692.

GEORGE, S. E., K. SIMOKAT, J. HARDIN and A. D. CHISHOLM, 1998 The VAB-1 Eph receptor tyrosine kinase functions in neural and epithelial morphogenesis in *C. elegans*. Cell **92:** 633-643.

GOLDSMITH, A. D., S. SARIN, S. LOCKERY and O. HOBERT, 2010 Developmental control of lateralized neuron size in the nematode *Caenorhabditis elegans*. Neural Dev **5:** 33.

GOMEZ, T. M., D. M. SNOW and P. C. LETOURNEAU, 1995 Characterization of spontaneous calcium transients in nerve growth cones and their effect on growth cone migration. Neuron **14:** 1233-1246.

GOMEZ, T. M., and N. C. SPITZER, 1999 *In vivo* regulation of axon extension and pathfinding by growth-cone calcium transients. Nature **397:** 350-355.

GU, C., and S. PARK, 2001 The EphA8 Receptor Regulates Integrin Activity through p110ϒ Phosphatidylinositol-3 Kinase in a Tyrosine Kinase Activity-Independent Manner. Mol Cell Biol **21:** 4579-4597.

GU, C., and S. PARK, 2003 The p110 gamma PI-3 kinase is required for EphA8-stimulated cell migration. FEBS Lett **540:** 65-70.

HANSEN, M. J., G. E. DALLAL and J. G. FLANAGAN, 2004 Retinal axon response to ephrin-as shows a graded, concentration-dependent transition from growth promotion to inhibition. Neuron **42:** 717-730.

HARBOTT, L. K., and C. D. NOBES, 2005 A key role for Abl family kinases in EphA receptor-mediated growth cone collapse. Mol Cell Neurosci **30:** 1-11.

HEDGECOCK, E. M., J. G. CULOTTI, J. N. THOMSON and L. A. PERKINS, 1985 Axonal guidance mutants of *Caenorhabditis elegans* identified by filling sensory neurons with fluorescein dyes. Dev Biol **111:** 158-170.

HEIMAN, M. G., and S. SHAHAM, 2009 DEX-1 and DYF-7 establish sensory dendrite length by anchoring dendritic tips during cell migration. Cell **137:** 344-355.

HENKEMEYER, M., D. ORIOLI, J. T. HENDERSON, T. M. SAXTON, J. RODER, T. PAWSON and R. KLEIN, 1996 Nuk controls pathfinding of commissural axons in the mammalian central nervous system. Cell **86:** 35-46.

HERTWECK, M., C. GOBEL and R. BAUMEISTER, 2004 *C. elegans* SGK-1 is the critical component in the Akt/PKB kinase complex to control stress response and life span. Dev Cell **6:** 577-588.

HIMANEN, J. P., M. J. CHUMLEY, M. LACKMANN, C. LI, W. A. BARTON, P. D. JEFFREY, C. VEARING, D. GELEICK, D. A. FELDHEIM, A. W. BOYD, M. HENKEMEYER and

D. B. NIKOLOV, 2004 Repelling class discrimination: ephrin-A5 binds to and activates EphB2 receptor signaling. Nat Neurosci **7:** 501-509.

HINDGES, R., T. MCLAUGHLIN, N. GENOUD, M. HENKEMEYER and D. D. O'LEARY, 2002 EphB forward signaling controls directional branch extension and arborization required for dorsal-ventral retinotopic mapping. Neuron **35:** 475-487.

HOBERT, O., R. J. JOHNSTON, JR. and S. CHANG, 2002 Left-right asymmetry in the nervous system: the *Caenorhabditis elegans* model. Nat Rev Neurosci **3:** 629-640.

HOLLAND, S. J., N. W. GALE, G. MBAMALU, G. D. YANCOPOULOS, M. HENKEMEYER and T. PAWSON, 1996 Bidirectional signalling through the EPH-family receptor Nuk and its transmembrane ligands. Nature **383:** 722-725.

HONG, K., M. NISHIYAMA, J. HENLEY, M. TESSIER-LAVIGNE and M. POO, 2000 Calcium signalling in the guidance of nerve growth by netrin-1. Nature **403:** 93-98.

HU, T., G. SHI, L. LAROSE, G. M. RIVERA, B. J. MAYER and R. ZHOU, 2009 Regulation of process retraction and cell migration by EphA3 is mediated by the adaptor protein Nck1. Biochemistry **48:** 6369-6378.

HURWITZ, M. E., P. J. VANDERZALM, L. BLOOM, J. GOLDMAN, G. GARRIGA and H. R. HORVITZ, 2009 Abl kinase inhibits the engulfment of apoptotic [corrected] cells in *Caenorhabditis elegans*. PLoS Biol **7:** e99.

IKEGAMI, R., K. SIMOKAT, H. ZHENG, L. BROWN, G. GARRIGA, J. HARDIN and J. CULOTTI, 2012 Semaphorin and Eph receptor signaling guide a series of cell movements for ventral enclosure in *C. elegans*. Curr Biol **22:** 1-11.

IKEGAMI, R., H. ZHENG, S. H. ONG and J. CULOTTI, 2004 Integration of semaphorin-2A/MAB-20, ephrin-4, and UNC-129 TGF-beta signaling pathways regulates sorting of distinct sensory rays in *C. elegans*. Dev Cell **6:** 383-395.

JOHNSTON, R. J., and O. HOBERT, 2003 A microRNA controlling left/right neuronal asymmetry in *Caenorhabditis elegans*. Nature **426:** 845-849.

KNOLL, B., and U. DRESCHER, 2004 Src family kinases are involved in EphA receptor-mediated retinal axon guidance. J Neurosci **24:** 6248-6257.

KULLANDER, K., and R. KLEIN, 2002 Mechanisms and functions of Eph and ephrin signalling. Nat Rev Mol Cell Biol **3:** 475-486.

LABOUESSE, M., S. SOOKHAREEA and H. R. HORVITZ, 1994 The *Caenorhabditis elegans* gene *lin-26* is required to specify the fates of hypodermal cells and encodes a presumptive zinc-finger transcription factor. Development **120:** 2359-2368.

LEE, R. Y., L. LOBEL, M. HENGARTNER, H. R. HORVITZ and L. AVERY, 1997 Mutations in the alpha1 subunit of an L-type voltage-activated Ca2+ channel cause myotonia in *Caenorhabditis elegans*. EMBO J **16:** 6066-6076.

LIM, Y. S., T. MCLAUGHLIN, T. C. SUNG, A. SANTIAGO, K. F. LEE and D. D. O'LEARY, 2008 p75(NTR) mediates ephrin-A reverse signaling required for axon repulsion and mapping. Neuron **59:** 746-758.

LIN, K., J. B. DORMAN, A. RODAN and C. KENYON, 1997 *daf-16*: An HNF-3/forkhead family member that can function to double the life-span of *Caenorhabditis elegans*. Science **278:** 1319-1322.

LUGO, T. G., A. M. PENDERGAST, A. J. MULLER and O. N. WITTE, 1990 Tyrosine kinase activity and transformation potency of bcr-abl oncogene products. Science **247:** 1079-1082.

MADURO, M., and D. PILGRIM, 1995 Identification and cloning of *unc-119*, a gene expressed in the *Caenorhabditis elegans* nervous system. Genetics **141:** 977-988.

MAEKAWA, H., Y. OIKE, S. KANDA, Y. ITO, Y. YAMADA, H. KURIHARA, R. NAGAI and T. SUDA, 2003 Ephrin-B2 induces migration of endothelial cells through the phosphatidylinositol-3 kinase pathway and promotes angiogenesis in adult vasculature. Arterioscler Thromb Vasc Biol **23:** 2008-2014.

MANNING, G., 2005 Genomic overview of protein kinases. WormBook**:** 1-19.

MARLER, K. J., E. BECKER-BARROSO, A. MARTINEZ, M. LLOVERA, C. WENTZEL, S. POOPALASUNDARAM, R. HINDGES, E. SORIANO, J. COMELLA and U. DRESCHER,

2008 A TrkB/EphrinA interaction controls retinal axon branching and synaptogenesis. J Neurosci **28:** 12700-12712.

MIAO, H., D. Q. LI, A. MUKHERJEE, H. GUO, A. PETTY, J. CUTTER, J. P. BASILION, J. SEDOR, J. WU, D. DANIELPOUR, A. E. SLOAN, M. L. COHEN and B. WANG, 2009 EphA2 mediates ligand-dependent inhibition and ligand-independent promotion of cell migration and invasion via a reciprocal regulatory loop with Akt. Cancer Cell **16:** 9-20.

MILLER, M. A., and I. D. CHIN-SANG, 2012 Eph receptor signaling in *C. elegans*. WormBook**:** 1-17.

MILLER, M. A., P. J. RUEST, M. KOSINSKI, S. K. HANKS and D. GREENSTEIN, 2003 An Eph receptor sperm-sensing control mechanism for oocyte meiotic maturation in *Caenorhabditis elegans*. Genes Dev **17:** 187-200.

MING, G., H. SONG, B. BERNINGER, N. INAGAKI, M. TESSIER-LAVIGNE and M. POO, 1999 Phospholipase C-gamma and phosphoinositide 3-kinase mediate cytoplasmic signaling in nerve growth cone guidance. Neuron **23:** 139-148.

MING, G. L., H. J. SONG, B. BERNINGER, C. E. HOLT, M. TESSIER-LAVIGNE and M. M. POO, 1997 cAMP-dependent growth cone guidance by netrin-1. Neuron **19:** 1225-1235.

MOHAMED, A. M., J. R. BOUDREAU, F. P. YU, J. LIU and I. D. CHIN-SANG, 2012 The *Caenorhabditis elegans* Eph receptor activates NCK and N-WASP, and inhibits Ena/VASP to regulate growth cone dynamics during axon guidance. PLoS Genet **8:** e1002513.

MOHAMED, A. M., and I. D. CHIN-SANG, 2006 Characterization of loss-of-function and gain-of-function Eph receptor tyrosine kinase signaling in *C. elegans* axon targeting and cell migration. Dev Biol **290:** 164-176.

NOREN, N. K., G. FOOS, C. A. HAUSER and E. B. PASQUALE, 2006 The EphB4 receptor suppresses breast cancer cell tumorigenicity through an Abl-Crk pathway. Nat Cell Biol **8:** 815-825.

NOREN, N. K., and E. B. PASQUALE, 2004 Eph receptor-ephrin bidirectional signals that target Ras and Rho proteins. Cell Signal **16:** 655-666.

NOREN, N. K., N. Y. YANG, M. SILLDORFF, R. MUTYALA and E. B. PASQUALE, 2009 Ephrin-independent regulation of cell substrate adhesion by the EphB4 receptor. Biochem J **422:** 433-442.

OGG, S., S. PARADIS, S. GOTTLIEB, G. I. PATTERSON, L. LEE, H. A. TISSENBAUM and G. RUVKUN, 1997 The Fork head transcription factor DAF-16 transduces insulin-like metabolic and longevity signals in *C. elegans*. Nature **389:** 994-999.

OGG, S., and G. RUVKUN, 1998 The *C. elegans* PTEN homolog, DAF-18, acts in the insulin receptor-like metabolic signaling pathway. Mol Cell **2:** 887-893.

PANDEY, A., D. F. LAZAR, A. R. SALTIEL and V. M. DIXIT, 1994 Activation of the Eck receptor protein tyrosine kinase stimulates phosphatidylinositol 3-kinase activity. J Biol Chem **269:** 30154-30157.

PARADIS, S., M. AILION, A. TOKER, J. H. THOMAS and G. RUVKUN, 1999 A PDK1 homolog is necessary and sufficient to transduce AGE-1 PI3 kinase signals that regulate diapause in *Caenorhabditis elegans*. Genes Dev **13:** 1438-1452.

PARADIS, S., and G. RUVKUN, 1998 *Caenorhabditis elegans* Akt/PKB transduces insulin receptor-like signals from AGE-1 PI3 kinase to the DAF-16 transcription factor. Genes Dev **12:** 2488-2498.

PASQUALE, E. B., 2005 Eph receptor signalling casts a wide net on cell behaviour. Nat Rev Mol Cell Biol **6:** 462-475.

PASQUALE, E. B., 2008 Eph-ephrin bidirectional signaling in physiology and disease. Cell **133:** 38-52.

PERKINS, L. A., E. M. HEDGECOCK, J. N. THOMSON and J. G. CULOTTI, 1986 Mutant sensory cilia in the nematode *Caenorhabditis elegans*. Dev Biol **117:** 456-487.

PIERCE-SHIMOMURA, J. T., S. FAUMONT, M. R. GASTON, B. J. PEARSON and S. R. LOCKERY, 2001 The homeobox gene *lim-6* is required for distinct chemosensory representations in *C. elegans*. Nature **410:** 694-698.

PROCKO, C., and S. SHAHAM, 2010 Assisted morphogenesis: glial control of dendrite shapes. Curr Opin Cell Biol **22:** 560-565.

ROSENBERG, S. S., and N. C. SPITZER, 2011 Calcium signaling in neuronal development. Cold Spring Harb Perspect Biol **3:** a004259.

SAHIN, M., P. L. GREER, M. Z. LIN, H. POUCHER, J. EBERHART, S. SCHMIDT, T. M. WRIGHT, S. M. SHAMAH, S. O'CONNELL, C. W. COWAN, L. HU, J. L. GOLDBERG, A. DEBANT, G. CORFAS, C. E. KRULL and M. E. GREENBERG, 2005 Eph-dependent tyrosine phosphorylation of ephexin1 modulates growth cone collapse. Neuron **46:** 191-204.

SATTERLEE, J. S., H. SASAKURA, A. KUHARA, M. BERKELEY, I. MORI and P. SENGUPTA, 2001 Specification of thermosensory neuron fate in *C. elegans* requires *ttx-1*, a homolog of otd/Otx. Neuron **31:** 943-956.

SEFTON, B. M., T. HUNTER and W. C. RASCHKE, 1981 Evidence that the Abelson virus protein functions in vivo as a protein kinase that phosphorylates tyrosine. Proc Natl Acad Sci U S A **78:** 1552-1556.

SHAMAH, S. M., M. Z. LIN, J. L. GOLDBERG, S. ESTRACH, M. SAHIN, L. HU, M. BAZALAKOVA, R. L. NEVE, G. CORFAS, A. DEBANT and M. E. GREENBERG, 2001 EphA receptors regulate growth cone dynamics through the novel guanine nucleotide exchange factor ephexin. Cell **105:** 233-244.

SHIN, J., C. GU, E. PARK and S. PARK, 2007 Identification of phosphotyrosine binding domain-containing proteins as novel downstream targets of the EphA8 signaling function. Mol Cell Biol **27:** 8113-8126.

SHTIVELMAN, E., B. LIFSHITZ, R. P. GALE and E. CANAANI, 1985 Fused transcript of abl and bcr genes in chronic myelogenous leukaemia. Nature **315:** 550-554.

SINGER, D., M. BIEL, I. LOTAN, V. FLOCKERZI, F. HOFMANN and N. DASCAL, 1991 The roles of the subunits in the function of the calcium channel. Science **253:** 1553-1557.

SMITH, A., V. ROBINSON, K. PATEL and D. G. WILKINSON, 1997 The EphA4 and EphB1 receptor tyrosine kinases and ephrin-B2 ligand regulate targeted migration of branchial neural crest cells. Curr Biol **7:** 561-570.

SRINIVASAN, D., and R. PLATTNER, 2006 Activation of Abl tyrosine kinases promotes invasion of aggressive breast cancer cells. Cancer Res **66:** 5648-5655.

SULSTON, J. E., E. SCHIERENBERG, J. G. WHITE and J. N. THOMSON, 1983 The embryonic cell lineage of the nematode *Caenorhabditis elegans*. Dev Biol **100:** 64-119.

TANG, F., E. W. DENT and K. KALIL, 2003 Spontaneous calcium transients in developing cortical neurons regulate axon outgrowth. J Neurosci **23:** 927-936.

TROEMEL, E. R., B. E. KIMMEL and C. I. BARGMANN, 1997 Reprogramming chemotaxis responses: sensory neurons define olfactory preferences in *C. elegans*. Cell **91:** 161-169.

TROEMEL, E. R., A. SAGASTI and C. I. BARGMANN, 1999 Lateral signaling mediated by axon contact and calcium entry regulates asymmetric odorant receptor expression in *C. elegans*. Cell **99:** 387-398.

TSUDA, H., S. M. HAN, Y. YANG, C. TONG, Y. Q. LIN, K. MOHAN, C. HAUETER, A. ZOGHBI, Y. HARATI, J. KWAN, M. A. MILLER and H. J. BELLEN, 2008 The amyotrophic lateral sclerosis 8 protein VAPB is cleaved, secreted, and acts as a ligand for Eph receptors. Cell **133:** 963-977.

VAN DER GEER, P., T. HUNTER and R. A. LINDBERG, 1994 Receptor protein-tyrosine kinases and their signal transduction pathways. Annu Rev Cell Biol **10:** 251-337.

VAN ETTEN, R. A., 1999 Cycling, stressed-out and nervous: cellular functions of c-Abl. Trends in cell biology **9:** 179-186.

WAHL, S., H. BARTH, T. CIOSSEK, K. AKTORIES and B. K. MUELLER, 2000 Ephrin-A5 induces collapse of growth cones by activating Rho and Rho kinase. J Cell Biol **149:** 263-270.

WANG, X., P. J. ROY, S. J. HOLLAND, L. W. ZHANG, J. G. CULOTTI and T. PAWSON, 1999 Multiple Ephrins Control Cell Organization in *C. elegans* Using Kinase-Dependent and -Independent Functions of the VAB-1 Eph Receptor. Mol Cell **4:** 903-913.

WARD, S., N. THOMSON, J. G. WHITE and S. BRENNER, 1975 Electron microscopical reconstruction of the anterior sensory anatomy of the nematode *Caenorhabditis elegans*. J Comp Neurol **160:** 313-337.

WITTE, O. N., A. PONTICELLI, A. GIFFORD, D. BALTIMORE, N. ROSENBERG and J. ELDER, 1981 Phosphorylation of the Abelson murine leukemia virus transforming protein. J Virol **39:** 870-878.

YOKOYAMA, N., M. I. ROMERO, C. A. COWAN, P. GALVAN, F. HELMBACHER, P. CHARNAY, L. F. PARADA and M. HENKEMEYER, 2001 Forward signaling mediated by ephrin-B3 prevents contralateral corticospinal axons from recrossing the spinal cord midline. Neuron **29:** 85-97.

YOSHIMURA, S., J. I. MURRAY, Y. LU, R. H. WATERSTON and S. SHAHAM, 2008 *mls-2* and *vab-3* Control glia development, *hlh-17*/Olig expression and glia-dependent neurite extension in *C. elegans*. Development **135:** 2263-2275.

YU, H. H., A. H. ZISCH, V. C. DODELET and E. B. PASQUALE, 2001 Multiple signaling interactions of Abl and Arg kinases with the EphB2 receptor. Oncogene **20:** 3995-4006.

YU, S., L. AVERY, E. BAUDE and D. L. GARBERS, 1997 Guanylyl cyclase expression in specific sensory neurons: a new family of chemosensory receptors. Proc Natl Acad Sci U S A **94:** 3384-3387.

ZALLEN, J. A., S. A. KIRCH and C. I. BARGMANN, 1999 Genes required for axon pathfinding and extension in the *C. elegans* nerve ring. Development **126:** 3679-3692.

ZISCH, A. H., M. S. KALO, L. D. CHONG and E. B. PASQUALE, 1998 Complex formation between EphB2 and Src requires phosphorylation of tyrosine 611 in the EphB2 juxtamembrane region. Oncogene **16:** 2657-2670.

III. Suppression of Eph signaling guidance defects and enhancement of dendrite defects by elevated function of a voltage-gated calcium channel

Abstract

Developing neurons are highly reliant on calcium signaling to regulate cell differentiation, rate of outgrowth, and function. We find that overactivation of an L-type voltage gated calcium channel is able to suppress ephrin and netrin guidance defects. Unexpectedly, we also observe a significant increase in sensory dendrite detachment defects in ephrin signaling mutants, suggesting a previously uncharacterized relationship between VAB-1 and EGL-19 mediated calcium signaling during dendrite attachment and outgrowth.

Introduction

In *C. elegans,* EGL-19, UNC-2, and UNC-36 are homologs of known vertebrate VGCC components. *egl-19* encodes the α1 subunit of an L-type voltage-gated calcium channel which is expressed both in neurons and pharyngeal and body wall muscle. Gain-of-function mutations in *egl-19* cause prolonged muscle action potentials and contractions (LEE *et al.* 1997). Complete loss of *egl-19* function causes embryonic lethality reflecting the requirement for muscle function in embryonic elongation, but partial loss of function in this channel subunit leads to reduced egg laying, locomotion defects and reduction in pharyngeal pumping (LEE *et al.* 1997). *unc-2* encodes an α1

subunit of a non-L-type voltage-gated calcium channel similar to the human P/Q type responsible for neurotransmitter release (ESTEVEZ *et al.* 2004; SCHAFER and KENYON 1995). In contrast to *egl-19*, reduction of *unc-2* function leads to an locomoter defects and an egg-laying constitutive phenotype (SCHAFER and KENYON 1995). The last channel subunit, *unc-36*, encodes the main neuronal α2/δ subunit in *C. elegans* (SCHAFER *et al.* 1996).

Expression of UNC-2, UNC-36, and EGL-19 have all been detected in mechanosensory neurons and mutations in these genes affect cell body migration of AVM and ALM (FROKJAER-JENSEN *et al.* 2006; KINDT *et al.* 2002; TAM *et al.* 2000). Although UNC-2 is required in touch neurons for proper AVM and ALM cell migration, axon guidance of AVM in these mutants was unaffected. This suggests that UNC-2 specifically directs cell body migration rather than axon outgrowth (KINDT *et al.* 2002). In contrast, mutations in *egl-19* affected both the migration and axon outgrowth of the AVM (TAM *et al.* 2000). Similarly, in *unc-36* mutants, ALM and AVM cell bodies are misplaced and axon guidance defects were noted in ALM (FROKJAER-JENSEN *et al.* 2006). It is not known if calcium regulation by these channels may be important in amphid axon guidance.

Results

Gain of function in a voltage-gated calcium channel suppresses axon guidance defects and enhances dendrite extension defects

In *Drosophila,* calcium influx during presynaptic neurotransmitter release is modified by Eph receptors signaling through Ephexin and Cdc42 (FRANK *et al.* 2009). In *C. elegans*, mutations causing altered neuronal activity, including a gain-of-function mutation in the L-type voltage gated calcium channel (VGCC) α1 subunit *egl-19*, cause amphid neurons to extend ectopic axonal branches during larval development (PECKOL *et al.* 1999). However EGL-19 or neuronal activity have not so far been implicated in amphid axon outgrowth during embryogenesis.

To address whether Eph signals genetically interact with VGCC in amphid guidance, we examined the effects of an EGL-19 activating mutation *egl-19(ad695)* (AVERY 1993) on the guidance defects in *vab-1* mutants. We found that *egl-19(ad695)* caused significant suppression of amphid guidance defects in *vab-1(kd)* and *vab-1(0)* mutants. *egl-19(gf)* also suppressed guidance defects in *unc-6*/netrin mutants but not in *sax-3*/Robo mutants (**Fig 3.1A**). Assuming the effects of *egl-19(gf)* are mediated by increased intracellular calcium in neurons, these results suggest amphid guidance in part is promoted by calcium signals. Complete loss of function in *egl-19* results in embryonic lethality, precluding a clear test of its requirement in amphid guidance; partial loss of function in *egl-19* resulted in no defects in the single mutant, and no enhancement in the *vab-1(kd)* background (**Fig 3.1B**). Loss of function in other calcium channel subunits such as the α2/δ subunit *unc-36* and α1 subunit *unc-2* had no effect on amphid axon guidance as single mutants or double mutants with *vab-1(kd)* (**Fig 3.1B**). Therefore, activity of EGL-19-containing voltage gated calcium channels may specifically promote amphid axon guidance.

Although *egl-19(gf)* mutations suppressed *vab-1* axon guidance defects, we

noticed that they exacerbated *vab-1* defects in amphid dendrite development. Defects in the initial attachment of the amphid dendrite tip result in shortened dendrites that are unattached to the anterior, the dendrite extension (Dex) phenotype (HEIMAN and SHAHAM 2009). *vab-1(kd)* and *vab-1(0)* mutants display an impenetrant dendrite extension (Dex) defect (**Fig 3.2A**). The penetrance of the Dex phenotype was similar in L1 and L4 animals, indicating that the dendrite attachment defects arise in embryos and are not a result of fragility in larval growth. In *egl-19(gf)* double mutants with *vab-1(kd)* or *vab-1(0)*, and to a lesser extent with *vab-1(e2)* and *vab-1(zd118)*, we observed a significant increase in Dex phenotypes to around 20% (**Fig 3.2B**). However, *egl-19(gf); unc-6* and *egl-19(gf); sax-3* double mutants did not display enhanced Dex phenotypes, suggesting the specific combination of reduced VAB-1 signaling and elevated calcium impairs dendrite attachment (**Fig 3.2B**). Dye filling with DiI indicates that the *vab-1(kd)* Dex phenotype generally involves the entire left or right side amphid dendrite bundle (**Fig 3.2C**). The lengths of dendrites in the *vab-1 egl-19(gf)* double mutants followed a bi-modal distribution, similar to lengths reported in *dex-1* and *dyf-7* mutants (HEIMAN and SHAHAM 2009). This result suggests defects occur during an early attachement process, while subsequent steps continue normally if this first failure does not occur.

To address whether the improved axon guidance is a response to loss of dendrite attachment we scored guidance and Dex defects in a *vab-1(0); egl-19(gf)* animal and found no significant correlation ($\chi^2 = 1.14$; $p<0.28$). These results suggest the role of VAB-1 in dendrite attachment is independent of its function in axon guidance.

Discussion

In *Drosophila,* Eph receptors signal through Ephexin and Cdc42 to create a calcium influx through $Ca_V2.1$ channels that alters presynaptic neurotransmitter release (FRANK *et al.* 2009). We find that *egl-19* mediated upregulation of calcium is able to suppress guidance defects in both the kinase dead version of the Eph receptor and the null, while partial loss of function results in [testing currently]. The ability of *egl-19(ad695)* to suppress *unc-6* defects indicates that increased calcium flow acts in a non Eph specific manner and improves guidance overall. It is possible that calcium regulation is a convergence point between only the Eph and netrin parallel guidance pathways since no suppression of defects was noted in the *sax-3; egl-19(gf)* mutant. We observed an increase in dendrite extension (Dex) defects specifically in compound mutants between *egl-19(gf)* and ephrin signaling mutants. Although increased neuronal activity has been shown to cause outgrowth defects during later amphid development (PECKOL *et al.* 1999), these results might suggest a previously unreported role for VAB-1 and EGL-19 during dendrite attachment or outgrowth.

Materials and Methods

Strains and culture conditions

Worms were cultured on *E. coli* OP50 seeded NGM agar plates. Animals were grown and analyzed at room temperature (21-23°C). The following mutants were used: **LGII:** *vab-1(e118, e2027, e2, zd118)* **LGIII:** *unc-36(e251)*. **LGIV:** *egl-19(ad695, n2368cs, ad1006)* **LGX:** *sax-3(ky123), unc-6(ev400), unc-2(e55)*. Published transgenes

used: P*str-1*-GFP(*kyIs104)* (TROEMEL *et al.* 1997); P*gcy-8*-GFP*(oyIs17)* (SATTERLEE *et al.* 2001).

Scoring of amphid axon guidance and dendrite extension

To visualize the overall structure of the amphids, we used DiI and DiO staining to label ASI, ADL, ASK, AWB, ASH, and ASJ neurons. A DiI or DiO stock solution of 2mg/ml was diluted 1:200 in M9 to a final concentration of 10ng/μl. Mixed stages of worms were incubated in this solution for 4 hours, rotating, at room temperature. Worms were given a quick wash with M9, then allowed to destain on OP50 seeded plates for 2 hours. Images were taken on Zeiss 510 LSM confocal using the 543 nm laser.

To visualize the morphology of individual neurons we used transgenic markers specific to single amphid neuron types. We immobilized L4 stage hermaphrodites using 1% phenoxy-1-propanol in M9 and scored the morphology of 100-200 neurons per genotype under compound microscopy. In the wild type essentially 100% of amphid axons extend ventrally in the amphid commissure and then turn anteriorly into the nerve ring. We classified amphid axon guidance as Normal, Lateral, or Other. The "other" category was rare and only used if no axon was visible extending out of the cell body. No strain displayed more than 5% "other" defects. As far as possible the initial guidance decision of the axon was scored, even if it subsequently changed direction. For example, if outgrowth started normally and extended ventrally, but then changed direction halfway to the ventral nerve cord this would be classified as "normal". This change in direction was also rare. For the candidate gene screen, mutations were crossed into the *vab-1(e118)* kinase-dead allele. To assess the significance of differences in proportions we used Fisher's exact test or the chi-squared test.

To score dendrite extension defects (Dex), compound microscopy was used to record the length of shortened dendrites as a percentage of the total length from cell body to nose tip, as well as whether the defect occurred on the right or left hand side in each strain scored. Due to slight natural variation in dendrite lengths, a Dex defect was counted when dendrite length was shorter than 95% of the distance from the amphid cell body to the nose of the worm.

Acknowledgements

We would like to thank Andy Nguyen for help with strain construction.

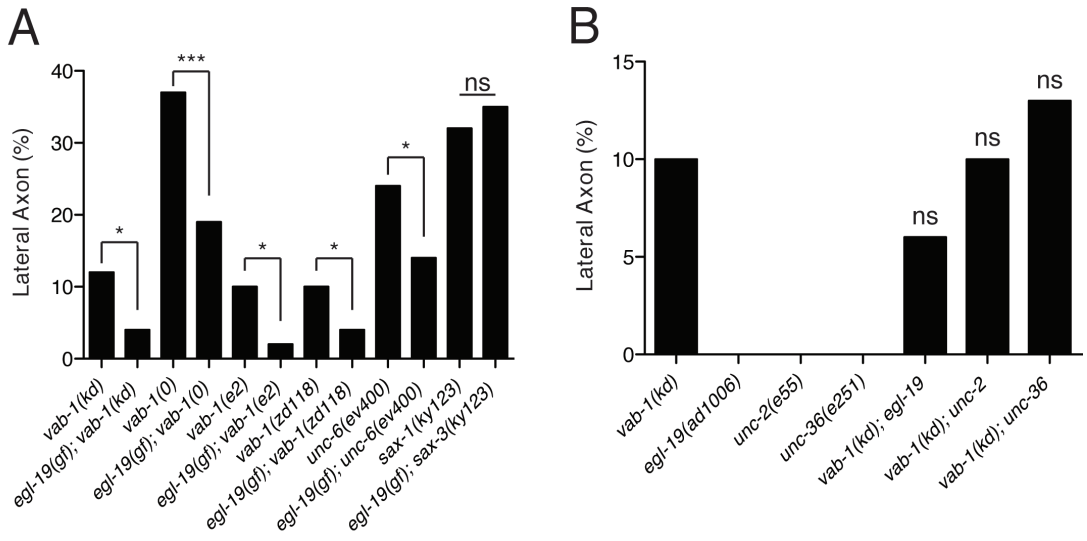

Figure 3.1 Voltage Gated Calcium Channel EGL-19 suppresses Eph guidance defects (A) *egl-19(ad695)* suppresses guidance defects in Eph and netrin signaling mutants. (B) Other calcium channel mutants do not show similar effects in compound mutants. *unc-2(e55)* guidance was examined in AFD neurons using P*gcy-8*-GFP(*oyIs17*).

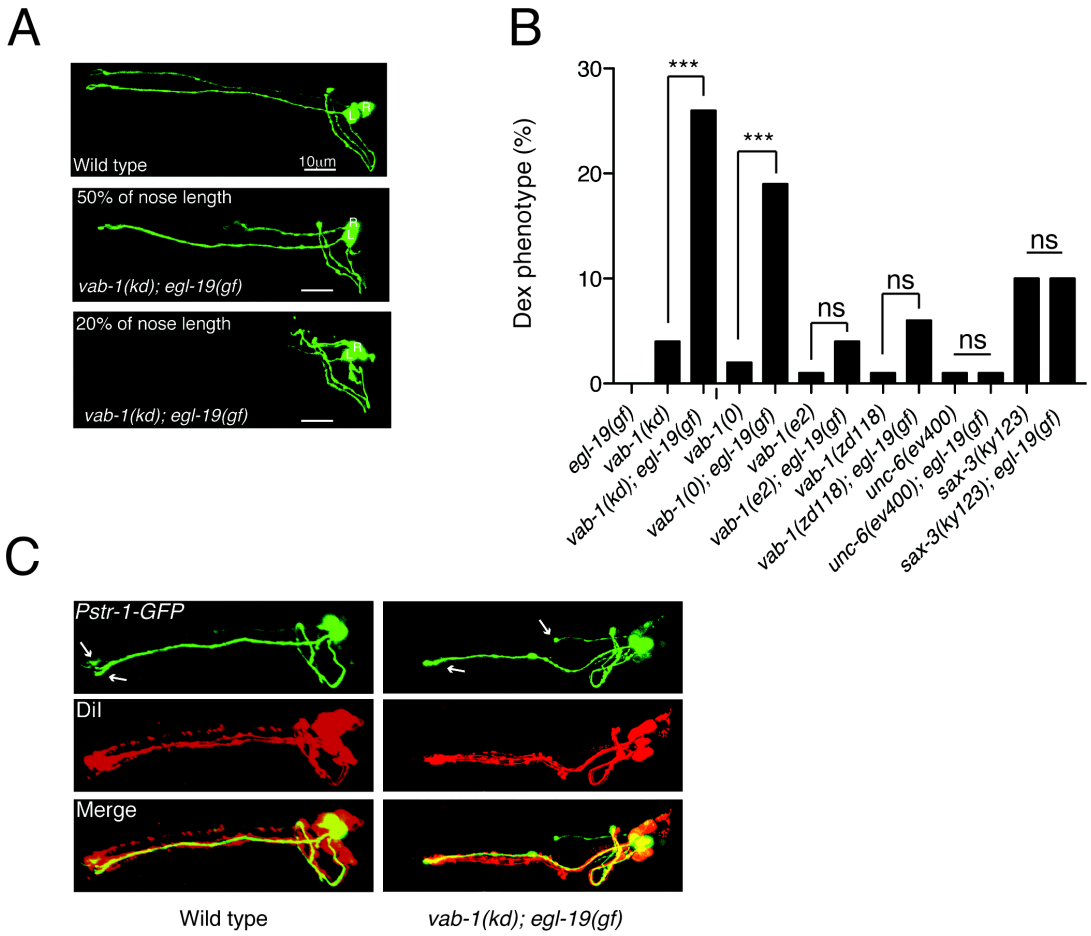

Figure 3.2 Dendrite defects in Eph double mutants with *egl-19(gf)* (A) Confocal images of wild type AWB dendrites and *vab-1(kd), egl-19(ad695); kyIs104* dendrites. Phenotypes observed include wild-type extension, right shortened, and both right and left shortened (as shown). (B) Only ephrin signaling mutants show a significant increase in Dex defects when combined with *egl-19(ad695).* (C) DiI staining in wild type (P*str-1*-GFP) and *vab-1(kd); egl-19(gf); kyIs104* mutants. Arrows show end of AWB dendrites. Complete failure to dye fill with DiI indicates all amphid dendrites are defective, suggesting total amphid bundle detachment.

References

AVERY, L., 1993 The genetics of feeding in *Caenorhabditis elegans*. Genetics **133:** 897-917.

ESTEVEZ, M., A. O. ESTEVEZ, R. H. COWIE and K. L. GARDNER, 2004 The voltage-gated calcium channel UNC-2 is involved in stress-mediated regulation of tryptophan hydroxylase. J Neurochem **88:** 102-113.

FRANK, C. A., J. PIELAGE and G. W. DAVIS, 2009 A presynaptic homeostatic signaling system composed of the Eph receptor, ephexin, Cdc42, and CaV2.1 calcium channels. Neuron **61:** 556-569.

FROKJAER-JENSEN, C., K. S. KINDT, R. A. KERR, H. SUZUKI, K. MELNIK-MARTINEZ, B. GERSTBREIH, M. DRISCOL and W. R. SCHAFER, 2006 Effects of voltage-gated calcium channel subunit genes on calcium influx in cultured *C. elegans* mechanosensory neurons. J Neurobiol **66:** 1125-1139.

HEIMAN, M. G., and S. SHAHAM, 2009 DEX-1 and DYF-7 establish sensory dendrite length by anchoring dendritic tips during cell migration. Cell **137:** 344-355.

KINDT, K. S., T. TAM, S. WHITEMAN and W. R. SCHAFER, 2002 Serotonin promotes G(o)-dependent neuronal migration in *Caenorhabditis elegans*. Curr Biol **12:** 1738-1747.

LEE, R. Y., L. LOBEL, M. HENGARTNER, H. R. HORVITZ and L. AVERY, 1997 Mutations in the alpha1 subunit of an L-type voltage-activated Ca2+ channel cause myotonia in *Caenorhabditis elegans*. EMBO J **16:** 6066-6076.

PECKOL, E. L., J. A. ZALLEN, J. C. YARROW and C. I. BARGMANN, 1999 Sensory activity affects sensory axon development in *C. elegans*. Development **126:** 1891-1902.

SATTERLEE, J. S., H. SASAKURA, A. KUHARA, M. BERKELEY, I. MORI and P. SENGUPTA, 2001 Specification of thermosensory neuron fate in *C. elegans* requires *ttx-1*, a homolog of otd/Otx. Neuron **31:** 943-956.

SCHAFER, W. R., and C. J. KENYON, 1995 A calcium-channel homologue required for adaptation to dopamine and serotonin in *Caenorhabditis elegans*. Nature **375:** 73-78.

SCHAFER, W. R., B. M. SANCHEZ and C. J. KENYON, 1996 Genes affecting sensitivity to serotonin in *Caenorhabditis elegans*. Genetics **143:** 1219-1230.

TAM, T., E. MATHEWS, T. P. SNUTCH and W. R. SCHAFER, 2000 Voltage-gated calcium channels direct neuronal migration in *Caenorhabditis elegans*. Dev Biol **226:** 104-117.

TROEMEL, E. R., B. E. KIMMEL and C. I. BARGMANN, 1997 Reprogramming chemotaxis responses: sensory neurons define olfactory preferences in *C. elegans*. Cell **91:** 161-169.

IV. The role of TRK-1 in *C. elegans* axon guidance

Abstract

We investigated the role of *trk-1,* a *C. elegans* neurotrophin receptor type B homolog, in two axonal outgrowth decisions. We first showed that *trk-1* is a true homolog of vertebrate TrkB receptors through analysis of the domains encoded in TRK-1 cDNA. Next, we examined expression of *trk-1* in a transcriptional reporter and observed widespread nervous system expression. This included expression in the nerve ring, ventral nerve cord, and tail neurons. Finally, utilizing both RNAi and genetic mutants, we demonstrated that TRK-1 seems to be required for proper PLM extension, but not for amphid commissure ventral guidance.

Introduction

Many developmental processes show a requirement for ephrin reverse signaling; specifically, signaling through ephrin-A type ligands. These include ephrin-A mediated repulsion in retinal ganglion cells (LIM *et al.* 2008), pathfinding of vomeronasal axons (KNOLL *et al.* 2001), and topographic mapping of the axons of olfactory neurons (CUTFORTH *et al.* 2003). ephin-A ligands are linked to the cell membrane only by a GPI linker and have no transmembrane domain. Therefore an outstanding question in the field remains how signals are propagated into the ephrin-A containing cell. A co-receptor has been found to be required, and three vertebrate receptors, p75, TrkB, and Ret have been demonstrated to play a role in reverse ephrin-A signaling (BONANOMI *et al.* 2012; LIM *et al.* 2008; MARLER *et al.* 2008). Although there are no homologs for p75 or Ret in *C.*

elegans, we were able to find a neurotrophin-like receptor protein, TRK-1. *trk-1* encodes a receptor tyrosine kinase that is most closely related to the vertebrate neurotrophin receptors (MANNING 2005). Very little is known about neurotrophins in *C. elegans*, and prior to the Manning publication they were not thought to be present in *C. elegans*. Although TRK-1 seems to encode a neurotrophin receptor, a *C. elegans* ligand has not been identified. We first verified the predicted protein structure of TRK-1 and examined RNAi knockdown as well as genetic mutants to determine their effect on axon guidance in *C. elegans.*

Results

The *trk-1* gene in *C. elegans* encodes a protein with sequence similarity to Trk receptors. To verify that *trk-1* is a homolog of vertebrate Trk receptors we sequenced two cDNA clones, yk1037d04 and yk1180e02, to confirm the published sequence. We were able to verify the sequence of the A isoform with these cDNA clones, but not the longer B isoform. When we compared the published (Wormbase) sequence to the cDNA clones, we found that the C-terminal end of the protein was annotated incorrectly on Wormbase and shortened the predicted protein sequence by seven amino acids. Additionally, using our corrected sequence, the last eleven amino acids of the protein are modified (**Fig 4.1A**). We next utilized NCBI BLAST to locate recognizable conserved protein domains. We were surprised to find that the 'A' isoform of the protein lacks 136 amin acids in the kinase domain that are present in the annotated 'B' isoform. However, in vertebrates several truncated isoforms of TrkB and TrkC that lack the tyrosine kinase

domain have been identified. These are thought to occur as a result of differential splicing (HUANG and REICHARDT 2003). Using the longer 'B' protein sequence, we find that the kinase domain shares 40% homology with the human TrkB kinase domain (**Fig 4.1B**). TRK-1 also has a Leucine Rich Repeat C-terminal Domain in its extracellular domain, which is characteristic of all Trk receptors. We were generously given a deletion mutant by S. Mitani, *tm3985*, which deletes most of exon 8 and 9 of the primary sequence, and we concluded that this mutation most likely truncates the protein between the kinase and transmembrane domain (**Fig 4.1A**). This theoretically should render the protein unable to propagate a reverse signal if it is acting in an adaptor capacity.

We next examined expression of *trk-1* by constructing a GFP transcriptional fusion utilizing 2 kb of genomic promoter sequence. We found that *trk-1::*GFP was expressed widely in the nervous system, including the nerve ring, ventral nerve cord, and tail neurons (**Fig 4.2A**). The widespread expression led us to question the potential role of TRK-1 in ephrin signaling, and we chose to examine two axon guidance decisions known to rely on VAB-1 signaling. First, we examined PLM extension using RNAi against *trk-1*. Both RNAi treatments resulted in worms that were sickly in appearance and had PLM extension defects. In wildtype worms, the PLM normally extends anteriorly past the PVM but stops short of the ALM cell body. We found that the RNAi treated worms had PLM axons that would aberrantly extend past the ALM cell body (**Fig 4.3A**). Next, we utilized *tm3985* to determine if TRK-1 has a role mediating ventral guidance in the amphid neurons. We observed no defects in the single mutant, and no enhancement was observed in a kinase dead background (**Fig 4.3B**). We also examined guidance in *tm4054*

mutants, but upon genotyping our strain seemed to have a deletion duplication and therefore was not included in the amphid guidance data.

Discussion

Although it seems like *trk-1* has some sort of role in PLM extension, it does not appear to play a role in amphid ventral guidance. The phenotype we observed in PLM axons mirrors those seen in *vab-1* mutants, so it would be interesting to follow up on any genetic relationship that exists between *vab-1* and *trk-1* in the mechanosensory neurons. In contrast to the sickly appearance of the RNAi treated worms, our *tm3985* genetic mutants were phenotypically wild type. This is most likely due to the genetically sensitized background of the RNAi treated worms. These worms (*mec-4*-GFP(*zdIs5*); *nre-1(hd20) lin-15b(hd126)*) are genetically sensitized to RNAi in the nervous system, but they also display brood size reduction and sterility at temperatures above 20°C (SCHMITZ *et al.* 2007). We've shown in this manuscript that ephrin signaling seems to be highly context specific, so it is possible that TRK-1 regulates PLM extension but not other axonal outgrowth decisions such as amphid commissure guidance.

Acknowledgements

We would like to thank S. Mitani for *tm3985* and *tm4054* deletion mutants. Thank you to Y. Kohara for *trk-1* cDNA clones yk1037d4 and yk1180e2.

Materials and Methods

Strains and culture conditions

Worms were cultured on *E. coli* OP50 seeded NGM agar plates. Animals were grown and analyzed at room temperature (21-23°C). The following mutants were used: **LGII:** *vab-1(e118)* **LGX:** *trk-1(tm3985, tm4054).*

RNAi experiments

Two RNAi clones were used, 4D17 and 4D21. L4440 vector alone was used as a negative control, and experiments were conducted in CZ8693 (*mec-4*-GFP(*zdIs5*); *nre-1(hd20) lin-15b(hd126)*) worms.

Trk-1 expression experiments

2 kb of upstream *trk-1* promoter was used to drive GFP expression in construct used. 30ng/ul of P*trk-1*-GFP was injected into N2 worms. Multiple lines were examined, representative line *juEx2917* is shown.

Scoring of amphid axon guidance

To visualize the morphology of individual neurons we used transgenic markers specific to single amphid neuron types. We immobilized L4 stage hermaphrodites using 1% phenoxy-1-propanol in M9 and scored the morphology of 100-200 neurons per genotype under compound microscopy. In the wild type essentially 100% of amphid axons extend ventrally in the amphid commissure and then turn anteriorly into the nerve ring. We classified amphid axon guidance as Normal, Lateral, or Other. The “other” category was rare and only used if no axon was visible extending out of the cell body.

No strain displayed more than 5% “other” defects. As far as possible the initial guidance decision of the axon was scored, even if it subsequently changed direction. For example, if outgrowth started normally and extended ventrally, but then changed direction halfway to the ventral nerve cord this would be classified as “normal”.

A

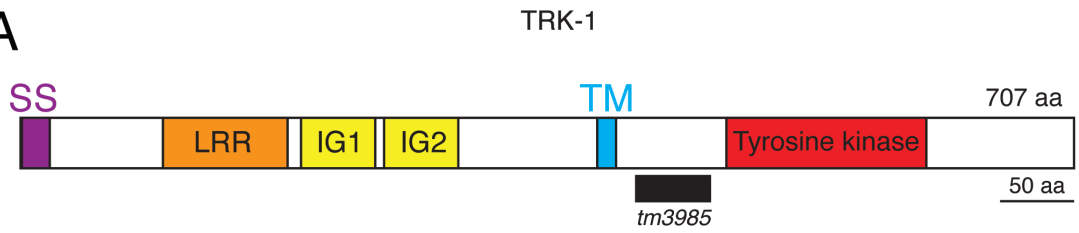

Isoform A

```
MILRILLTLL ILTYSPGVLT ISQCVKATRD TVRCDDFIDF NGTAKVLVVG NCSSLQNIDE  60
LGFGPFHSVT NVTFDCVVTH FPWEFANIFP NIRHIHINKC NLTSLPWQSI WTETLKTVDF 120
SSCPIQCSCQ NQWMRAKEIF EKITEPKSLR KCAWNCDPGK MMFPGVIYSK NGDNVTVHVG 180
FDDQVLNRTI DKPYFDWAFS KHPHKHEEII AEKGADLMIT NLKREDMGVI GVKCWHCLDF 240
LVGKIELRAN YPVKVAFVDK TRLDTDFLVV TGYPIDNISM AITKMQSNYS ETNFVGREKA 300
IFFSSLVVRM EKRPLFYQKT YRVFTKDAAE GDHLSGDLRF EVCTNGSCDA IEKHVSHLGL 360
INGTIDDFII VEYPYKQEIQ IVVFLIVICL LIVVSALAFY HRLKLQSFLR EKILSFRKRI 420
SLAQELQTRR ASQETEETLL RLEERSSLAS DYTNMTLPFI DMGNIEIHEM LGKGHFGEVY 480
LASWDYTGPR SVAVKSIRRV DMATEKEARV LQDLEHPNIV KLYGMTRNNF NLLLVFEHMH 540
GRQPFDGLSN LEVSSFTLAG MRPLKPERCP QDMYDLMVKC WHMEPVKRIT AKQILEDELF 600
DKIREGLPYR AANEANSLVS SCMLNINRYK DVVAETSFTT DPLNSSEIEV NDVPTENGKV 660
NGQTVEKAEY EKSESESDSG AVTFHGECSE DPLLCDQSDE LPIFASA
```

B

```
Query  3    LGKGHFGEVYLASWDYTGPRS----VAVKSIRRVDMATEK----EARVLQDLEHPNIVKL  54
            LG+G FG+V+LA       P      VAVK+++    +A  K     EA +L +L+H +IVK
Sbjct  544  LGEGAFGKVFLAECYNLSPTKDKMLVAVKALKDPTLAARKDFQREAELLTNLQHEHIVKF  603

Query  55   YGMTRNNFNLLLVFEHMNHGDLKTYLEQRAPVKSVYLQYPP-----PLVIDELKWIIKEI  109
            YG+  +    L++VFE+M HGDL  +L     P    + +     P       L + ++  I  +I
Sbjct  604  YGVCGDGDPLIMVFEYMKHGDLNKFLRAHGPDAMILVDGQPRQAKGELGLSQMLHIASQI  663

Query  110  TTGLVYLVEQSIVHRDLAARNCLVAGDSDLKATSHFERPPIRISDFGMSRRLYDHSEYYT  169
             +G+VYL  Q  VHRDLA RNCLV  +  +K           I DFGMSR +Y  ++YY
Sbjct  664  ASGMVYLASQHFVHRDLATRNCLVGANLLVK-----------IGDFGMSRDVYS-TDYYR  711

Query  170  MDHRGALPVRWLPPEAVQSHKFTYNSDIWSLGVTMWECMSYGRQPFDGLSNLEVSSFTLA  229
            +     LP+RW+PPE++    KFT  SD+WS GV +WE  +YG+QP+  LSN EV
Sbjct  712  VGGHTMLPIRWMPPESIMYRKFTTESDVWSFGVILWEIFTYGKQPWFQLSNTEVIECITQ  771

Query  230  GMRPLKPERCPQDMYDLMVKCWHMEPVKRITAKQI  264
            G    +P  CP+++YD+M+ CW  EP +R+  K+I
Sbjct  772  GRVLERPRVCPKEVYDVMLGCWQREPQQRLNIKEI  806
```

Figure 4.1 TRK-1 is the *C. elegans* homolog of vertebrate TrkB receptors (A) TRK-1 protein with conserved domains highlighted. SS=signal sequence (M1-T20), LRR=Leucine rich repeat, IG=immunoglobin domain, TM=transmembrane domain (I381-L399). Kinase domain from E471 to D597 in isoform A. (B) Alignment with human TrkB kinase domain, 40% homology. Green residues on C-terminal end of protein sequence corrected after cDNA clone sequencing.

A

Figure 4.2 P*trk-1*-GFP expression is observed pan-neuronally in *juEx2917* worms (A). Strong expression can be detected in nerve ring, ventral nerve cord, and tail neurons.

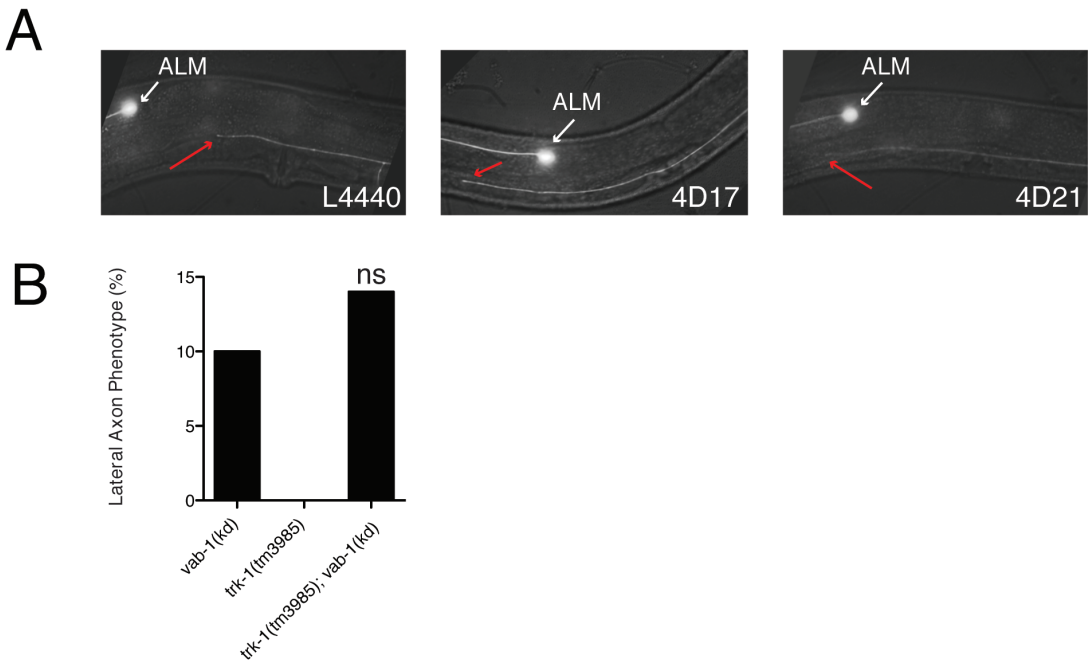

Figure 4.3 TRK-1 may have a role in regulation of PLM outgrowth, but does not seem to function in amphid axon guidance (A) ALM cell body placement and PLM extension in control (L4440) RNAi treated worms and two *trk-1* RNAi (4D17 and 4D21) treated worms. Red arrow points to end of PLM extension. PLM can be seen to extend anteriorly to ALM cell body in RNAi treated worms. (B) AWB guidance was scored in *tm3985* and *e118; tm3985* mutants. No enhancement over *vab-1(kd)* defects were observed.

References

BONANOMI, D., O. CHIVATAKARN, G. BAI, H. ABDESSELEM, K. LETTIERI, T. MARQUARDT, B. A. PIERCHALA and S. L. PFAFF, 2012 Ret is a multifunctional coreceptor that integrates diffusible- and contact-axon guidance signals. Cell **148:** 568-582.

CUTFORTH, T., L. MORING, M. MENDELSOHN, A. NEMES, N. M. SHAH, M. M. KIM, J. FRISEN and R. AXEL, 2003 Axonal ephrin-As and odorant receptors: coordinate determination of the olfactory sensory map. Cell **114:** 311-322.

HUANG, E. J., and L. F. REICHARDT, 2003 Trk receptors: roles in neuronal signal transduction. Annu Rev Biochem **72:** 609-642.

KNOLL, B., K. ZARBALIS, W. WURST and U. DRESCHER, 2001 A role for the EphA family in the topographic targeting of vomeronasal axons. Development **128:** 895-906.

LIM, Y. S., T. MCLAUGHLIN, T. C. SUNG, A. SANTIAGO, K. F. LEE and D. D. O'LEARY, 2008 p75(NTR) mediates ephrin-A reverse signaling required for axon repulsion and mapping. Neuron **59:** 746-758.

MANNING, G., 2005 Genomic overview of protein kinases. WormBook**:** 1-19.

MARLER, K. J., E. BECKER-BARROSO, A. MARTINEZ, M. LLOVERA, C. WENTZEL, S. POOPALASUNDARAM, R. HINDGES, E. SORIANO, J. COMELLA and U. DRESCHER, 2008 A TrkB/EphrinA interaction controls retinal axon branching and synaptogenesis. J Neurosci **28:** 12700-12712.

SCHMITZ, C., P. KINGE and H. HUTTER, 2007 Axon guidance genes identified in a large-scale RNAi screen using the RNAi-hypersensitive *Caenorhabditis elegans* strain *nre-1(hd20) lin-15b(hd126)*. Proc Natl Acad Sci U S A **104:** 834-839.

V. Discussion

Homologs of all the major guidance molecules and their receptors are encoded in the *C. elegans* genome, including netrin (ISHII *et al.* 1992; SERAFINI *et al.* 1994), slit (HAO *et al.* 2001), wnt (SHACKLEFORD *et al.* 1993), delta (TAX *et al.* 1994), ephrins (CHIN-SANG *et al.* 1999; CHIN-SANG *et al.* 2002; WANG *et al.* 1999), and semaphorins (ROY *et al.* 2000). Conservation of these molecules and signaling pathways allows us to study complex axon guidance signaling in a simpler organism, but still apply this knowledge to axon guidance in higher organisms. Using the amphid sensory neurons of *C. elegans* as a model, we have characterized an Eph kinase-independent forward signaling pathway required for axon guidance. Our work has uncovered novel roles in *C. elegans* for ABL-1, a non-receptor tyrosine kinase, as well as an unanticipated outgrowth asymmetry.

Role of Ephrin Ligands During Axon Guidance

In opposition to the roles they play in epidermal morphogenesis, EFN-2 and EFN-3 do not signal in a redundant fashion with EFN-1 to mediate amphid ventral guidance. Surprisingly, we found that EFN-2 and EFN-3 inhibit Eph kinase-independent signaling and are not required for amphid guidance. So why is there this difference in redundancy of ephrins between morphological development and axon guidance? One possible explanation is that axon guidance requires a more complex signaling relationship than ventral neuroblast migration and therefore the ephrins function in a more nuanced way as opposed to the redundant adhesive properties of neuroblast migration.

Kinase-independent Forward Signaling

We have demonstrated that ephrin signaling in amphid axon guidance signals primarily via a kinase-independent pathway for proper guidance. Based on the location of the components, the mechanism would fall into the "forward" classification since the Eph receptor is present on the amphid neuron, and therefore the signal is transduced through the receptor into the amphid cell. There are a number of processes in *C. elegans* that also require kinase-independent signaling by VAB-1, including neuroblast migration (GEORGE *et al.* 1998), PLM extension (MOHAMED and CHIN-SANG 2006), and gonadal sheath cell contraction (MILLER *et al.* 2003). However, we have contributed to the knowledge of the *in vivo* mechanism of this pathway.

ABL-1 has a Guidance Role in *C. elegans*

During axon guidance, we found that VAB-1 signals through a kinase-independent pathway that involves ABL-1. We believe this is the first evidence for a genetic interaction between an Eph receptor and Abl outside of cell culture, as well as the first evidence in *C. elegans* of a guidance role for *abl-1*. The mechanism of this interaction between *abl-1* and *vab-1* is still unclear, but it has been demonstrated using yeast-two-hybrid experiments that Abl is capable of binding to EphB2 through its C-terminal tail in an EphR kinase-independent manner (YU *et al.* 2001). We hypothesize that this mechanism could also be utilized during amphid guidance in *C. elegans*. The preferred binding site of the Abl SH2 domain (YXXP) (SONGYANG *et al.* 1993) is present

in both the kinase as well as the juxtamembrane domain of VAB-1, but it is unlikely this mechanism is utilized during amphid axon guidance because Eph kinase activity was also found to be required for Abl SH2 binding (YU *et al.* 2001). Recently, it was reported that the SH2 of ABL-1 and the kinase domain of VAB-1 do not interact (MOHAMED *et al.* 2012), but only one out of three possible ABL-1 SH2 binding sites in VAB-1 are present in this region. This could account for the lack of interaction observed.

Is VAB-1 Signaling Attractive or Repulsive?

Although there are many examples of ephrin signaling acting as a repulsive force (KLEIN 2012), there are also examples in which ephrin signaling is attractive (HOLMBERG and FRISEN 2002). For example, ephrinA5 and EphA7 are required for proper neural tube fusion during mouse embryogenesis (HOLMBERG *et al.* 2000), and EphB2 and EphB3/Sek4 are required for proper palatal shelf fusion (ORIOLI *et al.* 1996). In addition to regulating cellular adhesion, there are also examples of attractive Eph signaling during axon outgrowth. For the topographic targeting of vomeronasal axons, neurons with high expression of ephrin-A5 project to regions with high EphA6 expression, consistent with Eph signaling acting as an attractive force (KNOLL *et al.* 2001).

Interestingly, Abl also plays a role in both neuron outgrowth and retraction. Activated Abl promotes neurite outgrowth through its interaction with Cables (ZUKERBERG *et al.* 2000), whereas it promotes growth cone collapse downstream of Eph signaling (HARBOTT and NOBES 2005). This leads to the question of whether ephrin signaling during amphid outgrowth is attractive or repulsive. We believe that signaling in

this context is attractive due to the fact that *unc-6/unc-40, sax-3,* and *vab-1* mutants all give rise to similar lateral outgrowth guidance defects. This hypothesis then implies that ephrin ligands should be expressed along the ventral path of amphid. The opposing hypothesis would be that ephrin ligands act to repulse the growing axon from a lateral path. However if this were the case, we would expect the axons in a netrin mutant to be repulsed from taking a lateral path by the ephrins and therefore display no lateral guidance defects. Based on the observation that netrin mutants still display lateral defects, this suggests that ephrin signaling is attractive and EFN-1 is expressed along the path of amphid outgrowth.

Is Asymmetry in the Nervous System Beneficial?

Although there are many examples of asymmetry in the *C. elegans* nervous system, the mechanism of how this asymmetry occurs differs (BERTRAND *et al.* 2011; CHANG *et al.* 2003; TROEMEL *et al.* 1999). So why would nervous system benefit from being asymmetric? It is possible that neural asymmetry allows organisms, *C. elegans* in this case, to use the number of neurons it has most efficiently. For example, instead of detecting twelve hypothetical different cues (one for each pair of sensory neurons), having asymmetric expression of sensory receptors can increase detection up to twenty-four. This hypothesis is supported by evidence of chemosensory defects in a mutant that aberrantly expresses *str-2* in both AWC neurons instead of one (WES and BARGMANN 2001). In this work, we demonstrated that amphid neurons display an asymmetric guidance outgrowth defect implying a differing reliance on either kinase-dependent or –

independent Eph signaling. Perhaps by a similar logic, relying on different mechanisms to steer neurons to the correct target acts as a prevention of a mutation in the pathway from affecting all of the neurons. For example, if the kinase activity of the receptor is disrupted, this primarily affects neurons on the left, leaving guidance on the right unaffected for the most part.

Phosphatidylinositol-3-Kinase Signaling During Axon Guidance

The enhancement of defects observed in the *age-1 vab-1(0)* mutant can be interpreted a number of ways. First, this result could imply that *age-1*, and therefore PI3K signaling, signals completely in parallel to the Eph receptor. Since amphid guidance is guided by UNC-6/UNC-40, SAX-3, and VAB-1, we cannot rule out the hypothesis that PI3K signaling lies downstream of either UNC-40 or SAX-3. It has been shown that PI3K functions downstream of both netrin and slit in AVM neuron guidance (CHANG *et al.* 2006). However, we do believe that PI3K signals at least partially downstream of VAB-1 based on the evidence that VAB-1 physically interacts with and inhibits DAF-18 (BRISBIN *et al.* 2009). DAF-18/PTEN is a phosphatase responsible for inhibiting the PI3K signaling pathway. DAF-18 was identified as binding partner of VAB-1 in a yeast-two-hybrid screen. The C-terminal region of DAF-18 was shown to bind to the kinase domain of VAB-1, even in a kinase dead form of the receptor (BRISBIN *et al.* 2009). This evidence coupled with the suppression of defects observed in our *vab-1(kd); daf-18* mutant implies that VAB-1 is directly interacting with DAF-18 during amphid guidance, and therefore is responsible in part for regulation of PI3K signaling.

Another observation of interest, we found that PI3K signaling in axon guidance seems to follow a non-canonical pathway that does not agree with signaling implicated in *C. elegans* longevity. We find that PI3K signaling acts to promote ventral guidance, but that downstream genes such as AKT-1, SGK-1, and PDK-1 that are normally activated by products of PI3K signaling act as inhibitors to ventral guidance. To elucidate the relationship between the components, construction of genetic mutants such as *vab-1(kd), age-1, akt-1* should be done to better establish the genetic relationship between the components.

Is AWB A Pioneer Neuron?

We found that expressing ABL-1 exclusively in the AWB neurons could rescue the rest of the amphid neurons in the commissure. The mechanism of this non-cell autonomous rescue is unclear at this point, but we propose the following hypothetical models. First, AWB could be a pioneer axon, which the rest of the neurons in the amphid commissure follow. By rescuing AWB, this allows the rest of the amphid to guide correctly. Alternatively, expression of ABL-1 in AWB could endow this neuron with pioneer like cell identity. Additional experiments such as expression of ABL-1 under a different specific amphid pair promoter (*str-3, gcy-8,* etc.) should be done to determine if expression from another pair is able to rescue the entire amphid. If rescue is noted when expressed from a different neuron pair, this suggests that expression of ABL-1 is sufficient to cause those neurons to assume pioneer roles.

The Role of Calcium During Amphid Development

When a gain-of-function in the EGL-19 L-type voltage gated calcium channel is combined with ephrin signaling mutants, we find that although guidance defects are suppressed, dendrite detachment increases significantly. It has been demonstrated that growth cones producing a high frequency of calcium transients migrate slowly or retract, whereas growth cones generating a low frequency of calcium transients migrate rapidly (cite). It is possible that dendrite detachments during *C. elegans* embryogenesis could be occurring as a result of the increased calcium causing a reduction in dendrite extension. The amphid cell body will migrate posteriorly at a normal rate, but the reduction in dendrite growth could leads to stress on the attachment structure at the nose and detachment. Since these detachments are only seen in ephrin signaling mutants, this suggests that any calicum-mediated reduction of growth rate in dendrites might be dependent on UNC-6 and SAX-3.

Future Directions

Although we observed VAB-1 and EFN-1 expression during larval stages, it is still important to confirm their cellular localization during embryogenesis when axon outgrowth occurs. Attempts to fix and stain embryos using antibodies against GFP were not successful at detecting either EFN-1::GFP or VAB-1::GFP at a single cell resolution during embryogenesis. A co-localization marker that is expressed early, such as *dyf-7*, should be used to determine which component is expressed on the developing amphid

neurons. Additionally, determining expression of ABL-1 should be done to confirm its role downstream of VAB-1. Biochemical binding assays to determine if ABL-1 binds VAB-1 directly, and more specifically, which domains are necessary for their interaction are also suggested as a follow-up experiment. Lastly, to address the left/right guidance asymmetry noted in the amphid neurons, additional genes known to cause asymmetries in the *C. elegans* nervous system should be tested to assay their effect on amphid guidance. These include *gpa-16, nsy-4,* and *mir-273*.

References

BERTRAND, V., P. BISSO, R. J. POOLE and O. HOBERT, 2011 Notch-dependent induction of left/right asymmetry in *C. elegans* interneurons and motoneurons. Curr Biol **21:** 1225-1231.

BRISBIN, S., J. LIU, J. BOUDREAU, J. PENG, M. EVANGELISTA and I. CHIN-SANG, 2009 A role for *C. elegans* Eph RTK signaling in PTEN regulation. Dev Cell **17:** 459-469.

CHANG, C., C. E. ADLER, M. KRAUSE, S. G. CLARK, F. B. GERTLER, M. TESSIER-LAVIGNE and C. I. BARGMANN, 2006 MIG-10/lamellipodin and AGE-1/PI3K promote axon guidance and outgrowth in response to slit and netrin. Curr Biol **16:** 854-862.

CHANG, S., R. J. JOHNSTON, JR. and O. HOBERT, 2003 A transcriptional regulatory cascade that controls left/right asymmetry in chemosensory neurons of *C. elegans*. Genes Dev **17:** 2123-2137.

CHIN-SANG, I. D., S. E. GEORGE, M. DING, S. L. MOSELEY, A. S. LYNCH and A. D. CHISHOLM, 1999 The ephrin VAB-2/EFN-1 functions in neuronal signaling to regulate epidermal morphogenesis in *C. elegans*. Cell **99:** 781-790.

CHIN-SANG, I. D., S. L. MOSELEY, M. DING, R. J. HARRINGTON, S. E. GEORGE and A. D. CHISHOLM, 2002 The divergent *C. elegans* ephrin EFN-4 functions inembryonic morphogenesis in a pathway independent of the VAB-1 Eph receptor. Development **129:** 5499-5510.

GEORGE, S. E., K. SIMOKAT, J. HARDIN and A. D. CHISHOLM, 1998 The VAB-1 Eph receptor tyrosine kinase functions in neural and epithelial morphogenesis in *C. elegans*. Cell **92:** 633-643.

HAO, J. C., T. W. YU, K. FUJISAWA, J. G. CULOTTI, K. GENGYO-ANDO, S. MITANI, G. MOULDER, R. BARSTEAD, M. TESSIER-LAVIGNE and C. I. BARGMANN, 2001 *C. elegans* slit acts in midline, dorsal-ventral, and anterior-posterior guidance via the SAX-3/Robo receptor. Neuron **32:** 25-38.

HARBOTT, L. K., and C. D. NOBES, 2005 A key role for Abl family kinases in EphA receptor-mediated growth cone collapse. Mol Cell Neurosci **30:** 1-11.

HOLMBERG, J., D. L. CLARKE and J. FRISEN, 2000 Regulation of repulsion versus adhesion by different splice forms of an Eph receptor. Nature **408:** 203-206.

HOLMBERG, J., and J. FRISEN, 2002 Ephrins are not only unattractive. Trends Neurosci **25:** 239-243.

ISHII, N., W. G. WADSWORTH, B. D. STERN, J. G. CULOTTI and E. M. HEDGECOCK, 1992 UNC-6, a laminin-related protein, guides cell and pioneer axon migrations in *C. elegans*. Neuron **9:** 873-881.

KLEIN, R., 2012 Eph/ephrin signalling during development. Development **139:** 4105-4109.

KNOLL, B., K. ZARBALIS, W. WURST and U. DRESCHER, 2001 A role for the EphA family in the topographic targeting of vomeronasal axons. Development **128:** 895-906.

MILLER, M. A., P. J. RUEST, M. KOSINSKI, S. K. HANKS and D. GREENSTEIN, 2003 An Eph receptor sperm-sensing control mechanism for oocyte meiotic maturation in *Caenorhabditis elegans*. Genes Dev **17:** 187-200.

MOHAMED, A. M., J. R. BOUDREAU, F. P. YU, J. LIU and I. D. CHIN-SANG, 2012 The *Caenorhabditis elegans* Eph receptor activates NCK and N-WASP, and inhibits Ena/VASP to regulate growth cone dynamics during axon guidance. PLoS Genet **8:** e1002513.

MOHAMED, A. M., and I. D. CHIN-SANG, 2006 Characterization of loss-of-function and gain-of-function Eph receptor tyrosine kinase signaling in *C. elegans* axon targeting and cell migration. Dev Biol **290:** 164-176.

ORIOLI, D., M. HENKEMEYER, G. LEMKE, R. KLEIN and T. PAWSON, 1996 Sek4 and Nuk receptors cooperate in guidance of commissural axons and in palate formation. EMBO J **15:** 6035-6049.

ROY, P. J., H. ZHENG, C. E. WARREN and J. G. CULOTTI, 2000 *mab-20* encodes Semaphorin-2a and is required to prevent ectopic cell contacts during epidermal morphogenesis in *Caenorhabditis elegans*. Development **127:** 755-767.

SERAFINI, T., T. E. KENNEDY, M. J. GALKO, C. MIRZAYAN, T. M. JESSELL and M. TESSIER-LAVIGNE, 1994 The netrins define a family of axon outgrowth-promoting proteins homologous to *C. elegans* UNC-6. Cell **78:** 409-424.

SHACKLEFORD, G. M., S. SHIVAKUMAR, L. SHIUE, J. MASON, C. KENYON and H. E. VARMUS, 1993 Two wnt genes in *Caenorhabditis elegans*. Oncogene **8:** 1857-1864.

SONGYANG, Z., S. E. SHOELSON, M. CHAUDHURI, G. GISH, T. PAWSON, W. G. HASER, F. KING, T. ROBERTS, S. RATNOFSKY, R. J. LECHLEIDER and ET AL., 1993 SH2 domains recognize specific phosphopeptide sequences. Cell **72:** 767-778.

TAX, F. E., J. J. YEARGERS and J. H. THOMAS, 1994 Sequence of *C. elegans lag-2* reveals a cell-signalling domain shared with *Delta* and *Serrate* of *Drosophila*. Nature **368:** 150-154.

TROEMEL, E. R., A. SAGASTI and C. I. BARGMANN, 1999 Lateral signaling mediated by axon contact and calcium entry regulates asymmetric odorant receptor expression in *C. elegans*. Cell **99:** 387-398.

WANG, X., P. J. ROY, S. J. HOLLAND, L. W. ZHANG, J. G. CULOTTI and T. PAWSON, 1999 Multiple Ephrins Control Cell Organization in *C. elegans* Using Kinase-

Dependent and -Independent Functions of the VAB-1 Eph Receptor. Mol Cell **4:** 903-913.

WES, P. D., and C. I. BARGMANN, 2001 *C. elegans* odour discrimination requires asymmetric diversity in olfactory neurons. Nature **410:** 698-701.

YU, H. H., A. H. ZISCH, V. C. DODELET and E. B. PASQUALE, 2001 Multiple signaling interactions of Abl and Arg kinases with the EphB2 receptor. Oncogene **20:** 3995-4006.

ZUKERBERG, L. R., G. N. PATRICK, M. NIKOLIC, S. HUMBERT, C. L. WU, L. M. LANIER, F. B. GERTLER, M. VIDAL, R. A. VAN ETTEN and L. H. TSAI, 2000 Cables links Cdk5 and c-Abl and facilitates Cdk5 tyrosine phosphorylation, kinase upregulation, and neurite outgrowth. Neuron **26:** 633-646.

Appendix A. Transgenic *C. elegans* strains and plasmids

Table A.1 Transgenic Rescuing Arrays and Strains

Transgene	DNA constructs	Genotype	Strain #
juEx16	VAB-1(+) cosmid (M03A1)	*vab-1(0); kyIs104*	CZ11816
juEx2870	VAB-1(+) fosmid (WRM0617bA10) (100ng/µl)	*vab-1(0); kyIs104*	CZ14390
juEx3839	VAB-1(+) minigene (pCZ55) (1ng/µl)	*vab-1(0); kyIs104*	CZ14800
juEx3529	P*unc-33*-VAB-1 (*vab-1* 3'UTR) (pCZGY1859) (1ng/µl)	*vab-1(0); kyIs104*	CZ14078
juEx3470	P*rgef-1*-VAB-1 (*vab-1* 3'UTR) (pCZGY1847) (1 ng/µl)	*vab-1(0); kyIs104*	CZ14082
juEx3836	P*myo-2*-VAB-1 (*vab-1* 3'UTR) (pCZGY1854) (1 ng/µl)	*vab-1(0); kyIs104*	CZ14713
juEx4725	P*lin-26*-VAB-1 (*vab-1* 3'UTR) (pCZGY2220) (1 ng/µl)	*vab-1(0); kyIs104*	CZ16392
juEx4728	P*hlh-17*-VAB-1 (*vab-1* 3'UTR) (pCZGY1852) (1 ng/µl)	*vab-1(0); kyIs104*	CZ16835
juEx3308	P*dyf-7*-VAB-1 (*vab-1* 3'UTR) (pCZGY1342) (15 ng/µl)	*vab-1(0); kyIs104*	CZ13960
juEx4527	P*ttx-3*-VAB-1 (*vab-1* 3'UTR) (pCZGY1841) (5 ng/µl)	*vab-1(0); kyIs104*	CZ16033
juEx4857	P*str-1*-VAB-1 (*vab-1* 3'UTR) (pCZGY2221) (1 ng/µl)	*vab-1(0); kyIs104*	CZ17039
juEx3179	P*dyf-7*-EFN-1 (*unc-54* 3'UTR) (pCZGY1340) (1 ng/µl)	*vab-1(0); kyIs104*	CZ17654
juEx5418	P*dyf-7*-EFN-2 (*unc-54* 3'UTR) (pCZGY1343) (1 ng/µl)	*vab-1(0); kyIs104*	CZ18326

Table A.1 continued

Transgene	DNA constructs	Genotype	Strain #
juEx127	EFN-1(+) (pCZ126) (50 ng/µl)	*efn-1(0); kyIs104*	CZ14447
juIs52	EFN-1::GFP (pCZ131) (50 ng/µl)	*efn-1(0); kyIs104*	CZ13080
juEx3775	P*dpy-30*-EFN-1 (*unc-54* 3'UTR) (pCZGY1843) (1 ng/µl)	*efn-1(0); kyIs104*	CZ14487
juEx3577	P*unc-33*-EFN-1 (*efn-1* 3'UTR) (pCZGY1857) (1 ng/µl)	*efn-1(0); kyIs104*	n/a
juEx3476	P*unc-119*-EFN-1 (*unc-54* 3'UTR) (pCZGY1860) (1 ng/µl)	*efn-1(0); kyIs104*	CZ14086
juEx3158	P*rgef-1*-EFN-1 (*unc-54* 3'UTR) (pCZGY1344) (1 ng/µl)	*efn-1(0); kyIs104*	CZ13372
juEx3835	P*myo-2*-EFN-1 (*efn-1* 3'UTR) (pCZGY1853) (1 ng/µl)	*efn-1(0); kyIs104*	CZ14694
juEx4864	P*hlh-17*-EFN-1 (*efn-1* 3'UTR) (pCZGY1851) (1 ng/µl)	*efn-1(0); kyIs104*	CZ17042
juEx4524	P*ttx-3*-EFN-1 (*efn-1* 3'UTR) (pCZGY1839) (5 ng/µl)	*efn-1(0); kyIs104*	CZ16028
juEx4860	P*lin-26*-EFN-1 (*efn-1* 3'UTR) (pCZGY2223) (1 ng/µl)	*efn-1(0); kyIs104*	CZ16642
juEx3179	P*dyf-7*-EFN-1 (*unc-54* 3'UTR) (pCZGY1340) (1 ng/µl)	*efn-1(0); kyIs104*	CZ13373
juEx3272	P*dyf-7*-EFN-1 (*efn-1* 3'UTR) (pCZGY1341) (1 ng/µl)	*efn-1(0); kyIs104*	CZ13965
juEx4909	P*str-1*-EFN-1 (*efn-1* 3'UTR) (pCZGY2224) (1 ng/µl)	*efn-1(0); kyIs104*	CZ16743

Table A.1 continued

Transgene	DNA constructs	Genotype	Strain #
juEx4344	P*dyf-7*-ABL-1 (*abl-1* 3'UTR) (pCZGY1845) (1 ng/µl)	*vab-1(kd); abl-1; kyIs104*	CZ15789
juEx4345	P*dyf-7*-ABL-1 (*abl-1* 3'UTR) (pCZGY1845) (1 ng/µl)	*vab-1(kd); abl-1; kyIs104*	CZ15791
juEx4345	P*dyf-7*-ABL-1 (*abl-1* 3'UTR) (pCZGY1845) (1 ng/µl)	*vab-1(0); kyIs104*	CZ18522
juEx5055	P*str-1*-ABL-1 (*abl-1* 3'UTR) (pCZGY2227) (25 ng/µl)	*vab-1(kd); abl-1; kyIs104*	CZ17047
juEx5057	P*str-1*-ABL-1 (*abl-1* 3'UTR) (pCZGY2227) (25 ng/µl)	*vab-1(kd); abl-1; kyIs104*	CZ17049
juEx5059	P*str-1*-ABL-1 (*abl-1* 3'UTR) (pCZGY2227) (25 ng/µl)	*vab-1(kd); abl-1; kyIs104*	CZ17051
juEx5059	P*str-1*-ABL-1 (*abl-1* 3'UTR) (pCZGY2227) (25 ng/µl)	*vab-1(kd); kyIs104*	CZ18664

Appendix B. Strains Constructed

Table B.1 *C. elegans* Strains Constructed

Strain	Genotype
CZ9367	*Pstr-1-GFP(kyIs104)*
CZ9443	*vab-1(e118); Pgcy-7-GFP(otIs3)*
CZ9444	*vab-1(e118); Pgcy-8-GFP(oyIs17)*
CZ9445	*vab-1(e118); Pstr-3-GFP(kyIs128)*
CZ9553	*vab-1(e2027); Pgcy-7-GFP(otIs3)*
CZ9555	*vab-1(ju306); Pgcy-7-GFP(otIs3)*
CZ9556	*vab-1(ju306); Pgcy-8-GFP(oyIs17)*
CZ9878	*efn-2(ev658); Pstr-1-GFP(kyIs104)*
CZ9885	*efn-1(e96); Pstr-3-GFP(kyIs128)*
CZ9886	*vab-1(ju306); Pstr-1-GFP(kyIs104)*
CZ10141	*efn-2(ev658); Pstr-3-GFP(kyIs128)*
CZ10142	*efn-2(ev658); Pgcy-7-GFP(otIs3)*
CZ10229	*efn-1(e96); Pgcy-8-GFP(oyIs17)*
CZ10230	*efn-3(ev696); Pgcy-8-GFP(oyIs17)*
CZ10231	*Pgcy-7-GFP(otIs3); efn-3(ev696)*
CZ10232	*efn-2(ev658); Pgcy-8-GFP(oyIs17)*
CZ10582	*efn-1(e96); Pgcy-7-GFP(otIs3)*
CZ10700	*trk-1(tm3985); Pgcy-8-GFP(oyIs17)*
CZ10701	*trk-1(tm3985) Pstr-1-GFP(kyIs104)*
CZ11019	*efn-2(ev658) efn-1(e96); Pstr-1-GFP(kyIs104)*
CZ11020	*efn-1(e96); efn-3(ev696) Pstr-1-GFP(kyIs104)*
CZ11021	*efn-2(ev658); efn-3(ev696); Pstr-1-GFP(kyIs104)*
CZ11022	*vab-1(e118); efn-1(e96); Pstr-1-GFP(kyIs104)*
CZ11074	*vab-1(e2027); Pgcy-5-GFP(ntIs1)*
CZ11132	*jac-1(ok3000); Pstr-1-GFP(kyIs104)*
CZ11183	*vab-1(e118); trk-1(tm3985) Pstr-1-GFP(kyIs104)*
CZ11184	*vab-1(e118); jac-1(ok3000); Pstr-1-GFP(kyIs104)*
CZ11185	*vab-1(e118); efn-2(ev658); Pstr-1-GFP(kyIs104)*
CZ11395	*efn-3(ev696) Pstr-1-GFP(kyIs104)*
CZ11396	*ced-3(n717); Pstr-1-GFP(kyIs104); kyEx3294*
CZ11448	*src-2(ok819); Pstr-1-GFP(kyIs104)*
CZ11449	*vab-1(e118); efn-3(ev696) Pstr-1-GFP(kyIs104)*
CZ11493	*vab-1(dx31); Pstr-1-GFP(kyIs104)*

Table B.1 continued

Strain	Genotype
CZ11494	*goa-1(sa734); Pstr-1-GFP(kyIs104)*
CZ11535	*efn-2(ev658) efn-1(e96); efn-3(ev696) Pstr-1-GFP(kyIs104)*
CZ11815	*Pstr-1-GFP(kyIs104); vab-1(+) (juEx16)*
CZ11816	*vab-1(e2027); Pstr-1-GFP(kyIs104); vab-1(+) (juEx16)*
CZ11856	*sax-3(ky123) Pstr-1-GFP(kyIs104)*
CZ11892	*vab-1(e2027); efn-2(ev658); Pstr-1-GFP(kyIs104)*
CZ11933	*akt-1(ok525); Pstr-1-GFP(kyIs104)*
CZ11934	*vab-1(tm306); Pstr-1-GFP(kyIs104)*
CZ11961	*efn-2(ev658); EFN-1::GFP(juIs52)*
CZ12017	*Pdyf-7-mCherry(juEx2744)*
CZ12018	*Pdyf-7-mCherry(juEx2745)*
CZ12019	*Pdyf-7-mCherry(juEx2746)*
CZ12050	*vab-1(e2027); efn-3(ev696) Pstr-1-GFP(kyIs104)*
CZ12051	*vab-1(e2027); efn-1(e96); Pstr-1-GFP(kyIs104)*
CZ12220	*unc-40(e1430); Pstr-1-GFP(kyIs104)*
CZ12221	*unc-40(e1430); efn-2(ev658); Pstr-1-GFP(kyIs104)*
CZ12222	*vab-1(e118); abl-1(ok171) Pstr-1-GFP(kyIs104)*
CZ12268	*abl-1(ok171) Pstr-1-GFP(kyIs104)*
CZ12361	*efn-2(ev658); sax-3(ky123) Pstr-1-GFP(kyIs104)*
CZ12408	*vab-1(dx14); Pstr-1-GFP(kyIs104)*
CZ12409	*vab-1(ok1699); Pstr-1-GFP(kyIs104)*
CZ12410	*Ptrk-1-GFP(juEx2894)*
CZ12411	*Ptrk-1-GFP(juEx2895)*
CZ12412	*Ptrk-1-GFP(juEx2896)*
CZ12413	*Ptrk-1-GFP(juEx2897)*
CZ12433	*Ptrk-1-GFP(juEx2916)*
CZ12434	*Ptrk-1-GFP(juEx2917)*
CZ12435	*Ptrk-1-GFP(juEx2918)*
CZ12436	*vab-1(dx31); efn-2(ev658); Pstr-1-GFP(kyIs104)*
CZ12536	*arf-6(tm1447); Pstr-1-GFP(kyIs104)*
CZ12537	*shc-1(ok198); Pstr-1-GFP(kyIs104)*
CZ12538	*shc-1(ok198); vab-1(e118); Pstr-1-GFP(kyIs104)*
CZ12539	*shc-2(tm328); Pstr-1-GFP(kyIs104)*

Table B.1 continued

Strain	Genotype
CZ12581	*vab-1(e118); arf-6(tm1447); Pstr-1-GFP(kyIs104)*
CZ12582	*vab-1(e118); nck-1(ok694); Pstr-1-GFP(kyIs104)*
CZ12738	*vab-1(e1059); Pstr-1-GFP(kyIs104)*
CZ13016	*vab-1(e2027); trk-1(tm4054) Pstr-1-GFP(kyIs104)*
CZ13017	*vab-1(e2027); abl-1(ok171) Pstr-1-GFP(kyIs104)*
CZ13018	*wrk-1(ok695) Pstr-1-GFP(kyIs104)*
CZ13019	*vab-1(e118); wrk-1(ok695) Pstr-1-GFP(kyIs104)*
CZ13080	*efn-1(e96); EFN-1::GFP(juIs52), Pstr-1-GFP(kyIs104)*
CZ13084	*git-1(tm1962) Pstr-1-GFP(kyIs104)*
CZ13085	*vab-1(e118); git-1(tm1962) Pstr-1-GFP(kyIs104)*
CZ13086	*egl-19(ad695); Pstr-1-GFP(kyIs104)*
CZ13087	*vab-1(e118); egl-19(ad695), Pstr-1-GFP(kyIs104)*
CZ13100	*Prgef-1-EFN-1(juEx3158)*
CZ13101	*Pdyf-7-EFN-1(juEx3159)*
CZ13133	*Pdyf-7-EFN-1(juEx3178)*
CZ13134	*Pdyf-7-EFN-1(juEx3179)*
CZ13223	*Pstr-1-GFP(kyIs104); juEx2737*
CZ13226	*Pstr-1-GFP(kyIs104); juEx3178*
CZ13228	*efn-1(e141); Pstr-1-GFP(kyIs104)*
CZ13370	*ina-1(gm144); Pstr-1-GFP(kyIs104)*
CZ13371	*vab-1(e118); ina-1(gm144); Pstr-1-GFP(kyIs104)*
CZ13372	*efn-1(e96); Pstr-1-GFP(kyIs104); juEx3158*
CZ13373	*efn-1(e96); Pstr-1-GFP(kyIs104); juEx3179*
CZ13427	*Pdyf-7-mCherry(juEx3267)*
CZ13428	*Pdyf-7-mCherry(juEx3268)*
CZ13429	*Pdyf-7-mCherry(juEx3306)*
CZ13431	*Pdyf-7-VAB-1(juEx3269)*
CZ13432	*Pdyf-7-VAB-1(juEx3308)*
CZ13433	*Pdyf-7-VAB-1(juEx3309)*
CZ13434	*Pdyf-7-VAB-1(juEx3310)*
CZ13438	*Prgef-1-EFN-1(juEx3313)*
CZ13439	*Prgef-1-EFN-1(juEx3271)*
CZ13441	*Prgef-1-EFN-1(juEx3315)*

Table B.1 continued

Strain	Genotype
CZ13446	*Pstr-1-GFP(kyIs104); juEx3273*
CZ13448	*Pstr-1-GFP(kyIs104); juEx3320*
CZ13449	*Pstr-1-GFP(kyIs104); juEx3321*
CZ13614	*vab-1(e118); mig-10(ct41); Pstr-1-GFP(kyIs104)*
CZ13615	*EFN-1::GFP(juIs52); Pstr-1-GFP(kyIs104)*
CZ13616	*efn-2(ev658) efn-1(e141); Pstr-1-GFP(kyIs104)*
CZ13617	*vab-1(e118); ngn-1(ok2200); Pstr-1-GFP(kyIs104)*
CZ13618	*Pstr-1-GFP(kyIs104); juEx3269*
CZ13838	*Prgef-1-VAB-1(juEx3467)*
CZ13839	*Prgef-1-VAB-1(juEx3468)*
CZ13840	*Prgef-1-VAB-1(juEx3469)*
CZ13841	*Prgef-1-VAB-1(juEx3470)*
CZ13842	*Prgef-1-VAB-1(juEx3471)*
CZ13844	*Prgef-1-VAB-1(juEx3473)*
CZ13845	*Prgef-1-VAB-1(juEx3474)*
CZ13846	*Punc-119-EFN-1(juEx3475)*
CZ13847	*Punc-119-EFN-1(juEx3476)*
CZ13848	*vab-1(e118); juEx3477*
CZ13849	*aap-1(tm713); Pstr-1-GFP(kyIs104)*
CZ13850	*ephx-1(ok494); Pstr-1-GFP(kyIs104)*
CZ13851	*ngn-1(ok2200); Pstr-1-GFP(kyIs104)*
CZ13852	*vab-1(e2027); egl-19(ad695); kyIs014*
CZ13853	*egl-19(n2368cs); Pstr-1-GFP(kyIs104)*
CZ13854	*vab-1(e118); egl-19(n2368cs); Pstr-1-GFP(kyIs104)*
CZ13962	*Pstr-1-GFP(kyIs104); juEx3309*
CZ13963	*mig-10(ct41); Pstr-1-GFP(kyIs104)*
CZ13967	*Pstr-1-GFP(kyIs104); juEx3315*
CZ13968	*efn-1(e96); Pstr-1-GFP(kyIs104); juEx3315*
CZ13969	*Pstr-1-GFP(kyIs104); juEx3317*
CZ13971	*Punc-33-VAB-1(juEx3529)*
CZ13972	*Punc-33-VAB-1(juEx3530)*
CZ14074	*ephx-1(ok494) vab-1(e118); Pstr-1-GFP(kyIs104)*
CZ14075	*vab-1(e118); egl-19(ad695); Pgcy-8-GFP(oyIs17)*

Table B.1 continued

Strain	Genotype
CZ14076	*rga-5(ok2241); Pstr-1-GFP(kyIs104)*
CZ14077	*vab-1(e118); rga-5(ok2241); Pstr-1-GFP(kyIs104)*
CZ14078	*vab-1(e2027); Pstr-1-GFP(kyIs104); juEx3529*
CZ14079	*Pstr-1-GFP(kyIs104); juEx3529*
CZ14080	*vab-1(e2027); Pstr-1-GFP(kyIs104); juEx3530*
CZ14081	*Pstr-1-GFP(kyIs104); juEx3530*
CZ14083	*Pstr-1-GFP(kyIs104); juEx3470*
CZ14084	*efn-1(e96); Pstr-1-GFP(kyIs104); juEx3475*
CZ14085	*Pstr-1-GFP(kyIs104); juEx3475*
CZ14086	*efn-1(e96); Pstr-1-GFP(kyIs104); juEx3476*
CZ14087	*Pstr-1-GFP(kyIs104); juEx3476*
CZ14089	*Punc-33-EFN-1(juEx3575)*
CZ14090	*Punc-33-EFN-1(juEx3576)*
CZ14091	*Punc-33-EFN-1(juEx3577)*
CZ14095	*tag-341(ok1498); Pstr-1-GFP(kyIs104)*
CZ14177	*Pgcy-8-GFP(oyIs17); unc-2(e55)*
CZ14178	*vab-1(e118); Pgcy-8-GFP(oyIs17); unc-2(e55)*
CZ14387	*gap-2(tm748) Pstr-1-GFP(kyIs104)*
CZ14388	*efn-1(e96); Pstr-1-GFP(kyIs104); juEx3718*
CZ14389	*efn-1(e96); Pstr-1-GFP(kyIs104); juEx3719*
CZ14390	*vab-1(e2027); Pstr-1-GFP(kyIs104); juEx2870*
CZ14447	*efn-1(e96); Pstr-1-GFP(kyIs104); juEx127*
CZ14483	*vab-1(e118); akt-1(ok525); Pstr-1-GFP(kyIs104)*
CZ14484	*src-2(ok819); vab-1(e118); Pstr-1-GFP(kyIs104)*
CZ14485	*vab-1(e118); ngn-1(ok2200); Pstr-1-GFP(kyIs104)*
CZ14486	*aap-1(tm713); vab-1(e2027); Pstr-1-GFP(kyIs104)*
CZ14487	*efn-1(e96); Pstr-1-GFP(kyIs104); juEx3775*
CZ14629	*egl-19(ad695); efn-1(e96); Pstr-1-GFP(kyIs104)*
CZ14630	*age-1(hx546); efn-1(e96); Pstr-1-GFP(kyIs104)*
CZ14631	*Pmyo-2-EFN-1(juEx3835)*
CZ14632	*Pmyo-2-VAB-1(juEx3836)*
CZ14633	*Pmyo-2-VAB-1(juEx3837)*
CZ14634	*vab-1(+)(juEx3838)*

Table B.1 continued

Strain	Genotype
CZ14635	*vab-1(+)(juEx3839)*
CZ14693	*Pstr-1-GFP(kyIs104); juEx3835*
CZ14694	*efn-1(e96); Pstr-1-GFP(kyIs104); juEx3835*
CZ14712	*Pstr-1-GFP(kyIs104); juEx3836*
CZ14713	*vab-1(e2027); Pstr-1-GFP(kyIs104); juEx3836*
CZ14714	*Pstr-1-GFP(kyIs104); juEx3838*
CZ14715	*vab-1(e2027); Pstr-1-GFP(kyIs104); juEx3838*
CZ14716	*Pstr-1-GFP(kyIs104); juEx3839*
CZ14799	*unc-40(e1430); abl-1(ok171) Pstr-1-GFP(kyIs104)*
CZ14800	*vab-1(e2027); Pstr-1-GFP(kyIs104); juEx3839*
CZ14802	*dyf-7(juEx3925)*
CZ14803	*dyf-7(juEx3926)*
CZ14909	*abl-1(juEx3927)*
CZ14910	*abl-1(juEx3928)*
CZ14911	*Pabl-1-GFP(juEx3984)*
CZ14912	*age-1(hx546); Pstr-1-GFP(kyIs104)*
CZ14913	*vab-1(e118) age-1(hx546); Pstr-1-GFP(kyIs104)*
CZ14914	*vab-1(e118) tag-341(ok1498); Pstr-1-GFP(kyIs104)*
CZ15135	*Pdyf-7-VAB-1(juEx4113)*
CZ15136	*Pdyf-7-VAB-1(juEx4114)*
CZ15137	*Pdyf-7-VAB-1(juEx4115)*
CZ15138	*Pdyf-7-VAB-1(juEx4116)*
CZ15139	*Pdyf-7-VAB-1(juEx4117)*
CZ15294	*egl-19(ad695); unc-6(ev400) Pstr-1-GFP(kyIs104)*
CZ15295	*vab-1(e2); egl-19(ad695); Pstr-1-GFP(kyIs104)*
CZ15296	*Pstr-1-GFP(kyIs104); juEx4115*
CZ15297	*efn-1(e96); abl-1(ok171) Pstr-1-GFP(kyIs104)*
CZ15298	*vab-1(e118); akt-2(ok393) Pstr-1-GFP(kyIs104)*
CZ15507	*lsy-6(ot71); Pstr-1-GFP(kyIs104)*
CZ15508	*vab-1(e118); lsy-6(ot71); Pstr-1-GFP(kyIs104)*
CZ15567	*daf-18(ok480) Pstr-1-GFP(kyIs104)*
CZ15568	*vab-1(e118); daf-18(ok480) Pstr-1-GFP(kyIs104)*
CZ15589	*Pdyf-7-ABL-1(juEx4343)*

Table B.1 continued

Strain	Genotype
CZ15590	*Pdyf-7-ABL-1(juEx4344)*
CZ15591	*Pdyf-7-ABL-1(juEx4345)*
CZ15592	*Punc-33-ABL-1(juEx4346)*
CZ15781	*efn-1(e96); EFN-1::GFP(juIs52); juEx4421*
CZ15782	*efn-1(e96); EFN-1::GFP(juIs52); juEx4422*
CZ15783	*efn-1(e96); EFN-1::GFP(juIs52); juEx4423*
CZ15784	*efn-1(e96); EFN-1::GFP(juIs52); juEx4424*
CZ15785	*vab-1(e2027); lsy-6(ot71); Pgcy-5-GFP(ntIs1)*
CZ15786	*abl-1(ok171) Pstr-1-GFP(kyIs104); juEx4343*
CZ15787	*vab-1(e118); abl-1(ok171) Pstr-1-GFP(kyIs104); juEx4343*
CZ15788	*abl-1(ok171) Pstr-1-GFP(kyIs104); juEx4344*
CZ15789	*vab-1(e118); abl-1(ok171) Pstr-1-GFP(kyIs104); juEx4344*
CZ15790	*abl-1(ok171) Pstr-1-GFP(kyIs104); juEx4345*
CZ15791	*vab-1(e118); abl-1(ok171) Pstr-1-GFP(kyIs104); juEx4345*
CZ15792	*abl-1(ok171) Pstr-1-GFP(kyIs104); juEx4346*
CZ16027	*Pttx-3-EFN-1(juEx4524)*
CZ16028	*efn-1(e96); Pstr-1-GFP(kyIs104); juEx4524*
CZ16029	*Pttx-3-VAB-1(juEx4525)*
CZ16030	*Pttx-3-VAB-1(juEx4526)*
CZ16031	*Pttx-3-VAB-1(juEx4527)*
CZ16032	*Pttx-3-VAB-1(juEx4528)*
CZ16033	*vab-1(e2027);Pstr-1-GFP(kyIs104); juEx4527*
CZ16034	*vab-1(e2027); Pstr-1-GFP(kyIs104); juEx4346*
CZ16035	*akt-2(tm812) Pstr-1-GFP(kyIs104)*
CZ16036	*vab-1(e118); akt-2(tm812) Pstr-1-GFP(kyIs104)*
CZ16249	*nck-1(ok694) Pstr-1-GFP(kyIs104)*
CZ16250	*Pstr-1-GFP(kyIs104); juEx4345*
CZ16251	*Pstr-1-GFP(kyIs104); juEx4527*
CZ16386	*efn-1(e96); Pstr-1-GFP(kyIs104); juEx4719*
CZ16387	*efn-1(e96); Pstr-1-GFP(kyIs104); juEx4720*
CZ16388	*efn-1(e96); Pstr-1-GFP(kyIs104); juEx4721*
CZ16389	*Plin-26-VAB-1(juEx4722)*
CZ16390	*Plin-26-VAB-1(juEx4723)*

Table B.1 continued

Strain	Genotype
CZ16391	*Plin-26-VAB-1(juEx4724)*
CZ16392	*vab-1(e2027); Pstr-1-GFP(kyIs104); juEx4725*
CZ16393	*Pstr-1-GFP(kyIs104); juEx4725*
CZ16395	*Phlh-17-VAB-1(juEx4727)*
CZ16396	*Phlh-17-VAB-1(juEx4728)*
CZ16635	*age-1(hx546); abl-1(ok171) Pstr-1-GFP(kyIs104)*
CZ16636	*age-1(hx546); vab-1(e118); abl-1(ok171) Pstr-1-GFP(kyIs104)*
CZ16638	*Pstr-1-VAB-1(juEx4856)*
CZ16639	*Pstr-1-VAB-1(juEx4857)*
CZ16640	*Pstr-1-VAB-1(juEx4858)*
CZ16642	*efn-1(e96); Pstr-1-GFP(kyIs104); juEx4860*
CZ16643	*efn-1(e96); Pstr-1-GFP(kyIs104); juEx4861*
CZ16645	*Phlh-17-EFN-1(juEx4863)*
CZ16646	*Phlh-17-EFN-1(juEx4864)*
CZ16739	*Pstr-1-EFN-1(juEx4905)*
CZ16740	*Pstr-1-EFN-1(juEx4906)*
CZ16741	*Pstr-1-EFN-1(juEx4907)*
CZ16742	*Pstr-1-EFN-1(juEx4908)*
CZ16743	*efn-1(e96); Pstr-1-GFP(kyIs104); juEx4909*
CZ17033	*Pstr-1-GFP(kyIs104); juEx4728*
CZ17034	*Pstr-1-GFP(kyIs104); juEx4857*
CZ17035	*Pstr-1-GFP(kyIs104); juEx4858*
CZ17036	*Pstr-1-GFP(kyIs104); juEx4859*
CZ17037	*Pstr-1-GFP(kyIs104); juEx905*
CZ17038	*efn-1(e96); Pstr-1-GFP(kyIs104); juEx4905*
CZ17039	*vab-1(e2027); Pstr-1-GFP(kyIs104); juEx4857*
CZ17040	*efn-1(e96); Pstr-1-GFP(kyIs104); juEx4863*
CZ17041	*Pstr-1-GFP(kyIs104); juEx4864*
CZ17042	*efn-1(e96); Pstr-1-GFP(kyIs104); juEx4864*
CZ17043	*Pstr-1-VAB-1(juEx5052)*
CZ17044	*Pstr-1-VAB-1(juEx5053)*
CZ17045	*vab-1(e118); wsp-1(gm324); Pstr-1-GFP(kyIs104)*
CZ17046	*vab-1(e118); abl-1(ok171); Pstr-1-GFP(kyIs104); juEx5054*

Table B.1 continued

Strain	Genotype
CZ17047	*vab-1(e118); abl-1(ok171); Pstr-1-GFP(kyIs104); juEx5055*
CZ17048	*vab-1(e118); abl-1(ok171); Pstr-1-GFP(kyIs104); juEx5056*
CZ17049	*vab-1(e118); abl-1(ok171); Pstr-1-GFP(kyIs104); juEx5057*
CZ17050	*vab-1(e118); abl-1(ok171); Pstr-1-GFP(kyIs104); juEx5058*
CZ17051	*vab-1(e118); abl-1(ok171); Pstr-1-GFP(kyIs104); juEx5059*
CZ17052	*vab-1(e118); abl-1(ok171); Pstr-1-GFP(kyIs104); juEx5060*
CZ17296	*cog-1(sy275); Pgcy-7-GFP(otIs3)*
CZ17297	*wsp-1(gm324); Pstr-1-GFP(kyIs104)*
CZ17298	*vab-1(e2027); Pstr-1-GFP(kyIs104); juEx5053*
CZ17647	*daf-18(nr2037) Pstr-1-GFP(kyIs104)*
CZ17648	*vab-1(e118); daf-18(nr2037) Pstr-1-GFP(kyIs104)*
CZ17649	*daf-16(mu86); Pstr-1-GFP(kyIs104)*
CZ17650	*daf-16(mu86); vab-1(e118); Pstr-1-GFP(kyIs104)*
CZ17651	*aap-1(m889); Pstr-1-GFP(kyIs104)*
CZ17652	*aap-1(m889); vab-1(e118); Pstr-1-GFP(kyIs104)*
CZ17653	*efn-1(e96); Pstr-1-GFP(kyIs104); juEx3273*
CZ17654	*vab-1(e2027); Pstr-1-GFP(kyIs104); juEx3179*
CZ17679	*sgk-1(ok538) Pstr-1-GFP(kyIs104)*
CZ17680	*vab-1(e118); sgk-1(ok538) Pstr-1-GFP(kyIs104)*
CZ17765	*sgk-1(ft15) kyIs014*
CZ17766	*vab-1(e118); sgk-1(ft15) Pstr-1-GFP(kyIs104)*
CZ17767	*Punc-33-AAP-1(juEx5302)*
CZ17768	*Punc-33-AAP-1(juEx5303)*
CZ17769	*Punc-33-AAP-1(juEx5304)*
CZ17770	*Punc-33-AAP-1(juEx5305)*
CZ17861	*zfp-1(ok554); Pstr-1-GFP(kyIs104)*
CZ17862	*vab-1(e118); zfp-1(ok554); Pstr-1-GFP(kyIs104)*
CZ17863	*vab-1(e2027); sgk-1(ok538) Pstr-1-GFP(kyIs104)*
CZ17864	*vab-1(e118); Pstr-1-GFP(kyIs104); juEx5302*
CZ17865	*vab-1(e118); Pstr-1-GFP(kyIs104); juEx5304*
CZ18028	*Pdyf-7-tagRFP-T(juEx5385)*
CZ18029	*Pdyf-7-tagRFP-T(juEx5386)*
CZ18030	*vab-1(e118); Pstr-1-GFP(kyIs104); juEx3529*

Table B.1 continued

Strain	Genotype
CZ18031	*vab-1(e118); Pstr-1-GFP(kyIs104); juEx3530*
CZ18032	*vab-1(e118); Pstr-1-GFP(kyIs104); juEx4857*
CZ18033	*daf-16(mu86); vab-1(e2027); Pstr-1-GFP(kyIs104)*
CZ18034	*age-1(hx546); vab-1(e2027); Pstr-1-GFP(kyIs104)*
CZ18125	*aap-1(m889); efn-1(e96); Pstr-1-GFP(kyIs104)*
CZ18126	*daf-16(mu86); sgk-1(ok538); Pstr-1-GFP(kyIs104)*
CZ18127	*daf-16(mu86); abl-1(ok171); Pstr-1-GFP(kyIs104)*
CZ18128	*aap-1(m889); abl-1(ok171); Pstr-1-GFP(kyIs104)*
CZ18129	*Pdyf-7-EFN-2(juEx5417)*
CZ18130	*Pdyf-7-EFN-2(juEx5418)*
CZ18131	*vab-1(e118); Pstr-1-GFP(kyIs104); juEx3269*
CZ18132	*vab-1(e118); Pstr-1-GFP(kyIs104); juEx3309*
CZ18133	*vab-1(e2027); VAB-1::GFP(juIs24); juEx5431*
CZ18249	*efn-1(ju90); Pstr-1-GFP(kyIs104)*
CZ18250	*efn-2(ev658) efn-1(ju90); Pstr-1-GFP(kyIs104)*
CZ18251	*akt-2(ok393) Pstr-1-GFP(kyIs104)*
CZ18252	*vab-1(ju426); Pstr-1-GFP(kyIs104)*
CZ18253	*vab-1(qa2211); Pstr-1-GFP(kyIs104)*
CZ18323	*Pstr-1-GFP(kyIs104); juEx5417*
CZ18324	*vab-1(e118); Pstr-1-GFP(kyIs104); juEx5417*
CZ18325	*Pstr-1-GFP(kyIs104); juEx5418*
CZ18326	*vab-1(e118); Pstr-1-GFP(kyIs104); juEx5418*
CZ18327	*Pdyf-7-AAP-1(juEx5477)*
CZ18328	*Pdyf-7-AAP-1(juEx5478)*
CZ18329	*Pdyf-7-AAP-1(juEx5479)*
CZ18330	*Pdyf-7-AAP-1(juEx5480)*
CZ18331	*Pdyf-7-AAP-1(juEx5481)*
CZ18332	*Pdyf-7-AAP-1(juEx5482)*
CZ18449	*egl-19(ad695); sax-3(ky123); Pstr-1-GFP(kyIs104)*
CZ18450	*vab-1(e118); Pstr-1-GFP(kyIs104); juEx5478*
CZ18451	*vab-1(e118); Pstr-1-GFP(kyIs104); juEx5480*
CZ18452	*vab-1(e118); Pstr-1-GFP(kyIs104); juEx5482*
CZ18463	*Pstr-1-AAP-1(juEx5524)*

Table B.1 continued

Strain	Genotype
CZ18464	*Pstr-1-AAP-1(juEx5525)*
CZ18465	*Pstr-1-AAP-1(juEx5526)*
CZ18466	*Pstr-1-AAP-1(juEx5527)*
CZ18467	*Pstr-1-AAP-1(juEx5528)*
CZ18468	*Pstr-1-AAP-1(juEx5529)*
CZ18469	*efn-1(e96); EFN-1::GFP(juIs52); juEx5530*
CZ18470	*efn-1(e96); EFN-1::GFP(juIs52); juEx5531*
CZ18471	*efn-1(e96); EFN-1::GFP(juIs52); juEx5532*
CZ18514	*vab-1(e2027); pdk-1(mg142)*
CZ18515	*akt-1(ok525); vab-1(e2027); Pstr-1-GFP(kyIs104)*
CZ18516	*Pstr-1-GFP(juEx5535)*
CZ18517	*Pstr-1-GFP(juEx5536)*
CZ18518	*efn-1(e96); Pstr-1-GFP(kyIs104); EFN-1::GFP(juIs52); juEx5537*
CZ18519	*efn-1(e96); Pstr-1-GFP(kyIs104); EFN-1::GFP(juIs52); juEx5538*
CZ18520	*efn-1(e96); Pstr-1-GFP(kyIs104); EFN-1::GFP(juIs52); juEx5539*
CZ18521	*efn-1(e96); Pstr-1-GFP(kyIs104); EFN-1::GFP(juIs52); juEx5540*
CZ18522	*vab-1(e2027); Pstr-1-GFP(kyIs104); juEx4345*
CZ18584	*vab-1(e118); pdk-1(sa709)*
CZ18585	*vab-1(e2027); pdk-1(sa709)*
CZ18586	*aap-1(m889), Pstr-1-GFP(kyIs104); juEx5478*
CZ18587	*aap-1(m889); Pstr-1-GFP(kyIs104); juEx5480*
CZ18588	*aap-1(m889); vab-1(e118); Pstr-1-GFP(kyIs104); juEx5478*
CZ18589	*abl-1(ok171); Pstr-1-GFP(kyIs104); juEx5059*
CZ18663	*Pstr-1-GFP(kyIs104); juEx5059*
CZ18664	*vab-1(e118); Pstr-1-GFP(kyIs104); juEx5059*
CZ18665	*vab-1(e118); Pstr-1-GFP(kyIs104); juEx4345*
CZ18666	*vab-1(e118); Pstr-1-GFP(kyIs104); juEx5526*
CZ18667	*vab-1(e118); Pstr-1-GFP(kyIs104); juEx5529*
CZ18853	*vab-1(e2027); Pstr-1-GFP(kyIs104); juEx5059*